ABSTRACT

YAO, ZHEN. Design and Synthesis of Porphyrins for Targeted Molecular Brachytherapy. (Under the direction of Dr. Jonathan S. Lindsey).

New approaches are urgently needed for treatment of cancer. The inherent heterogeneity of cells in solid tumors has thwarted most approaches developed to date. A fundamentally new approach, targeted molecular brachytherapy, also known as selective targeted amplified radiotherapy (S.T.A.R.), is attractive conceptually but has not yet been implemented. This new method selectively accumulates radioactive precipitates in tumor sites by systemic treatment of distinct agents in a sequential manner. One of the key agents for such a therapy is a soluble, precipitable reagent (SPR). The essence of this thesis includes design, synthesis and evaluation of porphyrin-based SPRs for the S.T.A.R. method. Three distinct designs of porphyrin-based SPRs were proposed. Synthetic approaches for target SPRs were explored, and several model compounds were synthesized. The development of a new synthetic approach to *trans*-AB-porphyrins, which are essential structures in the designs of SPRs, is also described in this thesis. Several target SPRs have not yet been synthesized due to synthetic difficulties as well as limitations related to water-solubility or stability of compounds. On the other hand, a diphosphate porphyrin exhibited successful enzymatic conversion from the water-soluble form to a porphyrin precipitate. Future work toward SPRs will focus on new designs that incorporate such diphosphate porphyrins.

Design and Synthesis of Porphyrins for Targeted Molecular Brachytherapy

By
Zhen Yao

A dissertation submitted to the Graduate Faculty of

North Carolina State University

in partial fulfillment of the

requirements for the Degree of

Doctor of Philosophy

Chemistry

Raleigh, North Carolina, USA

Fall, **2006**

Approved by:

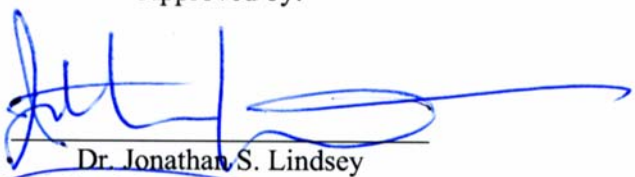

Dr. Jonathan S. Lindsey
Chair of the Advisory Committee

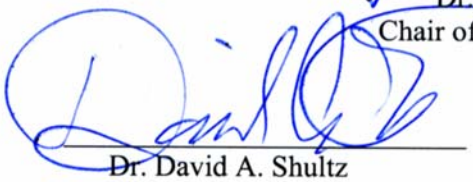

Dr. David A. Shultz

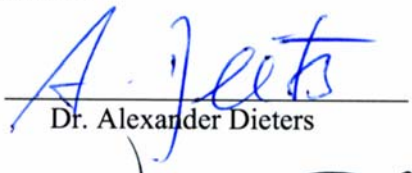

Dr. Alexander Dieters

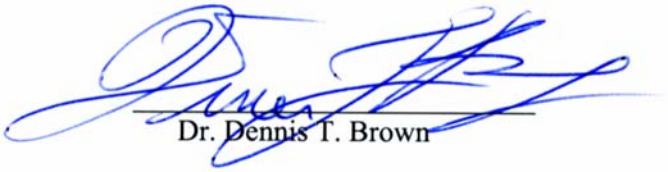

Dr. Dennis T. Brown

Dr. Winston Salser

BIOGRAPHY

Zhen Yao was born on September 12, 1975 in Shanghai, China. He spent his childhood with his grandparents in East China University of Science and Technology, where his grandfather used to work as a professor. Zhen's parents joined the same university in 1980s and obtained their professorships later. Although his name was never on the student list, Zhen stayed in his first university for 18 years and received his pre-college education from a primary school and a high school nearby.

Zhen entered Fudan University in Shanghai for his undergraduate study in genetics in 1994 and obtained his B.S. degree in 1998. After his graduation, Zhen looked for opportunities to continue his postgraduate education in the United States. With help from Dr. Jonathan Lindsey, he was accepted by North Carolina State University in 1999 and joined the Chemistry Department in the fall of that year. Zhen's first research project in Lindsey's group was related to ligation of DNA fragments on a solid support. He started the project presented in this thesis in 2002.

Zhen met Yi Lei, a new graduate student in the Industrial Engineering Department, in 2000. They were married in October, 2003. Two and a half years after their marriage, their lovely daughter, Evelyn, was born in Raleigh on March 14th, 2006. Life has been hectic but enjoyable everyday ever since.

ACKNOWLEDGMENTS

First I'd like to express my deepest thanks to my advisor, Dr. Jonathan Lindsey, for supervising my research and study, for providing me financial assistantship and for teaching me a lot more than just chemistry. All other Lindsey's group members over the past 7 years should also be thanked for every bit of help they offered me, for their effort to make the lab better and for being good friends. Among them, I specially thank Dr. Dhanalekshmi Savithri for working with me on this project, Dr. K. Eszter Borbas for providing a water-soluble porphyrin for enzymatic study, Dr. Marcin Ptaszek for preparing precursors that are potentially valuable for this project, Dr. Masahiko Taniguchi for advice on various topics, Dr. Arounaguiry Ambroise for teaching me organic synthesis, and fellow graduate student Jayeeta Bhaumik for the help with imidazolyl-porphyrins and also for taking good care of the lab.

I also want to thank my committee members, Dr. Alexander Dieters, Dr. David Shultz, Dr. Dennis Brown and previous members Dr. Binghe Wang and Dr. Bruce Eaton who have left the department, for their valuable advice. I am grateful that Dr. Winston Salser of Oncologic, Inc. traveled across the country to attend my thesis defense.

I have been given strong support from my family over these years. My wife, Yi Lei, shoulders the majority of the burden at home so that I can focus on research. My parents in China always encourage me on the phone and my mother-in-law came to help us through the most difficult time when our daughter, Evelyn, was born.

Finally, I'd like to thank Oncologic, Inc. for financial support to help me with my research.

TABLE OF CONTENTS

LIST OF CHARTS

LIST OF EQUATIONS

LIST OF FIGURES

LIST OF SCHEMES

LIST OF TABLES

LIST OF ABBREVIATIONS

Ac	acetyl
ADEPT	antibody-directed enzyme-prodrug therapy
BChl *c*	bacteriochlorophyll *c*
Boc	*tert*-butoxycarbonyl
BSA	bovine serum albumin
Bu_2B-OTf	dibutylboryl trifluoromethanesulfonate
CDI	carbonyldiimidazole
COSY	correlation spectroscopy
CTA	cancer targeting agent
DCC	1,3-dicyclohexylcarbodiimide
DDQ	2,3-Dichloro-5,6-dicyano-1,4-benzoquinone
DHB	2,5-dihydroxybenzoic acid
DHFR	dihydrofolate reductase
DMSO	dimethyl sulfoxide
DMAP	4-(dimethylamino)pyridine
DMF	*N*,*N*-dimethylformamide
ECF	extracellular fluid
EPR	enhanced permeability and retention
ESI-MS	electrospray ionization mass spectrometry
FAB-MS	fast atom bombardment mass spectrometry

Fb-OH/PO_4	5-(4-bromophenyl)-15-[(1-dihydroxyphosphoryloxy-5-hydroxy)pent-3-yl]porphyrin (swallowtail monophosphate free-base porphyrin)
Fb-$(OH)_2$	5-(4-bromophenyl)-15-(1,5-dihydroxypent-3-yl)porphyrin (swallowtail dihydroxyl free-base porphyrin)
Fb-$(PO_4)_2$	5-(4-bromophenyl)-15-[1,5-bis(dihydroxyphosphoryloxy)pent-3-yl]porphyrin (swallowtail diphosphate free-base porphyrin)
FH_2	dihydrofolate
FH_4	tetrahydrofolate
GDEPT	gene-directed enzyme-prodrug therapy
GPAT	genetic prodrug activation therapy
HSA	human serum albumin
LD-MS	laser desorption mass spectrometry
MDEPT	macromolecule-directed enzyme-prodrug therapy
MDR	multidrug resistance
Mes	mesityl
MTX	methotrexate
NMR	nuclear magnetic resonance
NBS	*N*-bromosuccinimide
NOESY	nuclear overhauser enhancement spectroscopy
PDEPT	polymer-directed enzyme-prodrug therapy
PDT	photodynamic therapy
Pgp	P glycoprotein

RIT	radioimmunotherapy
SAP	shrimp alkaline phosphatase
SEC	size exclusion chromatography
SEM	2-(trimethylsilyl)ethoxymethyl
SPR	soluble precipitable reagents
S.T.A.R.	selectively targeted amplified radiotherapy
TBAF	tetrabutylammonium fluoride
TBDMS	*tert*-butyldimethylsilyl
TEA	triethylamine
TFA	trifluoroacetic acid
THF	tetrahydrofuran
TLC	thin-layer chromatography
TMS	trimethylsilyl
TMSE	2-(trimethylsilyl)ethanol
VDEPT	virus-directed enzyme-prodrug therapy

Chapter 1

Cancer and Cancer Therapies

1.1. Carcinogenesis

Cancer is a disease with the capacity for uncontrolled growth and the ability to spread to different parts of the body. The development of cancer is a complex multi-step process in which malignant cells gradually evolve as a result of a series of mutations.[1.1] The alterations in DNA caused by various carcinogens, such as chemicals, radiation and viruses, result in genetic instability and remove normal regulatory mechanisms for cell growth. Tumor progression thus involves the accumulation of multiple mutations, which lead to the formation of more rapidly growing and increasingly malignant cells within the tumor population. Eventually tumor progression leads to the development of metastatic cancers, which invade the circulation system and spread to distant body sites.[1.2]

The majority of somatic mutations, both natural and those induced by carcinogens, take place in non-coding DNA, and carcinogenesis thus will not occur. On the other hand, genes modified by certain mutations directly contribute to the development of cancer. Those modified genes are known as oncogenes. Oncogenes are the mutant versions of either proto-oncogenes, which are normal cellular genes whose functions are enhanced by mutations in carcinogenesis, or tumor suppressor genes, whose cellular functions are inactivated. When functioning normally, proto-oncogenes and tumor suppressor genes are responsible for controlling cell growth by up-regulating or down-regulating cell division. Therefore, oncogenes can cause cancer development by stimulating cell proliferation or disabling regular growth suppression mechanisms.[1.3]

Figure 1.1 shows examples of irregular cell division caused by the proto-oncogene *ras* and the tumor suppressor gene p53. RAS protein, encoded by the *ras* gene, is a regulatory GTP hydrolase that cycles between two conformations: the activated RAS-GTP and the inactivated RAS-GDP (Figure 1.1a). The binding of growth factors to cell-surface receptors leads to the phosphorylation of RAS-GDP. The resulting RAS-GTP initiates a cascade of phosphorylation reactions, which lead eventually to the expression of proteins that stimulate cell cycles. GTPase-activating proteins (GAPs) can deactivate RAS-GTP by increasing the rate of GTP hydrolysis that regenerates RAS-GDP. RAS oncogenes can be activated by point mutations. The activity of the mutant RAS protein is no longer stimulated by GAPs, thus the half-life of active RAS-GTP increases due to the suppressed GTP hydrolysis. Therefore, the downstream signal transfer is locked permanently in the "On" state thereby activating cell cycles without growth signals.[1.4] Another example of carcinogenesis caused by oncogenes is related to the tumor suppressor gene *TP53* (Figure 1.1b). In normal cells, the p53 protein is deactivated by forming a complex with another peptide. DNA damage induced by carcinogens such as UV irradiation, oncogenes and DNA-damaging drugs leads to the phosphorylation of p53. The phosphorylated p53 is then released from the complex and plays an important role in growth arrest, DNA repair and apoptosis. Mutant p53 proteins can not respond to DNA damage, thereby allowing duplication of damaged DNA during cell growth. Therefore, mutations accumulate and lead to carcinogenesis.[1.5]

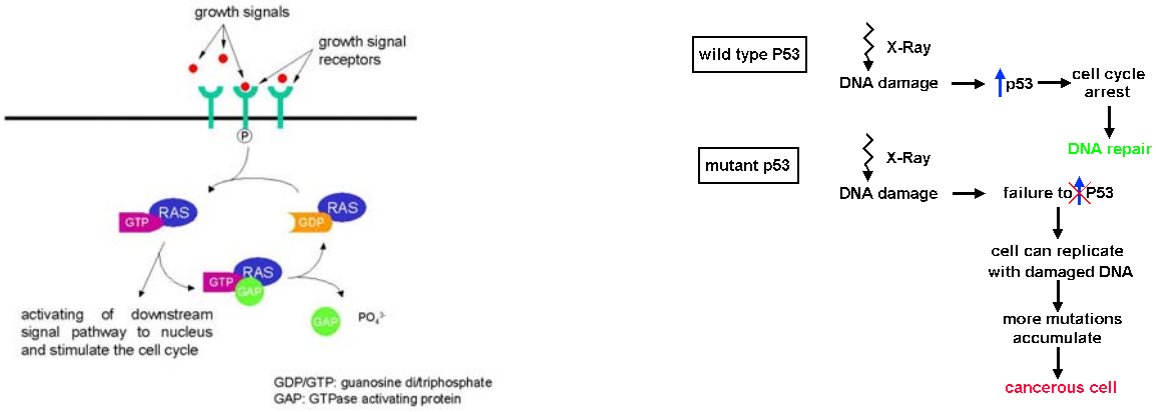

(a) (b)

Figure 1.1. Roles of oncogenes in carcinogenesis: (a) Proto-oncogene *ras* and (b) Tumor suppressor gene *TP53*.

1.2. Cancer Therapies

The goal of cancer treatment is to generate modalities that specifically target tumor cells, thereby avoiding unnecessary side effects to normal tissue. Surgical treatment, chemotherapy and radiotherapy are the most traditional treatments and remain the major clinical methods at present. With improved understanding of the specific biological processes involved in the proliferation of tumor cells, and technological advances that allow more refined manipulation of nucleic acids and proteins, a number of new strategies have been established. Such strategies include photodynamic therapy (PDT) and biological approaches such as immunotherapy and gene therapy.

1.2.1. Cancer Surgery

Cancer surgery refers to the surgical excision of tumor tissues and organs. Cancer surgery is most effective against benign tumors and early-stage malignant tumors wherein migration has not yet occurred. The major limitation of surgical treatments is that they are

effective only in the area of the operative field. However, when a tumor has become visible or palpable for possible surgical treatment, the neoplasm is usually already beyond the confines of the operative field, and the recurrence of the malignant neoplasm after the surgery is likely to happen.[1.6]

Cancer surgery has become a more effective method in treating cancer. The improvement mainly stems from more advanced surgical techniques that reduce operative death and the development of detection methods that help diagnose cancer at an early stage. Moreover, applying radiotherapy or chemotherapy as an adjunct therapy, usually closely following cancer surgery can avoid the recurrence of the tumor caused by inadequate excision.[1.7]

1.2.2. Radiotherapy

The radiation employed in cancer radiotherapy is characterized by sufficient energy to cause ionization of atoms in tissue and consequently to form highly reactive radicals that damage DNA in various ways. The radiation is either electromagnetic (x-rays, gamma rays) or corpuscular (electrons, protons, neutrons) in nature. The absorption of energy from ionizing radiation by cells and tissues is followed by radiochemical events that occur within 10^{-10} seconds. The presence of water during those radiochemical events results in highly reactive products such as hydrogen free radicals ($H^{\bullet}$) and hydroxyl free radicals ($OH^{\bullet}$), which have lifetimes (10^{-5} to 10^{-10} seconds) so short as to limit diffusion.[1.8] Therefore, radiochemical changes are localized and radiotherapy is relatively free of systemic cytotoxicity. This pattern of localization also causes radiotherapy to be more effective against cancers without metastases. Other than certain treatments of leukemia or lymphomas,

total-body irradiation is not common in the clinic because of accompanying damage to normal tissues at high dosage (Figure 1.2).[1.9] Therefore, similar to cancer surgery, radiotherapy is mostly used for regional control of tumors.

Radionuclides, such as radiolabeled metabolic agents and antibodies, are of great interest due to their potential tumor selectivity. Treatments involving radioactive antibodies are known as radioimmunotherapy and will be discussed in Chapter 2.1. Radiotherapy is also combined with chemotherapy and surgery to improve the effectiveness of the treatment.

Clinically, radiation can be applied by an external beam or by interstitial implantation. The latter method is also known as brachytherapy in which radiation sources are surgically implanted into a tumor and the immediately surrounding tissues. A fundamentally new, molecular approach to brachytherapy, which is capable of depositing radiation sources in both the primary tumor site and the metastatic sites by systemic treatment with distinct agents, will be discussed in Chapter 2.2. This thesis focuses on the development of agents for such a molecular brachytherapy.

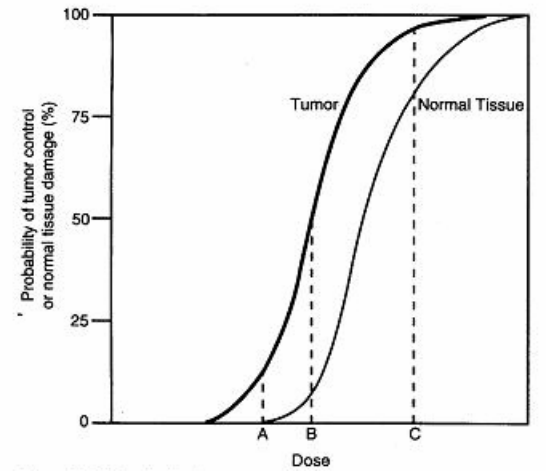

Figure 1.2. The relation between x-ray dose and outcome of radiotherapy.[1.9] Reproduced with permission.

1.2.3. Chemotherapy

Chemotherapy is a systemic therapy that involves the use of cytotoxic drugs and hormones to destroy tumor cells. Although side effects are a serious concern, systemic therapies are so far the only effective methods to treat metastatic cancer.

Cancer chemotherapy inhibits cancer via several potential mechanisms. The treatment may induce cell death, trap cell growth at a certain stage, or induce cell differentiation. For most chemotherapeutic agents, the target is a substance that is related to DNA synthesis or function. Consequently, these drugs exert their major toxic effects by inhibiting cells from undergoing DNA synthesis, including normal dividing cells. Figure 1.3 shows some common chemotherapy drugs and their purported anti-cancer mechanisms.[1.10]

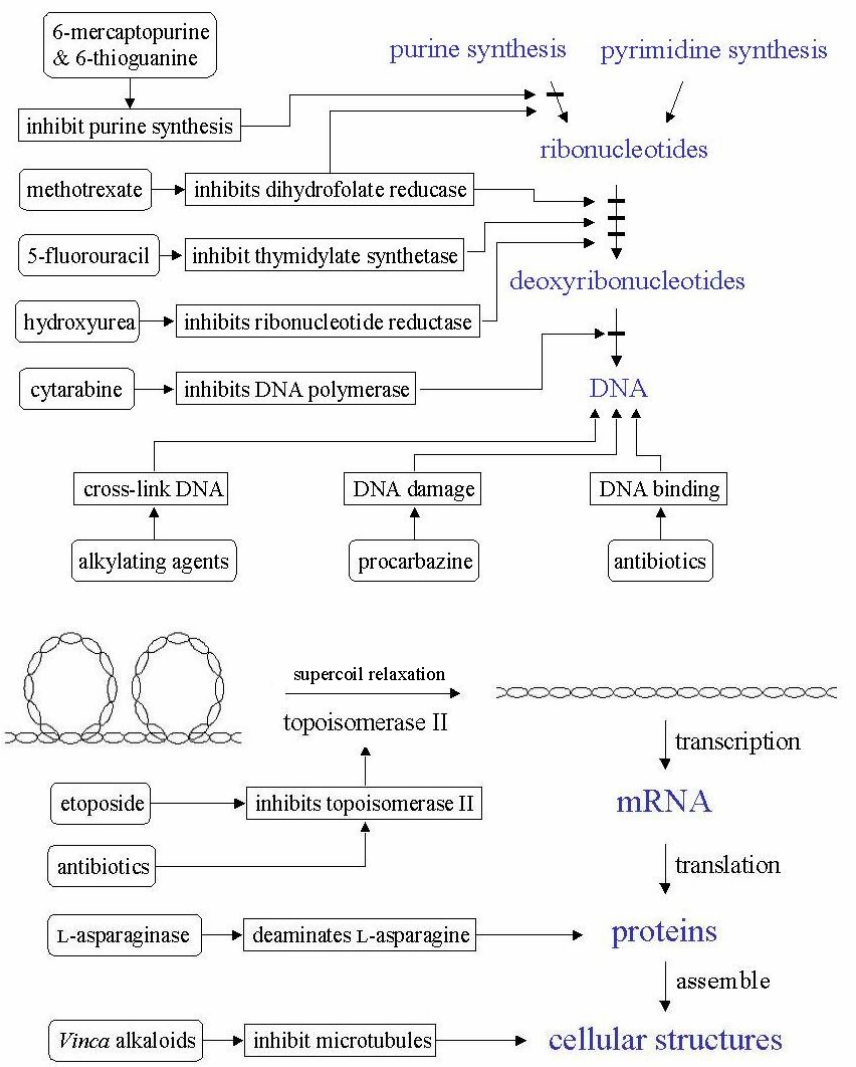

Figure 1.3. Common chemotherapeutic drugs and their targets. The round-cornered frames represent drugs; the rectangular frames represent the corresponding cellular effect. Adapted from ref. 1.10.

Selective toxicity of chemotherapy is possible because of the quantitative differences in the amounts of certain chemicals consumed or in the rates of various chemical reactions in cancer cells versus normal cells. For example, cancer cells consume large amounts of glucose as a source of energy to permit the exaggerated utilization of amino acids and nucleosides in gene expression or DNA synthesis. On the other hand, since the differences are quantitative, it is unavoidable that there is at least some degree of injury to normal tissues

during treatment by chemotherapeutic agents. In fact, many regenerating normal tissues, such as bone marrow elements and hair follicles, also have a high proliferative capacity that is comparable to that of malignant cells. Such normal tissues are comparable to tumors in bearing the same impact of the toxic effects of anti-cancer drugs. Considering that the safety margin of the treatment is often very narrow, the success of chemotherapy is not simply a matter of excessive toxicity for rapidly proliferating neoplasm.[1.6]

The clinical usefulness of a chemotherapeutic agent may be severely limited by the emergence of a line of malignant cells resistant to that drug. There are three different types of drug resistance: (1) apparent drug resistance is related to the clinic treatment procedure; (2) intrinsic resistance arises from pharmacological and kinetic issues; (3) acquired resistance is the result of biochemical and genetic events.[1.11] The molecular mechanisms underlying intrinsic and acquired resistance include decreased drug uptake, increased drug extrusion, competition with natural substrates, etc. (Figure 1.4a).[1.12] Tetrahydrofolate (FH_4) is a key ingredient in the de novo biosynthesis of thymidine nucleotide and thus is more abundant in cancer cells with active DNA duplication. Figure 1.4b shows that methotrexate (MTX) blocks FH_4 production by inhibiting dihydrofolate reductase (DHFR), which reduces dihydrofolate (FH_2) to FH_4. Six distinct mechanisms are known to result in MTX resistance in cancer: (1) decreased uptake of MTX; (2) decreased polyglutamylation of MTX and, as a result, diminished affinity to DHFR and abbreviated duration of retention in cells; (3) production of an altered DHFR that has lower affinity for MTX; (4) increased production of normal DHFR; (5) a decreased level of thymidylate synthase and consequent lowered demand for FH_4; (6) increased nucleoside salvage that suppresses the de novo synthesis of dTMP.[1.11]

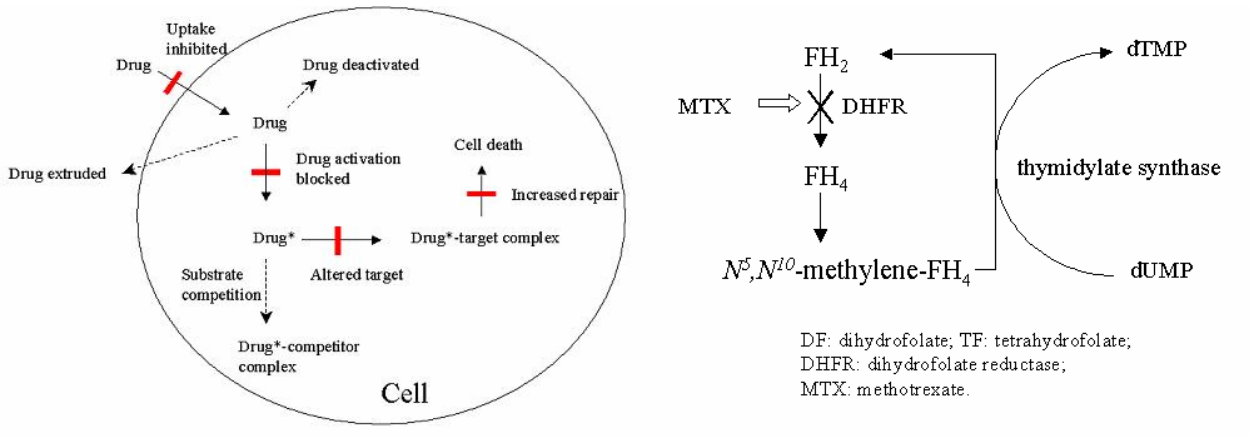

Figure 1.4. Drug resistance in chemotherapy: (a) Common mechanisms of drug resistance. The solid arrows represent the metabolic pathways that lead to cytotoxicity; the bars on arrows represent mechanisms that block those pathways; the dashed arrows represent the metabolic pathways that consume the drug without causing cell death. (b) Mechanism of action of methotrexate (MTX).

Single drug resistance can be overcome by increased dosage or by use of a combination of different drugs. In some cases, resistance to one drug may confer resistance to other, biochemically distinct drugs, to which tumor cells have not been exposed. This phenomenon is known as multidrug resistance (MDR), which may involve overexpression of membrane protein P glycoprotein (Pgp), or alteration of topoisomerase II or other enzymes with detoxification or DNA repair functions.[1.6] Pgp is an example of a family of molecular pump proteins with each such pump having the surprising ability to pump several different chemotherapy agents out of the cell, even if these agents have radically different chemical structures.

1.2.4. Photodynamic Therapy

Compared to surgery, radiotherapy and chemotherapy, photodynamic therapy (PDT) is a relatively new cancer treatment. PDT involves the localization of a light-absorbing drug

(photosensitizer) in the target tissue followed by illumination at an appropriate wavelength. Cytotoxic agents generated upon illumination trigger a cascade of biochemical responses that inactivate cancer cells either directly or through the induction of vascular stasis. One of the key mechanisms of PDT is illustrated in Figure 1.5. Upon illumination, the photosensitizer is excited from the ground state to the first excited singlet state, followed by intersystem crossing to the triplet state. The longer lifetime of the triplet state enables the excited photosensitizer to interact with ground state molecular oxygen ($^3O_2$) to generate excited singlet oxygen ($^1O_2$), which is believed to be the primary cytotoxic agent responsible for the biological effects in PDT.[1.13]

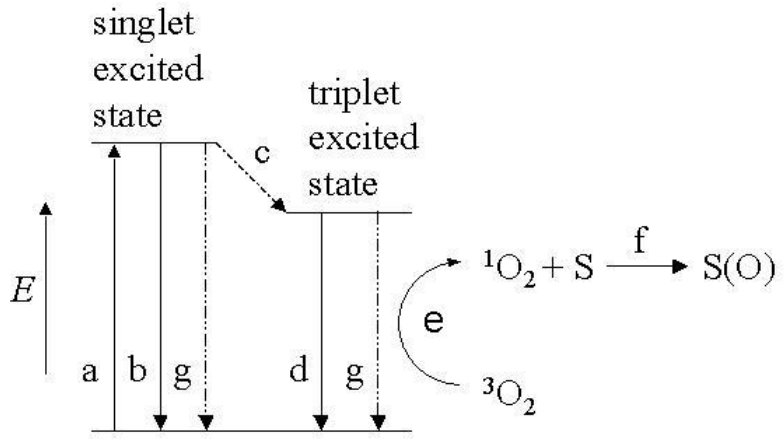

Figure 1.5. Mechanism of action in PDT. (a) excitation; (b) fluorescence; (c) intersystem crossing; (d) phosphorescence; (e) non-radiation transfer of energy to singlet oxygen; (f) substrate oxidation by singlet oxygen; (g) internal conversion.

The major feature of PDT is that cytotoxicity is generated by combining three nontoxic components: the photosensitizer, the activating light and molecular oxygen. The selectivity of the treatment is typically achieved by preferential uptake of the photosensitizer by the tumor tissue and the ability to confine activation of the photosensitizer to the tumor site by restricting the illumination to a specific region. Therefore, although photosensitizers

can be administered to patients systemically like chemotherapeutic drugs, PDT is not a systemic treatment in current clinical applications.[1.14] Hematoporphyrin-type photosensitizers have been found to concentrate around tumor blood vessels. The reason for such accumulation is not clear. One possible explanation concerns the inability of immature tumor blood vessels and lymphatics to clear large aggregates of the lipophilic photosensitizer.[1.15]

Most of the photosensitizers available to date absorb light in the visible region of the spectrum. The use of photosensitizers that absorb visible light has two major disadvantages. The first one is normal-tissue toxicity triggered by sunlight, which the photosensitizers also absorb, during or after the treatment. The second advantage is that the activating light can not penetrate deeply into soft tissue. Therefore, PDT is mostly used to treat superficial tumors such as skin cancers.[1.16]

An ideal photosensitizer must have little retention in normal tissues to allow total-body illumination, and is activated by light outside the visible region to avoid side effects by sunlight. Therefore, the current research for the new generation of photosensitizers focuses on improved harmacokinetics, tumor selectivity and photochemical properties. With such improved features, PDT has the potential to become a systemic method for treating disseminated cancers.

1.2.5. Immunotherapy and Gene Therapy

Although still at an early stage, cancer biotherapy probably attracts more interest than any other therapeutic modality because biological approaches may offer more physiologic and systemic treatments that also are less toxic. Instead of killing the tumor directly,

biotherapy focuses on the alteration of the host-tumor relationship in order to regain control of the growth of cancer cells. Immunotherapy and gene therapy are the two major approaches in this category.

The direct proof of the relationship between cancer and the immune system is that patients with immunodeficiency or immunosuppression are much more likely to develop cancer. The uncontrolled growth of cancer cells indicates that the disease has escaped the monitoring of the immune system despite detectable immune responses.[1.17] Cancer immunotherapy focuses on restoring or enhancing the functions of the immune system so that tumors can be eliminated by the patient's own biological mechanisms. The therapeutic methods of immunotherapy include: (1) stimulation of the intrinsic immune system of the host; (2) replenishment of a depressed host immunologic response; (3) transfer of effector cells to the host; and (4) up-regulation of tumor-associated antigens on the surface of tumor cells.[1.18]

Cancer gene therapy was at first considered a type of treatment to restore functions of normal genes to cancer cells. However, many applications to date do not have the expected direct therapeutic functions. Instead, more effort has been focused on using recombinant DNA techniques to improve existing therapies. The current approaches of gene therapy include (1) the use of recombinant vaccines as immunotherapeutics; (2) the protection of bone marrow during chemotherapy by transducing a drug-resistance gene into marrow stem cells; (3) gene replacement and oncogene inactivation; and (4) suicide gene therapy (see Chapter 2.1).[1.19] DNA transport, vector targeting, and gene integration/expression are the critical areas for future development in gene therapy.[1.20]

1.2.6. Summary

Fundamental understanding of the molecular genetics of cancer and the mechanisms underlying carcinogenesis is expanding rapidly and consequently allows the design and testing of novel cancer treatments and prevention strategies. Many new methods integrate techniques from multiple fields (immunology, genetics, radiology, etc.) to overcome the disadvantages of each single strategy. However, surgery, radiotherapy and chemotherapy are still the most prevalent methods in treating cancer patients in the clinic. Moreover, a large number of successful cases of cancer treatment in recent years are attributable to the improvement of early-detection techniques. If those cases are not taken into consideration, the mortality rates for most cancers have not changed significantly in the past 30 years.[1.21] The side effects of systemic treatments still limit the applications of many newly discovered anti-cancer agents. Thus, the development of targeted, systemic treatments for disseminated cancers is of great research interest. The essence of this thesis is to design and synthesize distinct agents for a targeted molecular brachytherapy, a therapeutic approach that has remarkable advantages over other existing therapies.

REFERENCES

(1.1) Klein, G. *Adv. In Cancer Res.* **1998**, *72*, 1–23.

(1.2) Cooper, G. M. *The Cancer Book: a guide to understanding the causes, prevention, and treatment of cancer*; Jones and Bartlett Publishers: Boston, MA, 1993; Vol 1, pp 15–25.

(1.3) Ibid., pp 82–95.

(1.4) (a) Bos, J. L. *Cancer Res.* **1989**, *49*, 4682–4689. (b) Reuter, C.; Morgan, M.;

Bergmann, L. *Blood* **2000**, *96*, 1655–1669.

(1.5) Vogelstein, B.; Lane, D.; Levine, A. J. *Nature* **2000**, *408*, 307–310.

(1.6) Cooper, G. M. *The Cancer Book: a guide to understanding the causes, prevention, and treatment of cancer*; Jones and Bartlett Publishers: Boston, MA, 1993; Vol 1, pp 127–144.

(1.7) (a) Benjamin, D. J. *Med. Hypotheses* **1993**, *40*, 129–138. (b) Mintzer, D. *Am. J. Med.* **1999**, *106*, 81–89.

(1.8) Steel, G. G. In *Oxford Textbook of Oncology*; Peckham, M.; Pinedo, H. M.; Veronesi, U., Eds.; Oxford University Press Inc.: New York, NY, 1995; Vol. 1, pp 668–680.

(1.9) Withers H. R. *Lancet* **1992**, *339*, 156–159.

(1.10) *Cancer chemotherapy and biotherapy: principles and practice*; Chabner, B. A.; Longo, D. L., Eds; Lippincott Williams & Wilkins: Philadelphia, PA, 2001; 2nd edition.

(1.11) Borst, P.; Pinedo, H. M. In *Oxford Textbook of Oncology*; Peckham, M.; Pinedo, H. M.; Veronesi, U., Eds.; Oxford University Press Inc.: New York, NY, 1995; Vol. 1, pp 586–601.

(1.12) (a) Takacova, M.; Imrichova, D.; Cernicka J.; Gbelska, Y.; Subik, J. *Curr. Genet.* **2004**, *45*, 1–8. (b) Banerjee, D.; Mayer-Kuckuk, P.; Capiaux, G.; Budak-Alpdogan, T.; Gorlick, R.; Bertino, J. R. *Biochim. Biophys. Acta* **2002**, *1587*, 164–173.

(1.13) (a) Macdonald, I. J.; Dougherty, T. J. *J. Porphyrins Phthalocyanines* **2001**, *5*, 105–129. (b) Sharman, W. M.; Allen, C. M.; van Lier, J. E. *Drug Discovery Today* **1999**, *4*, 507–517.

(1.14) Capella M. A. M.; Capella L.S. *J. Biomed. Sci.* **2003**, *10*, 361–366.

(1.15) Kessel, D.; Chou, T. H. *Cancer Res.* **1983**, *43*, 1994–1999.

(1.16) Sternberg, E. D.; Dolphin, D.; Brückner, C. *Tetrahedron* **1998**, *54*, 4151–4202.

(1.17) Baldwin, R. W.; Klein, G. *Cancer Res.* **1982**, *42*, 1608–1609.

(1.18) (a) Davis, I. D.; Jefford, M.; Parente, P.; Cebon, J. *J. Leuko. Biol.* **2003**, *73*, 3–29. (b) Jaffee, E. M. *Ann. NY Acad. Sci.* **1999**, *886*, 67–72. (c) Pandey, M.; Mathew, A.; Nair, M. K. *Eur. J. Surg. Oncol.* **1999**, *25*, 209–214. (d) Armstrong, A. C.; Hawkins, R. E. *Br. J. Radiol.* **2001**, *74*, 991–1002.

(1.19) (a) Roth, J. A.; Cristiano, R. J. *J. Natl. Cancer Inst.* **1997**, *89*, 1712–1714. (b) Wadhwa, P. D.; Zielske, S. P.; Roth, J. C.; Ballas, C. B.; Bowman, J. E.; Gerson, S. L. *Annu. Rev. Med.* **2002**, *53*, 437–452.

(1.20) (a) Brunner, S.; Sauer, T.; Carotta, S.; Cotton, M.; Saltik, M.; Wanger, E. *Gene Ther*. **2000**, *7*, 401–407. (b) Vacik, J.; Dean, B. S.; Zimmer, W. E.; Dean, D. A. *Gene Ther*. **1999**, *6*, 1006–1014. (c) Weichselbaum, R. R.; Kufe, D. W.; Advani, S. J.; Roizman, B. *Acta Oncol*. **2001**, *40*, 735–738.

(1.21) Bailar, J. C.; Gornik, H. L. *N. Engl. J. Med.* **1997**, *22*, 1569–1574.

Chapter 2

A New Targeted Method to Treat Disseminated Solid Tumors

2.1. Background of Targeted Cancer Therapies

A major challenge in the treatment of cancer is to selectively destroy metastatic tumor cells by the use of systemic agents. The occurrence of unwanted, adverse side effects typically limits the maximum dose of the anti-cancer agent that can be administered. In principle, targeted cancer therapies can effectively reduce the systemic cytotoxicity by selectively delivering the therapeutic agents to the tumor location. The success of targeted cancer therapies depends on the viability of suitable targeting agents. An ideal targeting agent would exhibit the following features: (1) provide complete specificity for tumor versus non-tumor; (2) reach 100% of the target population; and (3) display negligible or no toxicity to non-cancer cells. Although the availability of such an ideal targeting agent seems impossible, new technologies and methods have been developed to improve the specificity of cancer treatments.

2.1.1. Targeting Strategies with Monoclonal Antibodies

A monoclonal antibody (mAb) is produced by a single clone of B lymphocytes or a single hybridoma cell line, which is formed by the fusion of a lymphocyte cell with a myeloma cell. The utility of a mAb lies in its specificity in recognizing a single pattern of molecular conformation in the stimulating epitope, such as an antigen. Monoclonal antibodies raised against tumor antigens can be attached to a variety of diagnostic or therapeutic agents to form conjugates for use in potential targeted applications.[2.1]

2.1.1.1. Radioimmunotherapy. One of the major applications of mAbs in cancer therapy is radioimmunotherapy (RIT), which employs radiolabelled mAbs to selectively deliver radiation to the tumor. However, the accumulation of mAbs in tumor tissues is a slow procedure; thus, the radioactive mAb while in circulation could cause extensive systemic damage to the patient. Therefore, an improved version of RIT called "pretargeted" RIT has been developed. In "pretargeted" RIT, the tumor is pretargeted with an antibody construct that has affinity for the tumor-associated antigen on one side and for a radiolabeled molecule on the other side. An example of such an antibody construct is a mAb-streptavidin conjugate. After the conjugates not bound to the antigen are cleared from the circulation, a radiolabeled biotin is introduced to specifically bind to the streptavidin on the pretargeted cancer cells. Therefore, systemic damage is diminished by using a nontoxic agent for the slow targeting step.[2.2]

2.1.1.2. Antibody-Directed Enzyme-Prodrug Therapy. Enzyme-prodrug therapy can be described as targeted chemotherapy that involves site-specific activation of chemotherapeutic agents. The selectivity of enzyme-prodrug therapy is achieved by two key components: a prodrug having low toxicity, which is a precursor of an active drug, and a tumor targeting agent conjugated with an enzyme capable of converting the prodrug to the cytotoxic drug. Since neither component alone is very toxic, they can both be administered systemically in a sequential manner. Toxicity will not be produced until the two components interact with each other and generate the active drug. Therefore, in the treatment, the enzyme-containing targeting agent, which has good tumor specificity, is introduced to the

patient first. A time interval is required to allow completion of the targeting step well as to ensure that non-binding targeting agents are cleared from the circulation. After the targeting agent is localized within tumor tissues, the prodrug is administered. Prodrugs do not necessarily need to possess tumor targeting ability given that only those molecules that reach the targeting agent can be converted to active drug molecules. The enzyme-prodrug combination has the potential to create much higher concentrations of the active, cytotoxic drug within the microenvironment of the tumor than can be achieved by systemic administration of the active drug itself. Moreover, the cytotoxic drug molecules generated at the targeted locations are able to diffuse and kill adjacent cells that are not targeted. This "bystander effect" obviates targeting all tumor cells, which is an unrealistic goal due to the typical cellular heterogeneity of tumors. The amplification effect of the enzyme allows a small amount of enzyme-bound targeting agent to generate a large number of drug molecules, thereby enhancing the therapeutic effect of the treatment.

The selectivity of drug delivery in enzyme-prodrug strategies depends on the specificity of the targeting process. Antibody-directed enzyme-prodrug therapy (ADEPT) is an enzyme-prodrug based therapy using a mAb-enzyme conjugate as the targeting agent (Figure 2.1).[2.3]

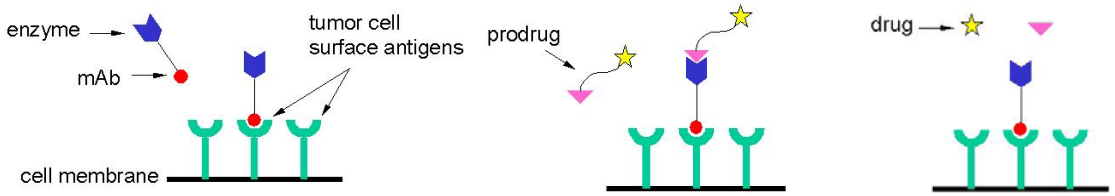

Figure 2.1. Schematic outline of antibody-directed enzyme prodrug therapy (ADEPT). (1) Antibodies conjugated with enzymes bind to tumor antigens. (2) Prodrugs reach the tumor where the enzyme is localized. (3) The enzyme cleaves the masking group on the prodrug to release the drug.

2.1.1.3. Problems with the mAb-Targeting Strategy. There is considerable evidence that the immune system responds to the antigens on tumor cells; however, the evidence for the existence of unique, tumor-specific antigens is circumstantial. Despite all the technical improvements in terms of mAb construction and screening and purification, clinical results so far have been relatively disappointing. Three problems that rationalize most of the unsuccessful mAb applications are as follows: (1) relatively low tumor affinity of the mAb; (2) nearly all antibodies also bind to some components of normal tissues; and (3) the large size of immunoglobulin molecules precludes penetrating the poorly vascularized tumor bed. Research efforts are now devoted to developing genetically engineered mAbs and fragments thereof to improve the therapeutic effects.[2.4]

2.1.2. Other Targeting Strategies

A wide variety of properties considered to be unique to tumors have also been exploited for cancer targeting, such as abnormal cell cycle and apoptosis, migration and metastasis, and specific transcriptional signals. Some examples of targeted therapies based on such tumor properties are described below.

It has been discovered that macromolecules can accumulate at the tumor site due to the enhanced permeability and retention (EPR) effect, which is attributed to the poorly organized tumor vasculature and the lack of lymphatic drainage inside tumor tissues. Therapeutic macromolecules such as conjugates of chemotherapeutic drugs and polymers are constructed for selective delivery to tumor sites.[2.5] The enzyme-prodrug therapy based on the targeting mechanism of macromolecules is called polymer-directed enzyme-prodrug therapy

(PDEPT) or macromolecule-directed enzyme-prodrug therapy (MDEPT). In PDEPT, both the targeting conjugate and the prodrug are constructed upon macromolecules and can preferentially accumulate at the tumor site, therefore enhancing the selectivity of the treatment.[2.6]

Another cancer therapy based on the enzyme-prodrug system is virus-directed enzyme-prodrug therapy (VDEPT), also known as gene-directed enzyme-prodrug therapy (GDEPT), genetic prodrug activation therapy (GPAT) or suicide gene therapy. VDEPT entails a combination of gene therapy and chemotherapy. Instead of targeting the enzyme as a protein to the surface of tumor cells, VDEPT introduces the DNA sequence that encodes the enzyme, whereupon the prodrug-to-drug conversion occurs inside tumor cells after the enzyme is produced. The targeting mechanism of VDEPT accrues by viral vectors preferentially attacking tumor cells[2.7] or by the tissue-specific transcription sequence controlling the expression of the enzyme[2.8] (Figure 2.2).

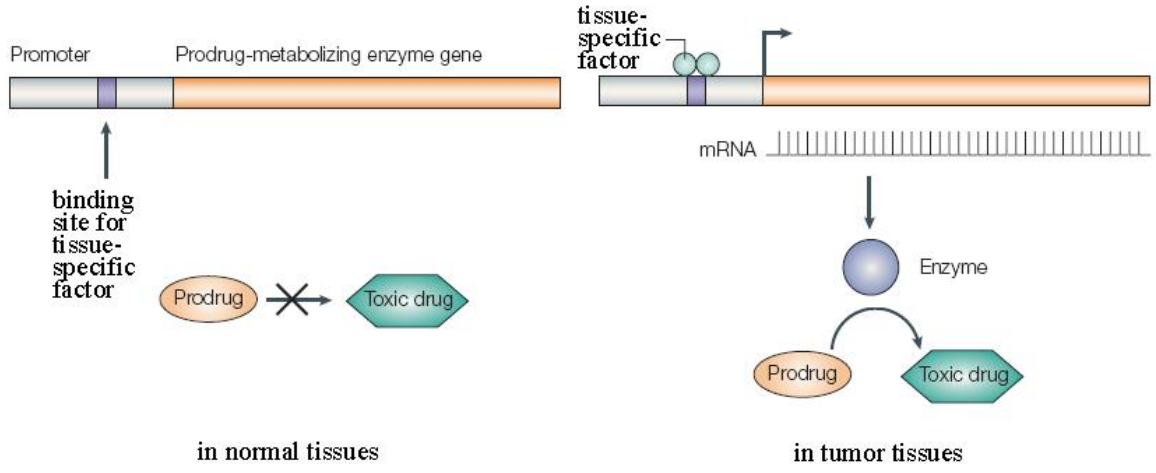

Figure 2.2. Schematic outline of virus-directed enzyme prodrug therapy (VDEPT). Adapted from ref. 2.8.

Solid tumors often contain regions at very low oxygen concentration (hypoxia), and

cells in the hypoxic regions are often resistant to both radiotherapy and chemotherapy. Although such resistance thwarts radiotherapy and chemotherapy, the existence of hypoxia also provides an opportunity for tumor-selective therapies such as hypoxia-prodrug therapy and hypoxia-specific gene therapy. Certain prodrugs can be activated in hypoxic regions by reduction reactions that can not occur in normal tissues where the oxygen concentration is much higher. Hypoxia-specific gene therapy is similar to VDEPT except that the transcription of the gene for the enzyme is controlled by factors that are only present in hypoxic cells.[2.9]

2.1.3. Limitations in the Current Targeted Cancer Therapies

Despite tremendous efforts in pursuing targeted treatments for cancer, the various targeted methods developed to date have generally not been successful for treating disseminated cancers. There appear to be three universal obstacles that impede further progress in cancer therapy: (1) The current therapeutic agents (e.g., drugs, radioactive compounds, vaccines) only target a subset of cancer cells, whereupon the remaining cell types survive because of the intrinsic heterogeneity of cancer; (2) It was hoped that the insufficient killing of cancer cells by a single agent could be circumvented by using a "cocktail" of multiple chemotherapeutic drugs each having chemical structure quite different from the others and each blocking a different biochemical pathway so that mutations conferring resistance to one drug could be unlikely to confer to any other drug in the "cocktail". Surprisingly, this was not very helpful in significantly prolonging the survival of cancer patients; (3) The agents also kill normal cells because their selectivity is not exclusive to cancer cells; and (4) The agents are not potent enough to kill resistant cancer cells or to

overcome the ability of cancer cells to adapt to the agents and become resistant. These obstacles stem from the inherent nature of solid tumors (i.e., heterogeneity), the cell-killing mechanisms of anti-cancer agents, and the current available targeting mechanisms. In order to gain control over cancer progression, an effective cure must overcome those obstacles.

2.2. Targeted Molecular Brachytherapy

2.2.1. General Information

In 1998, S. Rose proposed a fundamentally new strategy to treat cancer.[2.10] The proposed approach mimics the treatment of thyroid cancer with radioactive iodide. Compared to other types of cancer, thyroid cancer can often be successfully treated. The thyroid naturally absorbs iodide from body fluids to form a colloid. Therefore, the iodide concentration in the thyroid is much higher than in other parts of the body. When a radioactive iodide therapeutic agent is administered, most radiation damage is localized inside the thyroid. The systemic damage is insignificant because of the natural distribution pattern of iodide. Of crucial importance, the β-particles emitted from ^{131}I in each cell have an average range of approximately 50-cancer-cell diameters, reaching a "micro-region" containing approximately half a million cancer cells. Conversely, each cancer cell is being irradiated by β-particles from half-a-million of its neighbors. This circumvents the problem of the heterogeneity of cancer cells because those cancer cells that do not accumulate radioactivity are nevertheless killed by radiation from their neighbors.

Rose's approach is designed to mimic the process for thyroid cancer treatment, whereby radioactive material is accumulated in the tumor and causes micro-regional destruction via a multi-step process. One name for this procedure is "selectively targeted

amplified radiotherapy" (S.T.A.R.), which indicates the following features: (1) a combination of two "imperfect" targeting steps that causes localization in the most sensitive cancer cells; (2) generation of strong radioactivity to destroy every cell in a given micro-region; and (3) auto-catalyzed localization of radiotherapy sources in the tumor. Another name for this approach is "targeted molecular brachytherapy" to indicate the ability to selectively deposit radiation sources in tumor sites. Regardless, the net result is a targeted, auto-catalytic, micro-regional destruction of cancer cells.

The cornerstone of the S.T.A.R. method is a novel class of soluble chemical compounds. The compounds can be administered intravenously, circulate throughout body fluids, and be converted enzymatically into an insoluble material upon reaching targeted sites. Such compounds are called "soluble precipitable reagents" (SPR) to describe their ability to be converted from a soluble to an insoluble material. The insoluble material is called "platform" to suggest both a solid nature and the ability to bind various agents. The SPR compounds enable a four-step process to be devised whereby massive quantities of radionuclides are selectively delivered and retained in tumor tissue.

2.2.2. The Four-Step Procedure of the S.T.A.R. Method

The four-step procedure of the S.T.A.R. method is outlined as following. In the first step, a Step-1 SPR bearing a cancer targeting agent (CTA) and a binding handle is administered (Figure 2.3a). The CTA targets certain endocytosing receptors that are overexpressed in cancer cells. Due to up-regulated growth, tumor cells uptake a large variety of agents at higher levels than normal cells. Such agents potentially can be used as the CTA in the Step-1 SPR (see Chapter 3.1). The binding of the CTA to the receptors activates

endocytosis that transports the Step-1 SPR into the lysosome. The soluble Step-1 SPR is then converted into insoluble platform by lysosomal enzymes. The platform is neither digestible nor toxic and is retained and accumulated in cells. The platform contains binding handles that function as docking sites in a later step (Figure 2.3b). As mentioned in previous sections, the specificity of any current targeting mechanism is not perfect. Therefore, the targeting by the CTA on the Step-1 SPR also leads to the uptake of SPR by some normal cells, where platform also is formed.

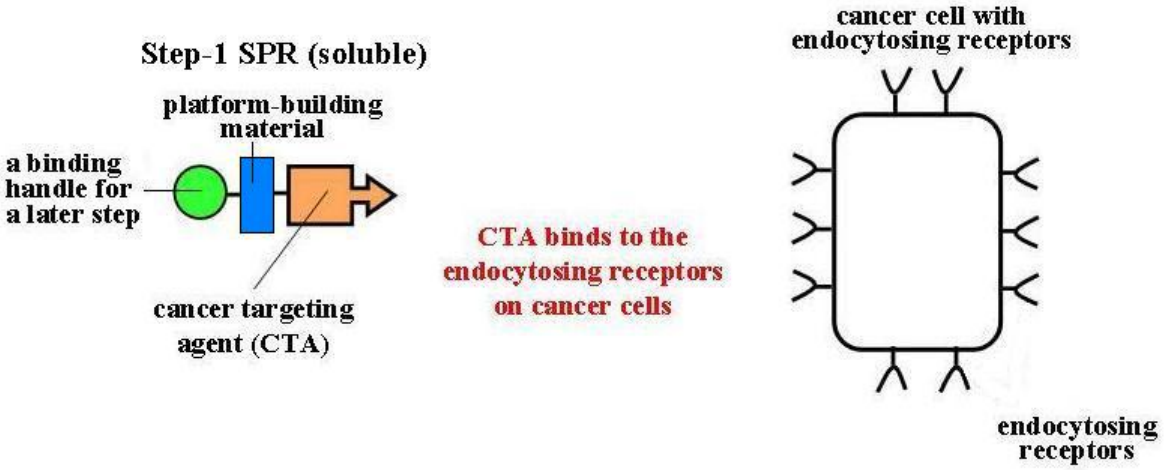

(a)

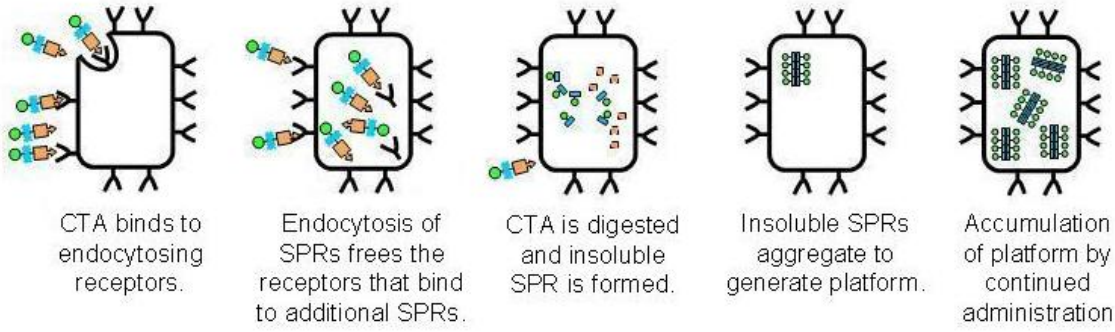

(b)

Figure 2.3. Step 1 of the S.T.A.R. method: (a) A Step-1 SPR and a cancer cell with endocytosing receptors and (b) Step-by-step: endocytosis of the Step-1 SPR and the formation and accumulation of platform. Adapted from ref. 2.11.

In step 2, a very low dose of the Step-2 agent, which typically is an approved anti-cancer drug, is administered to break open cancer cells and release the platform (Figure 2.4). The rationale behind step 2 is that the composition of cancer cells is highly heterogeneous, including super-resistant cells that are extremely hard to kill as well as super-sensitive cells that will be destroyed with a low dose of a toxic agent (Figure 2.5). In normal chemotherapy, a high dosage is routinely used in attempting to destroy all cancer cells including the super-resistant ones, and, as a result, causes serious systemic damage. This can be effective in leukemias, however seldom succeeds with solid cancer. In the S.T.A.R. approach, however, the purpose of the anti-cancer drug is to kill a subset of cancer cells (and release the platform stored within) while at the same time not damaging normal cells. Therefore, the dosage of the anti-cancer drug is set at a level so that a fraction of cancer cells will be destroyed while all normal cells will survive (or at least the damage to normal cells will be much less than in conventional chemotherapy). The resulting cell lysis releases the platform to the extracellular fluid (ECF). The platform is insoluble and is retained in the tumor much akin to the deposition of the material to form a tattoo. In combination with the specificity achieved in step 1, the chance for a normal cell to both accumulate platform and be destroyed in step 2 is extremely small. Thus, the second step of the S.T.A.R. method is a specificity-enhancing step, whereby insoluble platform is selectively released to the ECF.

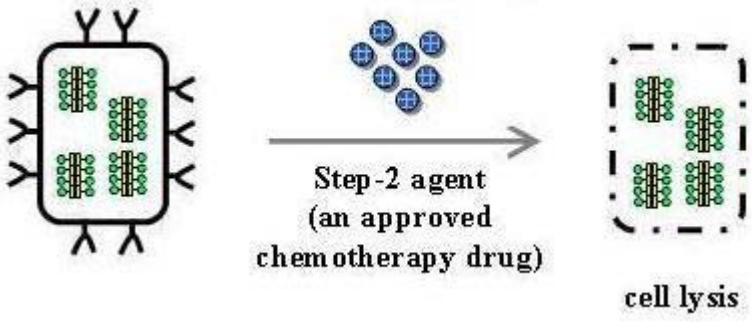

Figure 2.4. Step 2 of the S.T.A.R. method: Treatment with the Step-2 agent, an approved chemotherapy drug (e.g., doxorubicin), at a very low dose breaks open a fraction of the cancer cells and releases the platform to the extracellular area. Adapted from ref. 2.11.

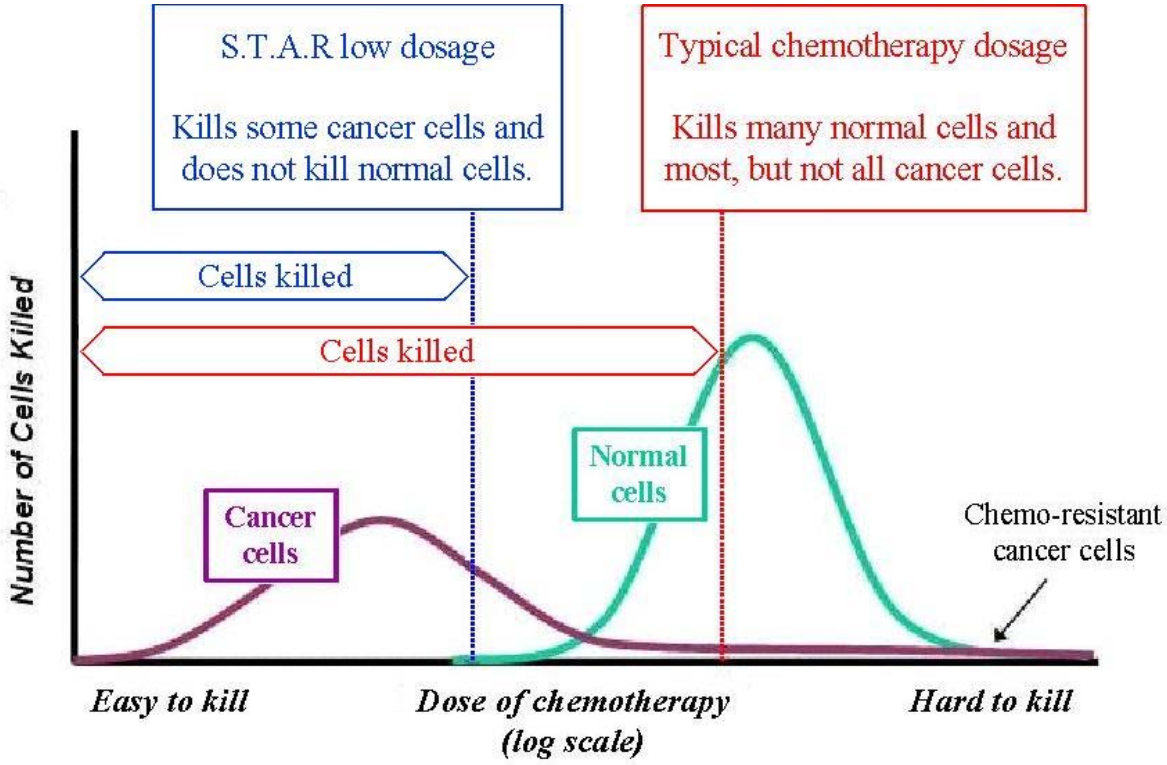

Figure 2.5. The effect of drug dosage on cell killing. Adapted from ref. 2.11.

The purpose of step 3 is to covalently attach an enzyme, which is not naturally present or accessible in normal tissues, to the platform released in step 2. The Step-3 agent consists of an enzyme and a binding moiety that specifically attaches to the handles on the platform (Figure 2.6a). The interaction between the binding moiety and the handle is both

specific and covalent, and the Step-3 agent is cell-impermeable (Figure 2.6b) so that it cannot bind to the platforms present inside of cells in normal tissues. Therefore, the Step-3 agent should not be retained in other parts of the body, nor bind to the platform inside surviving cells, whether they be tumor or normal cells. After step 3, the platform deposited in the ECF inside tumor tissues is armed with an enzyme with specificity that is absent anywhere else inside the patient. The choice of the enzyme for the Step-3 agent will be discussed in detail in Chapter 3.1.

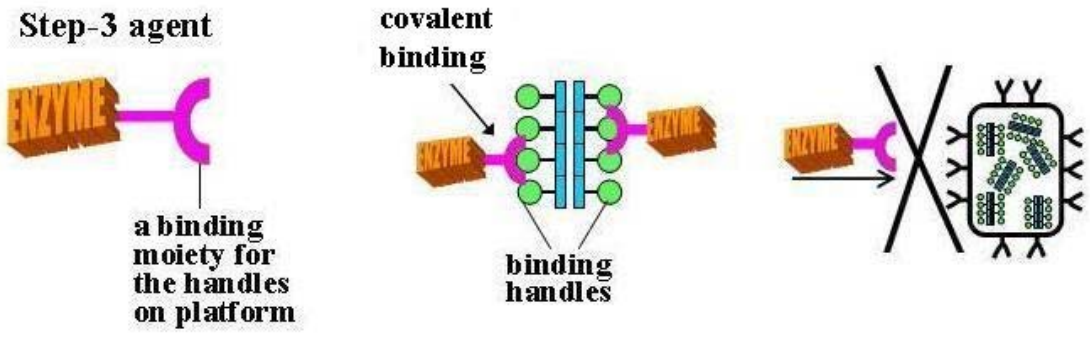

(a) (b)

Figure 2.6. Step 3 of the S.T.A.R. method: (a) the Step-3 agent; (b) the functionality of the Step-3 agent. Adapted from ref. 2.11.

The last step of the S.T.A.R. method is to localize a radiotherapy source inside the tumor. After any unbound Step-3 agent is cleared from the body, the Step-4 Agent, which is a radiolabeled SPR, is introduced. Unlike the Step-1 SPR, the Step-4 SPR is not equipped with the CTA or a binding handle. Instead, the Step-4 SPR carries enzymatically cleavable groups that will not be cleaved in normal tissues but will be cleaved by the enzyme docked on the platform, converting the soluble Step-4 SPR to the insoluble form. The radiolabeled SPRs are designed to be rapidly excreted so that those which do not reach the enzyme-bound

platform will not be retained in the body and thus will not produce serious systemic radiation toxicity (Figure 2.7). This autocatalytic deposition procedure can generate a large amount of radioactive precipitate from a small amount of platform. The resulting radioactive precipitate creates a radiation field that reaches hundreds of thousands of cancer cells in a surrounding micro-region whether those other cancer cells concentrate radiation or not (Figure 2.8). The micro-regional destruction overcomes the cellular heterogeneity of the solid tumor. Unlike chemotherapy, which kills only the sensitive cells, the S.T.A.R. mehod can kill all of the cancer cells regardless of how they may have mutated. Multiple such micro-regions overlap to form a large area of radiation that has the potential to kill all cancer cells at given sites in the body.

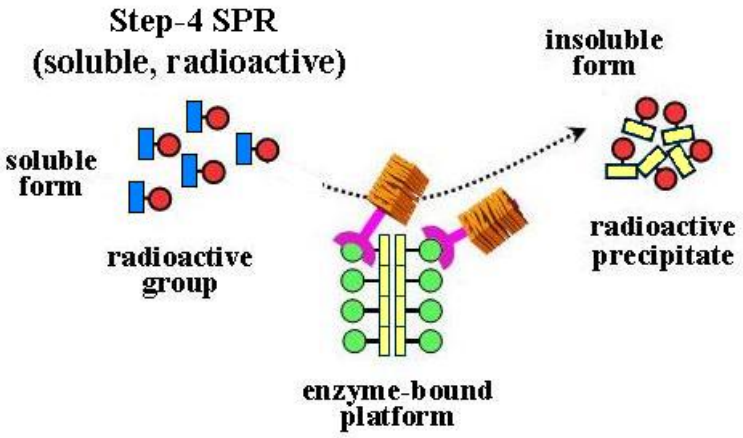

Figure 2.7. Step 4 of the S.T.A.R. method: the formation of radioactive precipitate by the soluble-to-insoluble conversion of the Step-4 SPR. Adapted from ref. 2.11.

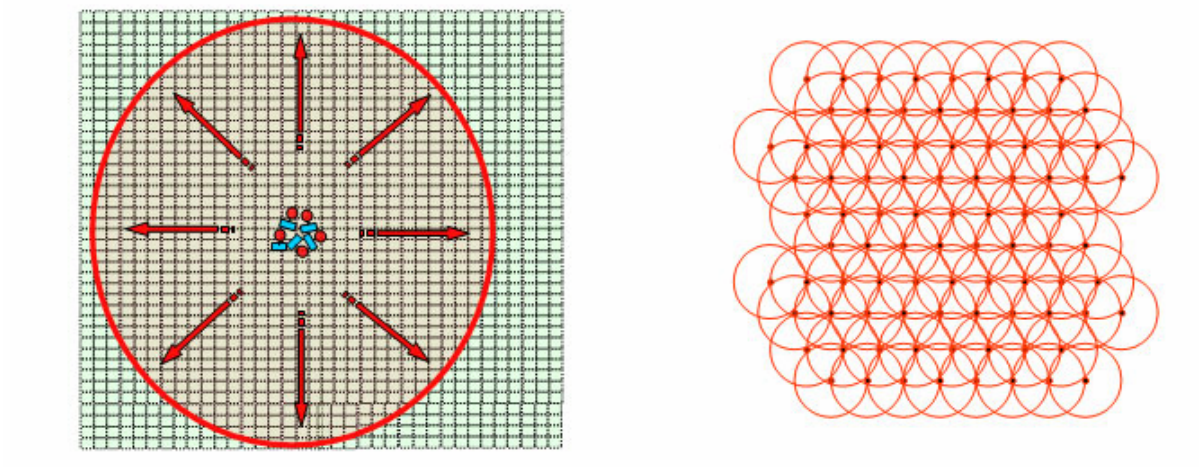

Figure 2.8. Tumor destruction in the S.T.A.R. method: (a) The radiation emitted by each radioactive precipitate can reach hundreds of thousands of surrounding cancer cells (the "micro-region"); (b) Even if only a small percentage of the cancer cells formed radioactive precipitates, the resulting micro-regions of destruction would so overlap that all of the cells in the cancer will be irradiated, covering the entire tumor. Adapted from ref. 2.11.

2.2.3. Summary of the S.T.A.R. Method

In summary, the S.T.A.R. method (wherein micro-regional fields of radiation are distributed throughout the tumor but little in normal tissues) lies intermediate between the two extremes of (1) surgical excision of the tumor, and (2) treatment with cell-specific cytotoxic drugs. The heterogeneity and plasticity of cancer cells can be circumvented by a micro-regional (instead of cell-by-cell) attack because the destruction is trait-independent. The tumor specificity can be enhanced by the additive contribution of multiple "imperfect" targeting steps that, taken together, minimize normal cells becoming the target of destruction. The advantages of the S.T.A.R. method compared to the other targeted cancer therapies include: (1) The primary and metastatic tumor sites are localized by a precipitate (i.e., platform) that is retained inside tumor tissues for an extended period of time compared to that of soluble targeting agents in other therapies; (2) The formation and the release of platform are both cancer-specific, thus the overall selectivity of tumor localization is improved by combining two "imperfect" targeting steps; (3) The enzyme is covalently bound to the

platform and thus also retained inside tumor tissues during the treatment; (4) Radiation destroys all cells in a micro-region to overcome the inherent heterogeneity of solid tumors; (5) The possibility to develop resistant cells by radiation is much lower than by cytotoxic drugs; and (6) The effective region of radiation is well defined due to the short lifetimes of the radiation-induced radicals (see Chapter 1.2), to be contrasted with cytotoxic drugs which can diffuse to normal tissues and cause systemic damage.

2.2.4. Progress in S.T.A.R. Development

This strategy, developed conceptually by S. Rose, to our knowledge, has not been applied in practice. A chief challenge lies in the creation of the molecular entities that constitute the SPRs. The Step-1 SPR needs to accomplish multiple tasks during the therapy. Those tasks include (1) cancer targeting; (2) forming precipitate upon enzymatic treatment; and (3) binding covalently to the Step-3 agent. The structures of the Step-1 SPR, both the soluble form and the insoluble form, are required to be non-toxic, non-immunogenic, stable in both intracellular and extracellular environments and endocytoxic (the soluble form). Therefore, the development of a successful Step-1 SPR is one of the essential tasks for the S.T.A.R. method and also poses great challenges due to the multiple functionalities on an SPR molecule. The Step-4 SPR may be considered as a radioactive version of the Step-1 SPR without the targeting moiety and the binding handle. Therefore, the fundamental structure of the Step-1 SPR for the soluble-to-insoluble conversion can be used to construct the Step-4 SPR.

Rose founded the company Oncologic, Inc. to develop the S.T.A.R. approach. One Step-1 SPR under development at Oncologic employs indoxyl glucoside tethered to

transferrin-labeled human serum albumin (HSA). Such a chemical structure was chosen because mammalian lysosomes contain enzyme activity which will remove the glucose to form an indoxyl. The indoxyl is soluble but very instable and rapidly undergoes oxidative dimerization to give insoluble indigo (Scheme 2.1). The indigo precipitate provides the platform for subsequent localization of radioactive material. A candidate for the Step-4 SPR is an ^{131}I-labeled indoxyl glucuronide, which upon enzymatic cleavage yields a radioactive precipitate. Although the complete four-step S.T.A.R. procedure has not yet been implemented or tested, Oncologic researchers have made major progress over the past 5 years in developing the Step-1 SPR, the Step-4 SPR, and the Step-3 enzyme conjugate. *In vitro* studies showed the accumulation of indigo (blue) inside the tumor cells, and the presence of the binding handle (a Loracarbef moiety, see Chapter 3.1) on the precipitate was demonstrated by an immunoassay.[2.12] These preliminary results prove the viability of the strategy on which the S.T.A.R. method is established. The research work presented in this thesis focuses on the design and synthesis of porphyrin-based SPRs (Step-1 and Step-4) and their soluble-to-insoluble conversion upon enzymatic treatment.

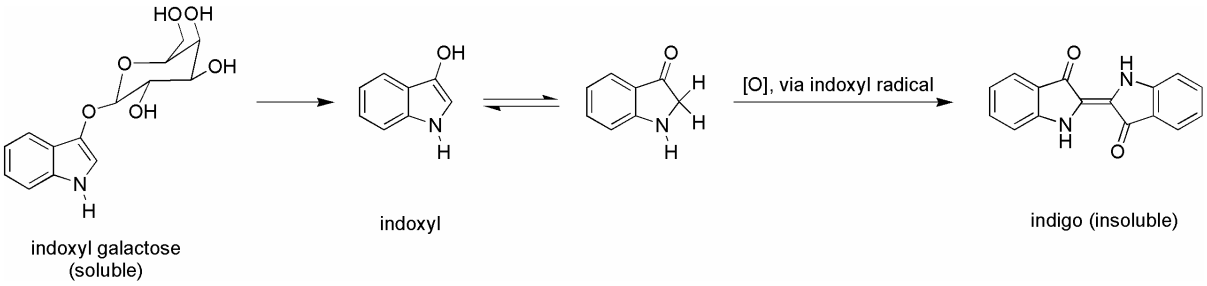

Scheme 2.1. Illustration of the soluble-to-insoluble conversion of an indoxyl-based system.

REFERENCES

(2.1) (a) Sikora, K. In *Oxford Textbook of Oncology*; Peckham, M.; Pinedo, H. M.; Veronesi, U., Eds.; Oxford University Press Inc.: New York, NY, 1995; Vol. 1, pp

659–680. (b) Krauss, W. C.; Park, J. W.; Kirpotin, D. B.; Hong, K.; Benz, C. C. *Breast Disease* **2000**, *11*, 113–124.

(2.2) (a) Hamblett, K. J.; Kegley, B. B.; Hamlin, D. K.; Chyan, M.-K.; Hyre, D. E.; Press, O. W.; Wilbur, D. S.; Stayton, P. S. *Bioconjugate Chem*. **2002**, *13*, 588–598. (b) Boerman, O. C.; van Schaijk, F. G.; Oyen, W. J. G.; Corstens, F. H. M. *J. Nucl. Med.* **2003**, *44*, 400–411. (c) Beeson, C.; Butrynski, J. E.; Hart, M. J.; Nourigat, C.; Matthews, D. C.; Press, O. W.; Senter, P. D.; Bernstein, I. D. *Bioconjugate Chem.* **2003**, *14*, 927–933.

(2.3) (a) Bagshawe, K. D. *Br. J. Cancer* **1987**, *56*, 531–532. (b) Houba, P. H. J.; Leenders, R. G. G.; Boven, E.; Scheeren, J. W.; Pinedo, H. M.; Haisma, H. *J. Biochem. Pharmcol.* **1996**, *52*, 455–463. (c) Webley, S. D.; Francis, R. J.; Pedley, R. B.; Sharma S. K.; Begent, R. H. J.; Hartley, J. A.; Hochhauser, D. *Br. J. Cancer* **2001**, *84*, 1671–1676. (d) Niculescu-Duvaz, I.; Springer, C. *J. Adv. Drug Deliv. Rev.* **1997**, *26*, 151–172. (e) Connors, T. A.; Duncan, R.; Knox, R. *J. Eur. J. Cancer* **1995**, *31A*, 1373–1378. (f) Senter, P. D.; Su, P. C. D.; Katsuragi, T.; Sakai, T.; Cosand, W. L.; Hellström, I.; Hellström, K. E. *Bioconjugate Chem.* **1991**, *2*, 447–451.

(2.4) (a) Weiner, L. M.; Adams, G. P. *Oncogene* **2000**, *19*, 6144–6151. (b) Chapman, A. P. *Adv. Drug Delivery Rev.* **2002**, *54*, 531–545.

(2.5) (a) Satchi-Fainaro, R.; Duncan, R.; Barnes, C. M. *Adv. Polym. Sci.* **2006**, *193*, 1–65. (b) Gianasi, E.; Wasil, M.; Evagorou, E. G.; Keddle, A.; Wilson, G.; Duncan, R. *Eur. J. Cancer* **1999**, *35*, 994–1002.

(2.6) (a) Duncan, R.; Gac-Breton, S.; Keane, R.; Musila, R.; Sat, Y. N.; Satchi, R.; Searle, F. *J. Control. Release* **2001**, *74*, 135–146. (b) Satchi-Fainaro, R.; Wrasidlo, W.; Lode, H.

N.; Shabat, D. *Bioorg. Med. Chem.* **2002**, *10*, 3023–3029. (c) Satchi-Fainaro, R.; Hailu, H.; Davies, J. W.; Summerford, C.; Duncan, R. *Bioconjugate Chem.* **2003**, *14*, 797–804.

(2.7) (a) Martin, L. A.; Vile, R.; Lemoine N. R.; Sikora, K.; Pandha, H. S. *Lancet* **1997**, *350*, 1993–1994. (b) Lipinski, K. S.; Djeha, A. H.; Ismail, T.; Mountain, A.; Young, L.; Wrighton, C. *J. Mol. Ther.* **2001**, *4*, 365–371. (c) Niculescu-Duvaz, I.; Springer, C. J. *Mol. Biotechnol.* **2005**, *30*, 71–88. (d) McNeish, I. A.; Green, N. K.; Gilligan, M. G.; Ford, M. J.; Mautner, V.; Young, L. S.; Kerr, D. J. *Gene Ther.* **1998**, *5*, 1061–1069.

(2.8) (a) Wagner, E.; Kircheis, R.; Walker, G. F. *Biomed. Pharmacother.* **2004**, *58*, 152–161. (b) Buchsbaum, D. J.; Curiel, D. T. *Cancer Biother. Radiopharm.* **2001**, *16*, 275–288.

(2.9) Brown, J. M.; Wilson, W. R. *Nat. Rev. Cancer* **2004**, *4*, 437–447.

(2.10) Rose, S. *J. Theor. Biol.* **1998**, *195*, 111–128.

(2.11) The company website of Oncologic Inc. (www.oncologic.net; Nov 20, 2006).

(2.12) Mayers, G. L. *Drug Dev. Res.* **2006**, *67*, 94–106.

Chapter 3

Porphyrin-Based Step-1 SPRs

3.1. Conceptual Design and Structural Features

The goal of my research has been to synthesize porphyrin-based SPRs that can be used in the S.T.A.R. approach, as alternatives to the indoxyl-based SPRs described in Chapter 2. There are several reasons for choosing porphyrins as the backbone of an SPR: (1) the extensive literature available concerning water-soluble porphyrins and aggregation of porphyrinic compounds; (2) the success of the rational synthesis of ABCD-porphyrins providing versatility in introducing different functional groups; (3) the robustness of the porphyrin macrocycle in biological systems; and (4) the ability to use metalloporphyrins as carriers for radioisotopic metals.

3.1.1. Conceptual Design

The conceptual structure of a porphyrin-based Step-1 SPR is shown in Figure 3.1. The SPR is composed of a metalloporphyrin, a CTA moiety, a binding handle for the Step-3 agent and intermolecular association moieties that are masked by water-solubilizing (cleavable) groups. Upon treatment by lysosomal enzymes, the CTA moiety and the water-solubilizing group are removed, and an intermolecular association group is exposed. The remaining porphyrin structure is insoluble and spontaneously aggregates. The pattern in which porphyrin molecules aggregate is determined by the interaction of the intermolecular association groups. Once the porphyrin-based aggregate reaches a certain size, the aggregate precipitates to form platform. The platform is equipped with binding handles for the Step-3

agent. The interaction of the intermolecular association groups may be covalent as in the dimerization to form indigo described in Chapter 2.2.4, or entail non-covalent interactions such as hydrogen-bonding, hydrophobic interaction, coordination and/or π-π interaction between the macrocycles. The central metal is required in some cases wherein the metal atom participates in the intermolecular association process. The structure of the actual molecule may deviate from the conceptual design shown in Figure 3.1. For example, different components may be attached to one meso position of the porphyrin through a multi-branched linker, or a pair of donor/acceptor-type intermolecular association groups may be employed so that masking of one of them by a water-solubilizing group is sufficient to block intermolecular association. The intermolecular association groups will be described in detail with each specific design in Chapter 5; the other components in the conceptual design will be discussed in the following sections.

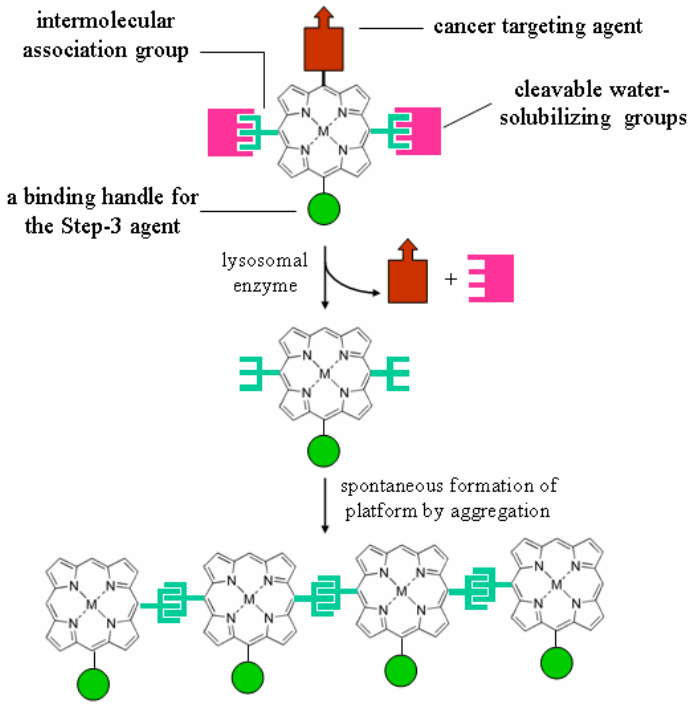

Figure 3.1. The conceptual design of a porphyrin-based Step-1 SPR.

3.1.2. The Cancer Targeting Agent (CTA)

The functions of the CTA include (1) targeting a receptor on a tumor cell and (2) initiating the internalization of the SPR molecule into the tumor cell. Therefore, the potential repertoire of CTAs for the Step-1 SPR includes any molecular structure that is capable of binding to an endocytosing receptor and undergoing transport into the targeted cell. Such targeting agents include transferrin, integrin, epidermal growth factor, folic acid, tumor specific antibodies, etc. Preferentially, following transport into the targeted tumor cell, the Step-1 SPR is delivered to the lysosomes where the enzymes convert the soluble SPR to platform. Oncologic, Inc., is currently employing transferrin as the CTA to construct Step-1 SPRs. Transferrin is a plasma protein that delivers iron into cells by binding to the transferrin receptor on the cell surface. Transferrin receptors is expressed on rapidly dividing cells, with 10,000 to 100,000 molecules per cell commonly found on tumor cells.[3.1] In contrast, in nonproliferating cells, expression of transferrin receptor is low or even undetectable.[3.2]

The Step-1 SPR can be synthesized with the CTA directly attached to the porphyrin. Alternatively, the CTA can be attached to a carrier moiety such as albumin that is preloaded with multiple porphyrins (Figure 3.2). The advantage of employing a carrier is that the targeting by one CTA and the subsequent endocytosis of the carrier will cause the internalization of multiple platform-building materials (i.e., porphyrins). For example, bovine serum albumin (BSA) bears 30 to 35 primary amino groups (lysine residues) that are capable of reacting with a functional group such as succinimide during conjugation. Transferrin can be derivatized with *N*-(ε-maleimidocaproyloxy)succinimide ester to

introduce a maleimidyl moiety, which can be coupled with another molecule bearing a thiol group.[2.12] Maleimide-activated BSA (commercially available with 15 to 25 maleimide groups on each BSA molecule) can be conjugated with reagents bearing a thiol group. While BSA can serve as the carrier in a model SPR compound, the actual SPR should employ human serum albumin (HSA). Representative commercial crosslinking reagents that can be used to connect the porphyrin and the carrier are listed in Table 3.1. We chose to introduce a thiol-terminated linker to the porphyrin because the thiol group can be conveniently conjugated to the carrier with either an amine or succinimide functionality.

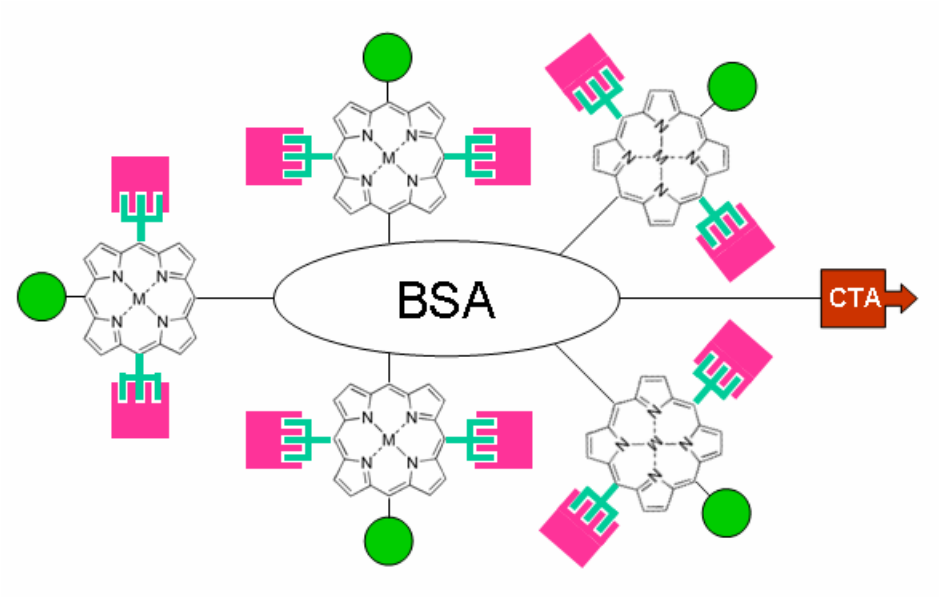

Figure 3.2. A schematic diagram of a human serum albumin (BSA) carrier loaded with porphyrins and a CTA. (Only seven porphyrins are shown in the diagram whereas the typical number of functional groups available on each albumin molecule is more than 20.)

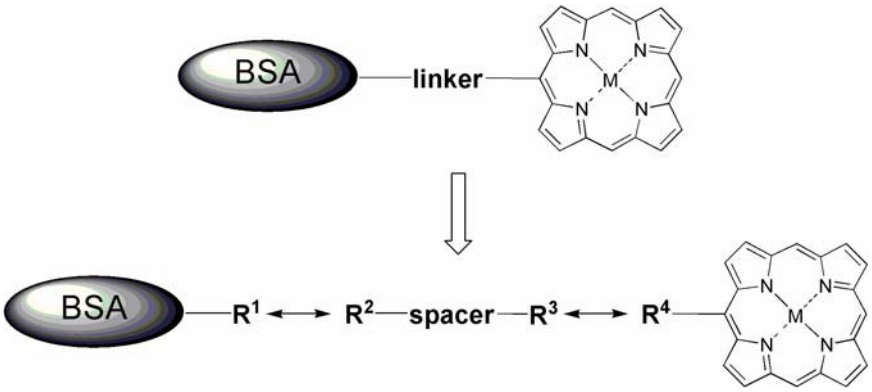

Table 3.1. The coupling of the porphyrin and the carrier by commercial crosslinking reagents. (Only one porphyrin attached to the carrier molecule is shown. The CTA, intermolecular association groups and water-solubilizing groups are omitted for clarity. The molecular components between functional groups such as those between BSA and R^1, R^2 and R^3, and porphyrin and R^4 are also omitted.)

R^1	R^2	R^3	R^4
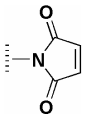	No additional linker is needed.		
	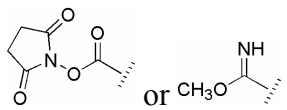	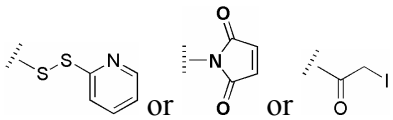	
	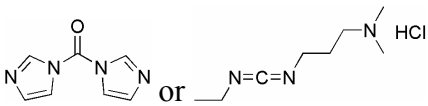		
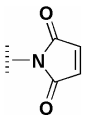	Thiolation reagents such as 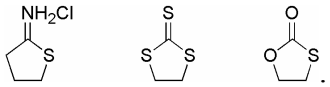 .		

3.1.3. The Water-solubilizing Groups

The primary function of the water-solubilizing group, as the name suggests, is to solubilize the highly hydrophobic porphyrin macrocycle. On the other hand, the water-solubilizing group also serves as a protecting group to mask the activity of the intermolecular association moiety. In order to accomplish the soluble-to-insoluble conversion, the water-

solubilizing group needs to be cleavable by an enzyme. Accordingly, some common solubilizing substituents for porphyrins such as the pyridyl (pyridinium) group are not suitable for porphyrin-based SPRs. The water-solubilizing group also needs to remain intact before being transported into cells to avoid premature deposition of platform in the ECF. For example, β-glucose can be used to solubilize the porphyrin because β-glucosidase, the enzyme that cleaves β-glucose, only exists in lysosomes in humans.

The water-solubilizing group for the Step-4 SPR, on the other hand, is determined by the enzyme employed in the Step-3 agent. The Step-3 agent has to possess an enzyme that is not accessible inside the body to avoid premature deposition of the radioactive precipitate from the Step-4 SPR. The candidates for such an enzyme include β-glucuronidase, phosphatase, sulfatase and β-galactosidase. The corresponding water-solubilizing groups are β-glucuronic acid, phosphate, sulfate and β-galactose, respectively.

We chose β-glucuronic acid, which can be cleaved by β-glucuronidase, as the water-solubilizing group for the Step-4 SPR. The mammalian β-glucuronidase is expressed only at a low level and is less active than the bacterial analogue under the pH conditions inside humans.[2.3d] Therefore, the presence of the mammalian β-glucuronidase in serum should not compromise the specificity of the bacterial β-glucuronidase during therapy. As for the porphyrin-based SPR, in addition to the advantages of employing β-glucuronidase in the therapy, the negtively charged glucuronide moieties will provide electrostatic repulsion between porphyrin molecules, and thus may impart greater solubility to porphyrins than is achieved with glucosyl groups. Although our work focuses on the Step-1 SPRs, we employed both glucose and glucuronic acid in our study to test the water-solubility of various sugar porphyrins.

3.1.4. The Binding Handle for the Step-3 agent

The Step-3 agent, which catalyzes the formation of the radioactive precipitate, is localized in the tumor milieu upon interaction with the binding handle on the platform. The specificity of the S.T.A.R. method thus relies on highly specific and irreversible (i.e., covalent) interaction between the Step-3 agent and the binding handle. An excellent model for such a system is an enzyme and its irreversible inhibitor. For example, Loracarbef, a penicillin analogue that is employed as the binding handle by Oncologic, Inc., is the substrate of a β-lactamase (Figure 3.3a). β-Lactamase catalyzes the hydrolysis of the β-lactam ring by forming a covalently linked intermediate with Lorcarbef (Figure 3.3b). A specifically designed mutant β-lactamase, however, lacks the amino acid residue that is responsible for the ring-opening reaction and the release of the corresponding product from the enzyme, and thus can be irreversibly inhibited by a penicillin analogue such as Loracarbef.[3.3] In order to comply with the S.T.A.R. method, the irreversible enzyme inhibitor, or at least the sub-structure motifs that will bind to the Step-3 agent, must remain intact in the presence of lysosomal enzymes and other intracellular and extracellular conditions. Owing to synthetic considerations, the inhibitor also needs to carry a functional group distant from the binding structure, for the attachment to other components to form the Step-1 SPR. Compared to other irreversible enzyme inhibitors that have been discovered to date, Loracarbef is relatively stable and also carries a primary amine group as a synthetic handle, thus affording an excellent candidate for the binding handle for the Step-3 agent.

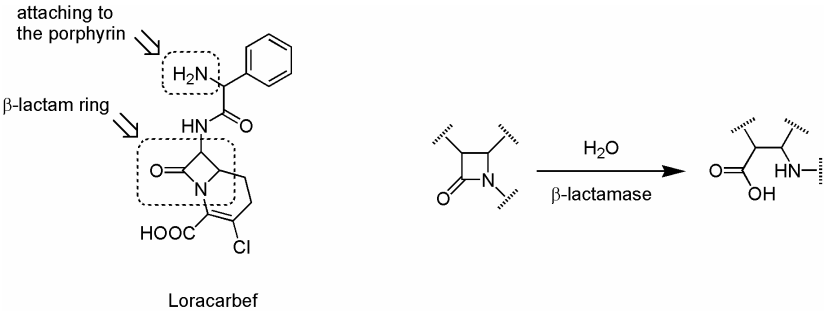

(a) (b)

Figure 3.3. The binding handle on the platform. (a) The structure of Loracarbef and (b) the ring-opening reaction of a β-lactam catalyzed by a β-lactamase.

3.1.5. Summary: A Porphyrin-Based Step-1 SPR

Oncologic, Inc., has developed a Step-1 SPR based on indoxyl glucoside and has successfully demonstrated the targeting of the SPR to cancer cells and subsequent endocytosis as well as the availability of the binding handles on the platform.[2.12] Therefore, we decided to employ the same CTA (transferrin) and the same binding handle for the Step-3 agent (the irreversible enzyme inhibitor Loracarbef) in porphyrin-based Step-1 SPRs. The porphyrin will also carry a thiol-terminated linker for attaching to the albumin carrier. The water-solubilizing group of our choice is glucose. Different intermolecular association groups were studied and will be discussed in detail in Chapter 5.

3.2. General Information on Porphyrin Synthesis

A porphyrin is a macrocyclic tetrapyrrolic compound with four meso-positions and eight β-positions. Four different substituents can be attached to the meso positions. The eight β-positions on the macrocycle can also be derivatized but are less synthetically accessible than the meso-positions. A porphyrin bearing the same substituents at all four meso-positions ("A_4-porphyrin") can be synthesized by the condensation of an aldehyde and

pyrrole.[3.4] When more than one aldehyde species is employed, the condensation reaction will yield a statistical mixture of porphyrins with different patterns of substitution.[3.5] The purification of any single porphyrin species from such a mixture is tedious. Therefore, the aldehyde and pyrrole condensation is generally not suitable for the synthesis of porphyrins bearing different meso substituents.

3.2.1. Rational Synthesis of Porphyrins Bearing Four Different Meso Substituents

Our group has developed a rational method to synthesize porphyrins bearing four different meso groups ("ABCD-porphyrin"). The synthesis begins with the condensation of an aldehyde with excess pyrrole to give a dipyrromethane (Scheme 3.1). The first ("A") substituent is introduced via the substituent on the aldehyde. The acylation of the dipyrromethane with an *S*-pyridyl thioester (Mukaiyama reagent) bearing the second ("B") substituent yields the corresponding 1-acyldipyrromethane. A second acylation reaction with a Mukaiyama reagent (or acyl chloride) bearing the third ("C") substituent yields a "BAC" 1,9-diacyldipyrromethane. The diacyldipyrromethane is reduced to afford the corresponding dicarbinol, which is then condensed with a dipyrromethane bearing the fourth ("D") substituent to yield the ABCD-porphyrin.[3.6]

The same fundamental approach can also be applied in the rational synthesis of porphyrins with a fewer number of distinct substituents, such as *trans*-A_2B_2- and *trans*-AB_2C-porphyrins (Scheme 3.2). A *trans*-A_2B_2-porphyrin can by synthesized from a 1-acyldipyrromethane bearing an "A" substituent at the 5-position and a "B" substituent at the 1-position. The acyldipyrromethane is reduced and the self-condensation of the resulting dipyrromethane-1-carbinol yields the *trans*-A_2B_2-porphyrin (Scheme 3.2a).[3.7] As discussed

in Chapter 3.1, the porphyrin molecule employed in a Step-1 SPR needs to carry various components. Therefore, an efficient synthetic method toward porphyrins bearing different substituents (as in ABCD-porphyrins) is essential to the success of constructing a porphyrin-based Step-1 SPR.

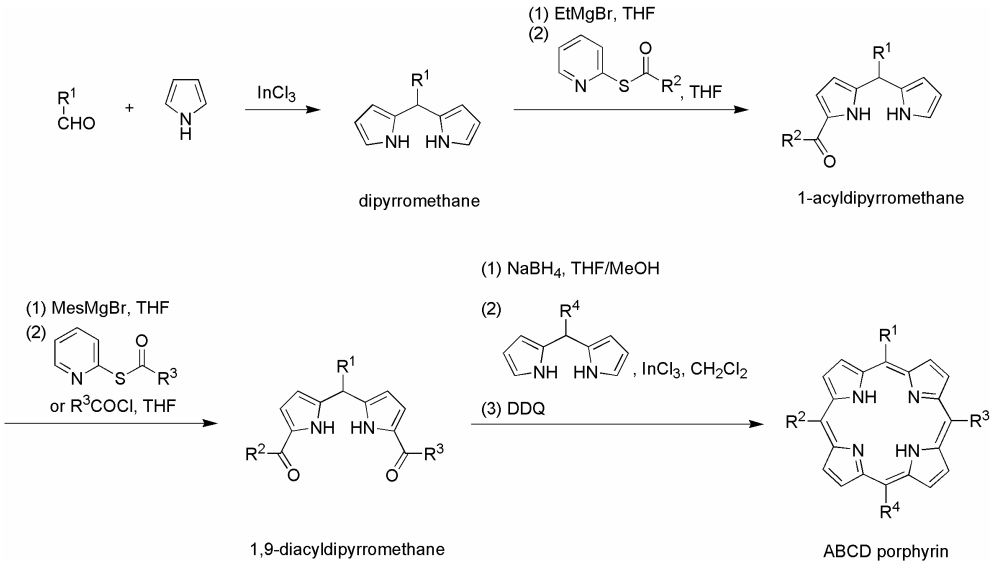

Scheme 3.1. The rational synthesis of a porphyrin bearing four different meso substituents.

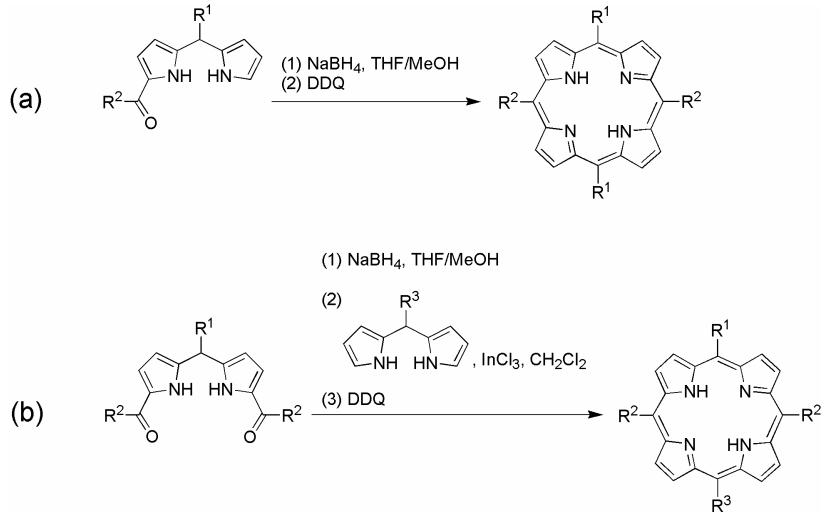

Scheme 3.2. The synthesis of (a) *trans*-A_2B_2-porphyrins and (b) *trans*-AB_2C-porphyrins from acyldipyrromethanes.

3.2.2. Other Synthetic Routes to Porphyrins

Between the two extremes of pyrrole-aldehyde condensation and the rational synthetic methods described in the previous section, porphyrins can also be synthesized via the condensation of a dipyrromethane and an aldehyde. A *trans*-A_2B_2-porphyrin can be obtained upon condensation of a dipyrromethane and an aldehyde. Although such a synthesis is rational and only one porphyrin product is expected, the dipyrromethane-aldehyde condensation frequently yields not only the desired *trans*-A_2B_2-porphyrin but also other porphyrins such as the *cis*-A_2B_2-isomer and A_3B-porphyrin. This major limitation is due to an acid-catalyzed polypyrrolic rearrangement called "scrambling" (Scheme 3.3).[3.8] In the limit of complete scrambling, a statistical mixture of porphyrins (A_4-, A_3B-, *trans*-A_2B_2-, *cis*-A_2B_2-, AB_3- and B_4-) is produced.

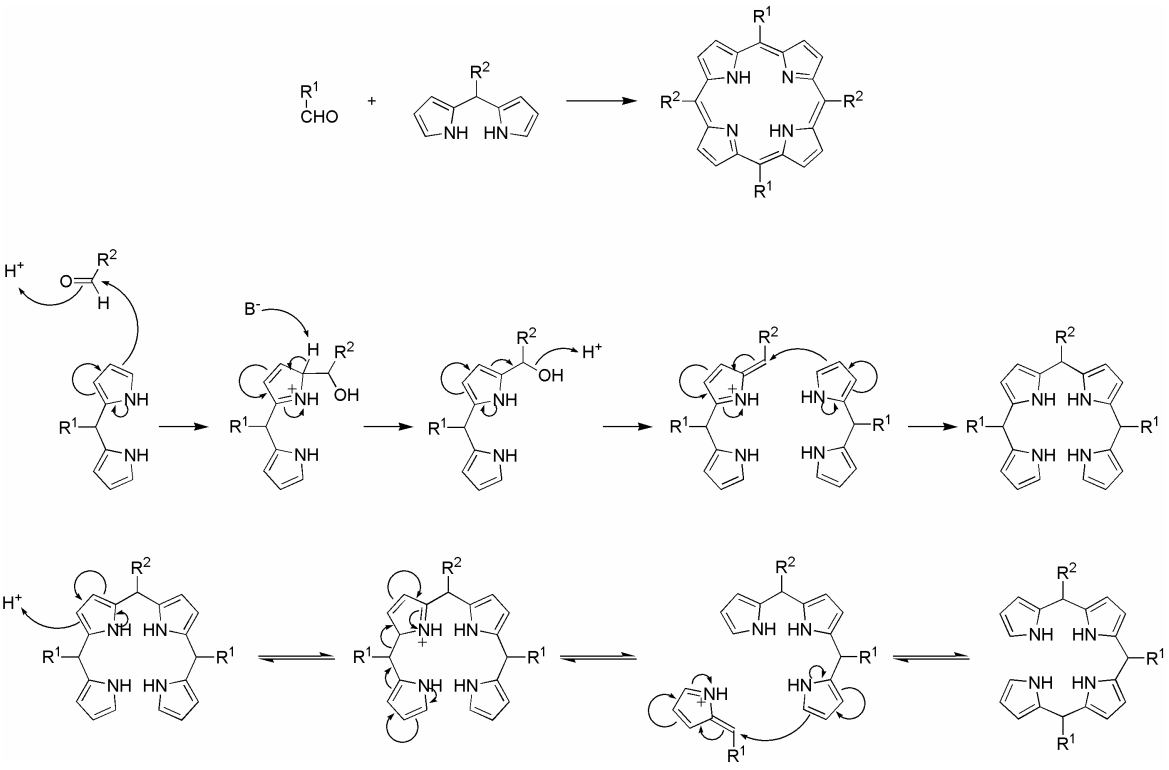

Scheme 3.3. The mechanism of scrambling during the synthesis of a *trans*-A_2B_2-porphyrin from a dipyrromethane and an aldehyde.

On the other hand, when one dipyrromethane or aldehyde and two different species of the other reactant are employed in the condensation, three different porphyrins, without counting the possible scrambled products, will be obtained statistically (Scheme 3.4).[3.9] Despite the disadvantages of statistical reactions, the porphyrin syntheses shown in Scheme 3.4 may be the only resort when certain functional groups in the substituents are not compatible with the conditions for rational syntheses. Therefore, we do not exclude statistical reactions in our synthesis of porphyrin-based SPRs.

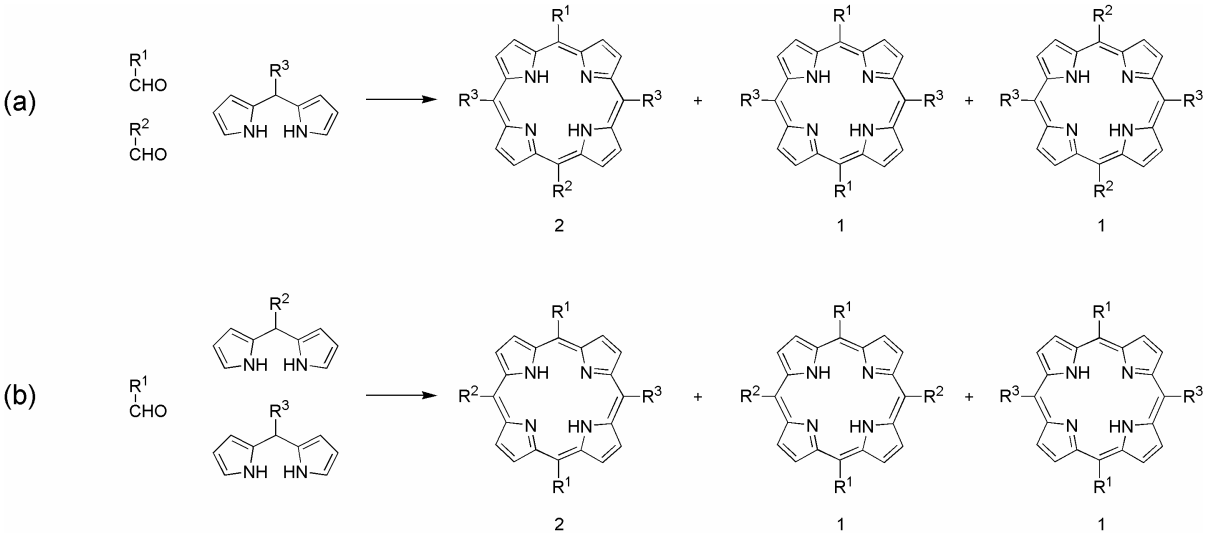

Scheme 3.4. Statistical synthesis of *trans*-AB_2C-porphyrins by the condensation of (a) two aldehydes and one dipyrromethane or (b) one aldehyde and two dipyrromethanes. The numbers indicate the ratio of the reactants and the theoretical ratio of the products.

3.2.3. Synthetic Routes to Porphyrins Bearing Unsubstituted Meso-Positions

In our study of porphyrin-based Step-1 SPRs, we employed ABCD-porphyrins as well as porphyrins bearing unsubstituted meso-positions such as *trans*-AB-porphyrins (see Chapter 5 for each specific design). The two free meso-positions on a *trans*-AB-porphyrin can be further elaborated to introduce moieties that may be labile in the rational synthesis of ABCD-porphyrins described previously. A new synthetic route to *trans*-AB-porphyrins has

been developed in our group and will be discussed in detail in Chapter 4.

3.3. Self-Immolative Linkers in Prodrug Applications

One similarity of a Step-1 SPR and a prodrug is that both are subject to distinct changes in molecular behavior upon enzymatic treatment. A Step-1 SPR can be converted from a soluble molecule to an insoluble one, whereas a prodrug can be converted from a less toxic or nontoxic molecule to a cytotoxic drug. Therefore, the same strategy for reducing the toxicity of prodrugs may also be suitable for solubilizing the hydrophobic porphyrin.

The most straightforward way to construct a prodrug is to attach the substrate of an enzyme to a functional group on the drug molecule. For example, glutamic acid, phosphate or glucuronic acid was attached to nitrogen mustard drugs to form the corresponding prodrugs (Equation 3.1).[2.3d] However, the direct attachment of the cleavable group to the drug limits possible modifications to improve the properties of the prodrug. Therefore, most prodrugs that have been reported contain "self-immolative" linkers that join the cleavable group and the drug.

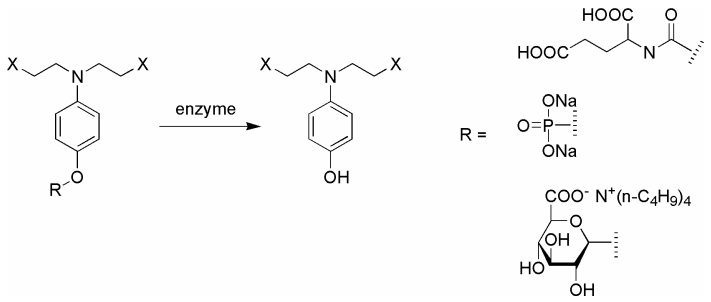

Equation 3.1. Constructing a prodrug by directly attaching a substrate of an enzyme.

Self-immolative linkers denote a specific group of linkers that contain a spacer structure and a trigger structure, where the trigger is normally located at the end of the linker. Upon removal of the trigger structure, the spacer structure collapses spontaneously, as the

name “self-immolative” suggests, and releases the molecule that is attached to the linker. A wide variety of self-immolative linkers have been reported in the field of prodrug research.[3.10] The self-immolative linkers can be distinguished in two categories by the mechanism of self-immolation: electron-transfer cascade linkers and cyclization linkers.

The self-immolation mechanism of electron-transfer cascade linkers is based on an elimination reaction initiated by a series of electron-transfer processes. The most prominent example of an electron-transfer cascade linker is the 1,6-elimination linker (Scheme 3.5).[3.11] The removal of the trigger structure unveils an aniline or phenol moiety, which initiates an electron-transfer cascade sequence and leads to the release of the drug molecule as well as fragments of the linker. The electron-cascade sequence can be adjusted by substituents such as a nitro or halide group on the aromatic ring.[3.12] Such electron-withdrawing groups can modify the electronic property of the ring, thus affecting the electron movement during the degradation of the linker. The name of the system, 1,6-elimination, indicates that electrons move along six continuous bonds before a covalent bond is broken. An aromatic system is normally required on the path of the electron movement (the only exception[3.13] that we found in the literature is shown in Scheme 3.6). Three types of elongated electron-transfer cascade linkers are shown in Equation 3.2, including the 1,8-elimination system based on naphthyl derivatives, the 1,10-elimination system based on biphenyl derivatives, and the system with linear multiple 1,6-elimination units.[3.14] Those lengthy linkers can reduce the steric hindrance between the drug moiety and the trigger structure, and thus facilitate both the synthesis and the enzymatic activation.

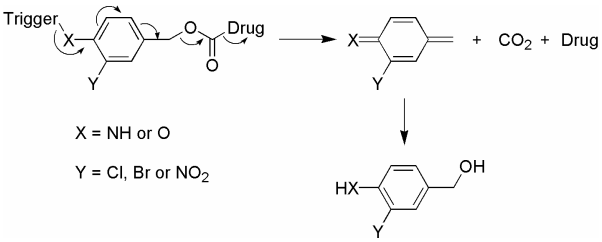

Scheme 3.5. The mechanism of self-immolation by an electron-transfer cascade.

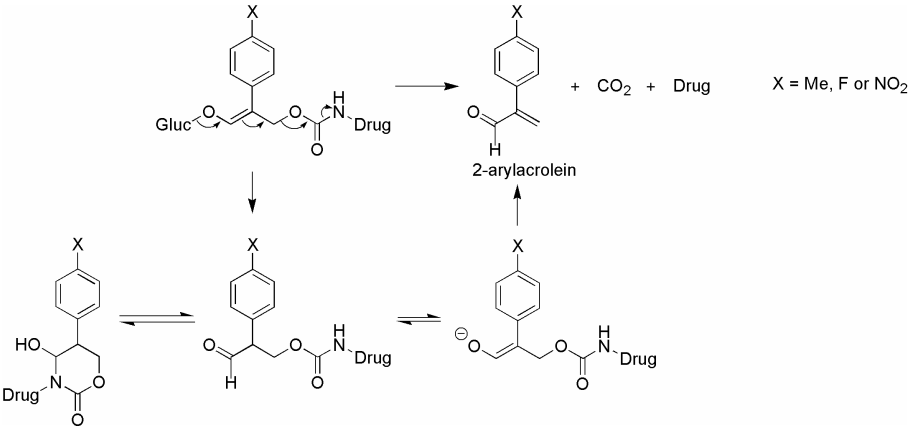

Scheme 3.6. An electron-transfer cascade linker that does not have any aromatic system on the path of electron transfer.

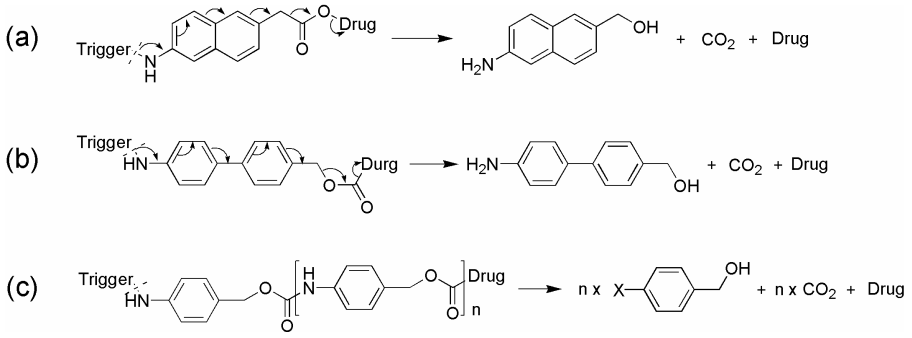

Equation 3.2. Elongated electron-transfer cascade linkers: (a) the 1,8-elimination system; (b) the 1,10-elimination system; (c) linear multiple 1,6-elimination systems.

The other type of self-immolative linker is the cyclization linker. The drug molecule on a cyclization linker is released via an intramolecular ring closure reaction. Two examples of cyclization linkers are shown in Scheme 3.7.[3.15] The removal of the trigger structure reveals an amino or hydroxyl group that attacks a carbonyl group in the same molecule and

forms a five-membered ring. The drug molecule is released as the leaving group in the cyclization reaction.

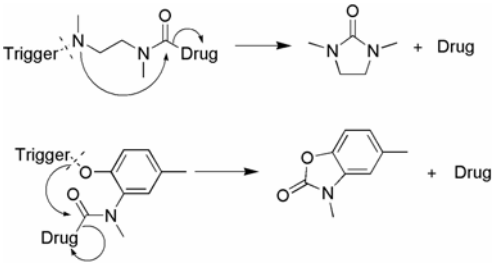

Scheme 3.7. The mechanism of self-immolation by ring closure.

Electron-transfer cascade linkers and cyclization linkers can also be combined in the same prodrug molecule. A dendritic prodrug that carries two drug moieties has been synthesized with both types of linkers and is capable of releasing two drug molecules simultaneously upon enzymatic treatment (Scheme 3.8).[3.15b] Scheme 3.9 shows a special prodrug that contains two drug molecules attached to a cephalosporin-based self-immolative linker.[3.16] The linker carries a β-lactam ring as the trigger structure that can be hydrolyzed by a β-lactamase. Two drug moieties are attached to different functional groups on the linker. Upon treatment with a β-lactamase, the first drug molecule is released by the electron-transfer cascade mechanism, and then the second drug molecule is released by the cyclization mechanism.

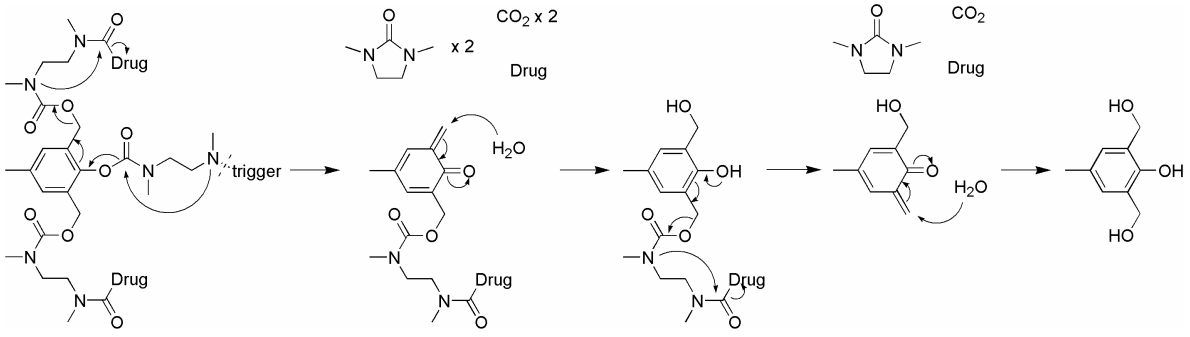

Scheme 3.8. A prodrug releases two drug molecules upon self-immolation of a linker by both

electron-transfer cascade and cyclization mechanisms.

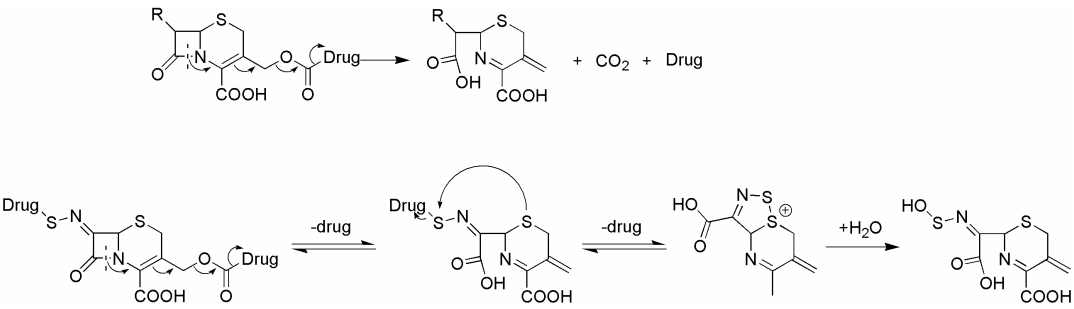

Scheme 3.9. A special prodrug constructed from a cephalosporin-based self-immolative linker: two drug molecules are released by two different mechanisms.

Although a self-immolative linker between the trigger structure and the drug molecule is not required, such a linker provides advantages in prodrug design, including (1) separating the drug and the trigger; (2) providing functionalities for attaching additional drug moieties or other required components; and (3) allowing various modifications in the designs. Therefore, we decided to employ a self-immolative linker between the water-solubilizing group and the intermolecular association group in the design of a porphyrin-based Step-1 SPR. The synthesis of self-immolative linkers will be described in Chapter 5.3.1.2.

REFERENCES

(3.1) Inoue, T.; Cavanaugh, P. G.; Steck, P. A.; Brunner, N.; Nicolson, G. L. *J. Cell Physiol.* **1993**, *156*, 212–217.

(3.2) Qian, Z. M.; Li, H.; Sun, H.; Ho, K. *Pharmacol. Rev.* **2002**, *54*, 561–587.

(3.3) Delaire, M.; Labla, R.; Samama, J. P.; Masson, J. M. *J. Biol. Chem.* **1992**, *267*, 20600–20606.

(3.4) Lindsey, J. S.; Schreiman, I. C.; Hsu, H. C.; Kearney, P. C.; Marguerettaz A. M. *J.*

Org. Chem. **1987**, *52*, 827–836.

(3.5) Lindsey, J. S.; Prathapan, S.; Johnson, T. E.; Wagner, R. W. *Tetrahedron* **1994**, *50*, 8941–8968.

(3.6) Rao, P. D.; Dhanalekshmi, S.; Littler, B. J.; Lindsey, J. S. *J. Org. Chem.* **2000**, *65*, 7323–7344.

(3.7) Rao, P. D.; Littler, B. J.; Geier, G. R., III; Lindsey, J. S. *J. Org. Chem.* **2000**, *65*, 1084–1092.

(3.8) Littler, B. J.; Ciringh, Y.; Lindsey, J. S. *J. Org. Chem*. **1999**, *64*, 2864–2872.

(3.9) Gryko, D. T.; Clausen, C.; Lindsey, J. S. *J. Org. Chem.* **1999**, *64*, 8635–8647.

(3.10) (a) Dubowchik, G. M.; Radia, S. *Tetrahedron Lett.* **1997**, *38*, 5257–5260. (b) Rawale, S.; Hrihorczuk, L. M.; Wei, W.-Z.; Zemlicka, J. *J. Med. Chem.* **2002**, *45*, 937–943. (c) Andrianomenjanahary, S.; Dong, X.; Florent, J.-C.; Gaudel, G.; Gesson, J.-P.; Jacquesy, J.-C.; Koch, M.; Michel, S.; Mondon, M.; Monneret, C.; Petit, P.; Renoux, B.; Tillequin, F. *Bioorg. Med. Chem. Lett.* **1992**, *2*, 1093–1096. (d) Antczak, C.; Bauvois, B.; Monneret, C.; Florent, J.-C. *Bioorg. Med. Chem.* **2001**, *9*, 2843–2848. (e) Niculescu-Duvaz, D.; Niculescu-Duvaz, I.; Friedlos, F.; Martin, J.; Spooner, R.; Davies, L.; Marais, R.; Springer, C. J. *J. Med. Chem.* **1998**, *41*, 5297–5309. (f) Niculescu-Duvaz, D.; Niculescu-Duvaz, I.; Friedlos, F.; Martin, J.; Lehouritis, P.; Marais, R.; Springer, C. J. *J. Med. Chem.* **2003**, *46*, 1690–1705. (g) Niculescu-Duvaz, I.; Niculescu-Duvaz, D.; Friedlos, F.; Spooner, R.; Martin, J.; Marais, R.; Springer, C. J. *J. Med. Chem.* **1999**, *42*, 2485–2489. (h) Mauger, A. B.; Burke, P. J.; Somani, H. H.; Friedlos, F.; Knox, R. J. *J. Med. Chem.* **1994**, *37*, 3452–3458. (i) Madec-Lougerstay, R.; Florent, J.-C.; Monneret, C. *J. Chem. Soc. Perkin Trans. 1* **1999**,

1369–1375.

(3.11) (a) Dubowchik, G. M.; Firestone, R. A.; Padilla, L.; Willner, D.; Hofstead, S. J.; Mosure, K.; Knipe, J. O.; Lasch, S. J.; Trail, P. A. *Bioconjugate Chem.* **2002**, *13*, 855–869. (b) de Groot, F. M. H.; Busscher, G. F.; Aben, R. W. M.; Scheeren, H. W. *Bioorg. Med. Chem. Lett.* **2002**, *12*, 2371–2376. (c) Walker, M. A.; Dubowchik, G. M.; Hofstead, S. J.; Trail, P. A.; Firestone, R. A. *Bioorg. Med. Chem. Lett.* **2002**, *12*, 217–219. (c) Dubowchik, G. M.; Mosure, K.; Knipe, J. O.; Firestone, R. A. *Bioorg. Med. Chem. Lett.* **1998**, *8*, 3347–3352. (d) Dubowchik, G. M.; Radia, S. *Tetrahedron Lett.* **1997**, *38*, 5257–5260. (e) Toki, B. E.; Cerveny, C. G.; Wahl, A. F.; Senter, P. D. *J. Org. Chem.* **2002**, *67*, 1866–1872. (f) de Groot, F. M. H.; van Berkom, L. W. A.; Scheeren, H. W. *J. Med. Chem.* **2000**, *43*, 3093–3102.

(3.12) Leenders, R. G. G.; Damen, E. W. P.; Bijsterveld, E. J. A.; Scheeren, H. W.; Houba, P. H. J.; van der Meulen-Muileman, I. H.; Boven, E.; Haisma, H. *Bioorg. Med. Chem.* **1999**, *7*, 1597–1610.

(3.13) Rivault, F.; Tranoy-Opalinski, I.; Gesson, J.-P. *Bioorg. Med. Chem.* **2004**, *12*, 675–682.

(3.14) de Groot, F. M. H.; Loos, W. J.; Koekkoek, R.; van Berkom, L. W. A.; Busscher, G. F.; Seelen, A. E.; Albrecht, C.; de Bruijn, P.; Scheeren, H. W. *J. Org. Chem.* **2001**, *66*, 8815–8830.

(3.15) (a) Gopin, A.; Pessah, N.; Shamis, M.; Rader, C.; Shabat, D. *Angew. Chem. Int. Ed.* **2003**, *42*, 327–332. (b) Shamis, M.; Lode, H. N.; Shabat, D. *J. Am. Chem. Soc.* **2004**, *126*, 1726–1731. (c) Schmidt, F.; Florent, J.-C.; Monneret, C.; Straub, R.; Czech, J.; Gerken, M.; Bosslet, K. *Bioorg. Med. Chem. Lett.* **1997**, *7*, 1071–1076. (d) Desbene,

S.; Van, H. D.-T.; Michel, S.; Tillequin, F.; Koch, M.; Schmidt, F.; Florent, J.-C.; Monneret, C.; Straub, R.; Czech, J.; Gerken, M.; Bosslet, K. *Anti-Cancer Drug Design* **1999**, *14*, 93–106.

(3.16) Smyth, T. P.; O'Donnell, M. E.; O'Connor, M. J.; Ledger, J. O. S. *J. Org. Chem.* **1999**, *64*, 3132–3138.

Chapter 4

Development of a New Route to *Trans*-AB-Porphyrins

4.1. A New Route to *Trans*-AB-Porphyrins

As mentioned in Chapter 3.2.3, *trans*-AB-porphyrins bearing unsubstituted meso-positions provide alternative components for use in constructing Step-1 SPRs. The rational synthesis of ABCD-porphyrins described previously could be used for preparing *trans*-AB-porphyrins by employing a meso-substituted dipyrromethane bearing primary carbinol groups (Equation 4.1a). However, the yields are typically lower than those achieved for ABCD-porphyrins, where the dipyrromethane bears secondary carbinol groups.[4.1] One possible way to improve such a reaction is to replace the primary carbinol groups (from the reduction of the formyl groups at 1- and 9-positions of the dipyrromethane) with other more reactive C1 synthons. Therefore, we developed new methodology for preparing *trans*-AB-porphyrins from 1,9-bis(*N*,*N*-dimethylaminomethyl)dipyrromethanes under acid-free conditions (Equation 4.1b). This work was carried out by Dazhong Fan, Masahiko Taniguchi, Savithri Dhanalekshmi and myself. A complete description of this work has been publish;[4.2] salient excerpts are described here.

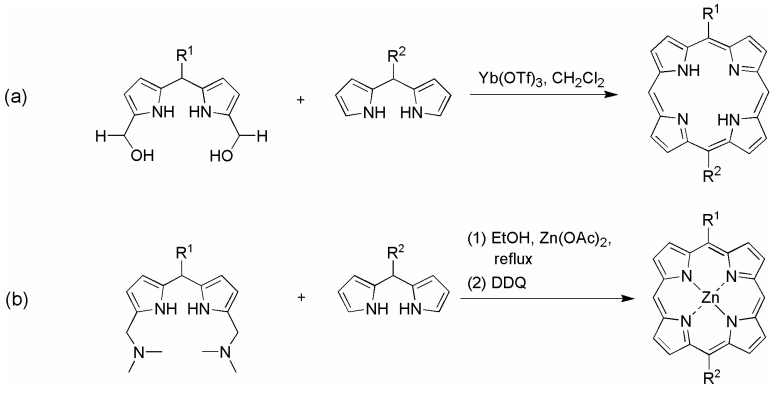

Equation 4.1. Synthesis of a *trans*-AB-porphyrin from (a) a dipyrromethane-1,9-dicarbinol

and a dipyrromethane; and (b) a 1,9-bis(*N*,*N*-dimethylaminomethyl)dipyrromethane and a dipyrromethane.

4.2. Synthesis of 5-Substituted-1,9-bis(*N*,*N*-dimethylaminomethyl)dipyrromethanes.

A series of known dipyrromethanes (**Ia-n**)[3.6,4.3-4.14] was prepared by application of a new solventless synthesis that entails treatment of an aldehyde dissolved in 100 equiv of pyrrole with a mild Lewis acid ($InCl_3$) at room temperature.[4.15] Each dipyrromethane (**Ia-n**) was reacted with Eschenmoser's reagent at room temperature followed by workup with aqueous $NaHCO_3$ (aqueous K_2CO_3 was used for the synthesis of **IIIi**), affording the corresponding free base 1,9-bis(*N*,*N*-dimethylaminomethyl)dipyrromethane (**IIIa-n**) in 43% to 91% yield (Table 4.1).

Table 4.1. Synthesis of 5-substituted-1,9-bis(*N*,*N*-dimethylaminomethyl)dipyrromethanes **IIIa-n**[a]

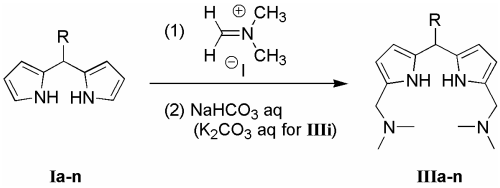

	R	Yield (%)[b]		R	Yield (%)[b]
a		68	**h**	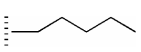	83
b	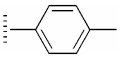	91	**i**		63
c	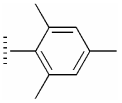	64	**j**	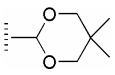	75
d	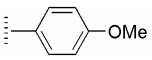	85	**k**		43
e	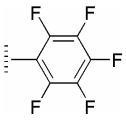	87	**l**	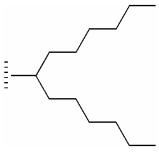	81
f		68	**m**		66

Table 4.1. (continued) Synthesis of 5-substituted-1,9-bis(*N*,*N*-dimethylaminomethyl)dipyrromethanes **IIIa-n**[a]

g	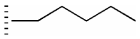	87	**n**	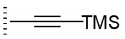	86

[a]Reaction conditions: 100 mM dipyrromethane **Ia-n** and 2 equiv of Eschenmoser's reagent in CH_2Cl_2 at room temperature for 1 h, then washed with saturated aqueous $NaHCO_3$ (K_2CO_3 for **Ii**). [b]Isolated yield.

4.3. Synthesis of *Trans*-AB-, *Trans*-A_2-, and A-porphyrins: Probing aryl/alkyl/H substituents at 5-position.

The scope of porphyrin formation was examined using the 1,9-bis(*N*,*N*-dimethylaminomethyl)dipyrromethanes (Equation 4.1b, Table 4.2). Emphasis was placed on (1) variation of the substituents, (2) assessment of any scrambling processes, and (3) yields of porphyrin. Altogether, the preparation of 28 *trans*-AB-porphyrins was examined. The yields of porphyrin were determined spectroscopically and ranged from <1% to 19% depending on the substituents and combination of the dipyrromethane precursors. Note that a given porphyrin can be made in two ways by switching the combination of the 1,9-bis(*N*,*N*-dimethylaminomethyl)dipyrromethane (**III**) and dipyrromethane (**I**). For example, **Ie** + **IIId** afforded the zinc porphyrin **ZnVde** in <1% yield while **Id** + **IIIe** gave **ZnVde** in 15% yield. In all cases where the better of the two possible combinations was employed, the yields ranged from 12% to 19%. In those cases where the porphyrin was isolated (**ZnVab** and **ZnVac**), the isolated yields compared well with the spectroscopic yield. Scrambling was observed only in the reaction of 5-(pentafluorophenyl)dipyrromethane (**Ie**) + 1,9-bis(*N*,*N*-dimethylaminomethyl)-5-pentyldipyrromethane (**IIIg**) (8% yield, level 2 scrambling). The scrambling problem could be overcome by reversal of the substituents; thus, reaction of **Ig** + **IIIe** afforded the same target porphyrin in 15% yield with no detectable scrambling. In

general, the reaction of 5-(pentafluorophenyl)dipyrromethane (**Ie**) proceeded in low yield and/or scrambling whereas the same meso-substituent could be well accommodated upon use of 1,9-bis(*N*,*N*-dimethylaminomethyl)-5-(pentafluorophenyl)dipyrromethane (**IIIe**). Taken together, the results upon condensation of a dipyrromethane + 1,9-bis(*N*,*N*-dimethylaminomethyl)dipyrromethane are superior to those of the reaction of a 1,9-bis(hydroxymethyl)-5-substituted-dipyrromethane + a 5-substituted-dipyrromethane, which resulted in extensive scrambling.[4.1]

The results illustrate the effects of substituents (alkyl or aryl) on the yields of the *trans*-AB-porphyrins and the relative reactivity of those groups when present on the dipyrromethane (**1**) versus 1,9-bis(dimethylaminomethyl)dipyrromethane (**3**). The yields of porphyrin are insensitive to the presence of an alkyl versus aryl group on either dipyrromethane or 1,9-bis(dimethylaminomethyl)dipyrromethane reactants. However, in the synthesis of porphyrins bearing only one meso-substituent (A-porphyrin), the combination of unsubstituted dipyrromethane and 5-substituted 1,9-bis(dimethylaminomethyl)dipyrromethane affords higher yields than the reverse combination.

Table 4.2. Formation of *trans*-AB- and A-Porphyrins **ZnV** via **IIIa-g,i** + **Ia-g,i**[a]

		IIIa 	**IIIb** 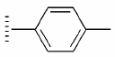	**IIIc** 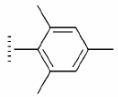	**IIId** 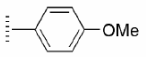	**IIIe** 	**IIIf** methyl	**IIIg** *n*-pentyl	**IIIi** H
Ia		–	13	11	11	18	7	15	5
Ib	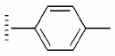	14 (16[b])	–	11	9	13	6	16	5
Ic	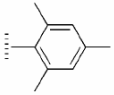	18 (15[b])	18	–	10	18	12	16	6
Id	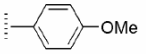	12	13	12	–	15	6	14	5
Ie	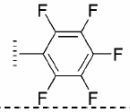	<1	6[c]	<1	<1	–	4	8[c]	2
If	methyl	13	13	16	12	12	–	16	4
Ig	*n*-pentyl	18	16	16	15	15	11	–	8
Ii	H	13	19	14	11	8	9	16	–

[a]The yields of porphyrin were determined by absorption spectroscopy of small aliquots from the reaction mixture. All reactions gave level 0 scrambling (detected by LD-MS analysis) unless noted otherwise. Reaction conditions: 10 mM reactants and 10 equiv of $Zn(OAc)_2$ in EtOH under reflux exposed to air for 3 h, then treated with 3/4 equiv of DDQ per pyrrole unit (30 mM). The combination that gives the better yield of porphyrin is underlined. [b]Isolated yield. [c]Level 2 scrambling.

4.4. Synthesis of *Trans*-AB-, *Trans*-A_2-, and A-porphyrins: Scope with diverse substituents.

We examined the synthesis of a series of *trans*-AB-, *trans*-A_2-, and A-porphyrins bearing diverse substituents (Table 4.3). Each porphyrin was purified by short passage over a pad of silica. 5-(*p*-Tolyl)dipyrromethane (**Ib**) was reacted with a series of 1,9-bis(dimethylaminomethyl)dipyrromethanes bearing diverse substituents **IIIj-m**, including acetal,[4.10] allyl,[4.11] swallowtail,[4.12] and carboethoxy[4.13] groups. In each case, no scrambling was observed and the isolated yields of the *trans*-AB-porphyrins ranged from 5-15%. In the same manner, a *trans*-AB-porphyrin (**ZnVgh**) bearing two alkyl groups was prepared in 17% yield. When a 5-TMS-ethynyldipyrromethane (**In**) was employed, the yield of porphyrin was low (**ZnVan** and **ZnVjn**). Very little change was obtained upon use of the TMS-ethynyl unit in the bis(*N*,*N*-dimethylaminomethyl)dipyrromethane species.

Table 4.3. Synthesis of *trans*-AB-, A_2-, and A-Porphyrins **ZnV** with diverse substituents[a]

Bis(aminomethyl) dipyrromethane		Dipyrromethane		Porphyrin	Yield (%)[b]
trans-AB-Porphyrin					
IIIj	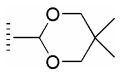	**Ib**	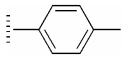	**ZnVbj**	10
IIIk		**Ib**	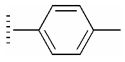	**ZnVbk**	14
IIIl	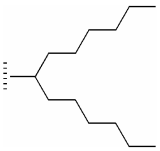	**Ib**	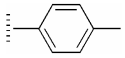	**ZnVbl**	15
IIIm		**Ib**	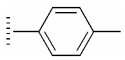	**ZnVbm**	5
IIIg	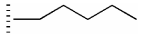	**Ih**	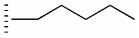	**ZnVgh**	17

Table 4.3. (continued) Synthesis of *trans*-AB-, A_2-, and A-Porphyrins **ZnV** with diverse substituents[a]

IIIa		**In**	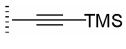	**ZnVan**	6
IIIj	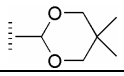	**In**	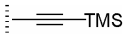	**ZnVjn**	1
		A-Porphyrin			
IIIj	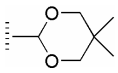	**Ii**		**ZnVij**	12
IIIk		**Ii**		**ZnVik**	17
IIIl	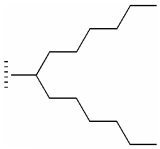	**Ii**		**ZnVil**	20
IIIm	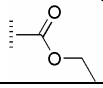	**1i**		**ZnVim**	5
		trans-A_2-Porphyrin			
IIIl	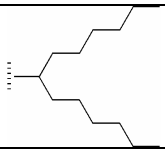	**Il**	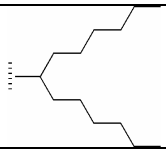	**ZnVll**	15

[a]All reactions give level 0 scrambling (assessed by LD-MS analysis). Reaction conditions: 10 mM reactants and 10 equiv of $Zn(OAc)_2$ in refluxing EtOH exposed to air for 2 h, then treated with 3/4 equiv of DDQ per pyrrole unit (30 mM). [b]Isolated yields.

A similar series of reactions was performed with unsubstituted dipyrromethane (**1i**) and 5-substituted 1,9-bis(*N*,*N*-dimethylaminomethyl)dipyrromethanes **IIIj-m**. The corresponding A-porphyrins (**ZnVij**, **ZnVik**, **ZnVil**, and **ZnVim**) were obtained in yields of 5-20%. *Trans*-AB-porphyrins bearing a single swallowtail substituent (**ZnVbl** and **ZnVil**) were obtained smoothly. A *trans*-A_2-porphyrin (**ZnVll**) was obtained by using a dipyrromethane and a bis(*N*,*N*-dimethylaminomethyl)dipyrromethane each bearing swallowtail substituents at the 5-position. The success of these approaches is in contrast to the failure encountered upon attempted reaction of a dipyrromethane-1-carbinol bearing a

swallowtail substituent at the 1-position.[4.12]

In general, the substituents that can be introduced with this method are quite diverse and open up a number of applications. The acetal group (**ZnVbj, ZnVij**) can be converted to an aldehyde,[4.10] the allyl group (**ZnVbk, ZnVik**) can be used for surface attachment,[28] the swallowtail group (**ZnVbl, ZnVil ZnVll**) can suppress aggregation and thereby increase the solubility of the porphyrin,[4.12] and the ester (**ZnVbm, ZnVim**) provides a motif for apical coordination in self-assembly processes.

4.5. Outlook

The synthesis of porphyrins bearing one or two meso-substituents (A-porphyrin, *trans*-AB-porphyrin) requires use of a C1 synthon that provides greater reactivity than that of a primary carbinol group. The *N*,*N*-dimethylaminomethyl group serves as an effective C1 synthon owing to the ease of introduction, reactivity in the absence of an added Brønsted acid, and reaction under mild conditions without detectable acidolysis. The method described herein affords rather modest yields of zinc porphyrins. The low yields are offset by the absence of scrambling, the broad scope, and the ease of implementation.

4.6. Experimental

4.6.1. General

All ^{1}H NMR (400 MHz) and ^{13}C NMR (100 MHz) spectra were obtained in $CDCl_3$ unless noted otherwise. Porphyrins were analyzed by laser desorption mass spectrometry without a matrix (LD-MS).[4.16] Fast atom bombardment mass spectrometry (FAB-MS) data are reported for the molecule ion or protonated molecule ion. Column chromatography was

performed with flash silica. Each new compound was >95% pure as determined by ^{1}H NMR spectroscopy.

4.6.2. Noncommercial compounds

The dipyrromethanes **Ia**,[4.3] **Ib**,[4.3] **Ic**,[4.5] **Id**,[4.6] **Ie**,[4.7] **If**,[4.8] **Ig**,[4.4] **Ih**,[3.6] **Ii**,[4.9] **Ij**,[4.10] **Ik**,[4.11] **Il**,[4.12] **Im**,[4.13] **In**[4.14] were prepared using a new method that entails reaction of an aldehyde in 100 equivalents of pyrrole containing a Lewis acid (e.g., $InCl_3$).[4.15]

4.6.3. Standard procedures

Aminomethylation of a dipyrromethane, exemplified for 1,9-bis(*N*,*N*-dimethylaminomethyl)-5-phenyldipyrromethane (IIIa). A solution of **Ia** (667 mg, 3.00 mmol) in CH_2Cl_2 (30 mL) at room temperature was treated with *N*,*N*-dimethylmethyleneammonium iodide (Eschenmoser's reagent; employed as a fine powder; 1.17 g, 6.30 mmol). After 1 h, CH_2Cl_2 (100 mL) and aqueous $NaHCO_3$ (100 mL) were added to the reaction mixture. The organic phase was dried (Na_2SO_4) and then concentrated to dryness. Addition of hexanes/CH_2Cl_2 afforded a precipitate, which upon filtration was obtained as a pale yellow solid (600 mg, 59%): mp 76–78 °C; ^{1}H NMR δ 2.17 (s, 12H), 3.33 (s, 4H), 5.37 (s, 1H), 5.72–5.74 (m, 2H), 5.89–5.91 (m, 2H), 7.19–7.31 (m, 5H), 8.07–8.18 (br, 2H); ^{13}C NMR δ 44.3, 45.0, 56.7, 106.8, 107.3, 126.7, 128.36, 128.48, 128.9, 132.5, 142.4; Anal. Calcd for $C_{21}H_{28}N_4$: C, 74.96; H, 8.39; N, 16.65. Found: C, 74.76; H, 8.63; N, 16.27.

Porphyrin formation from 1,9-bis(*N*,*N*-dimethylaminomethyl)dipyrromethanes,

exemplified for Zn(II)-5-mesityl-15-phenylporphyrin (ZnVac) via IIIa + Ic. A solution of **IIIa** (168 mg, 0.500 mmol) and 5-mesityldipyrromethane (**Ic**, 132 mg, 0.500 mmol) in ethanol (50 mL) at room temperature was treated with $Zn(OAc)_2$ (917 mg, 5.00 mmol). The mixture was heated to reflux. After 2 h, the reaction mixture was allowed to cool to room temperature. A sample of DDQ (340 mg, 1.50 mmol) was added and the mixture was stirred for 15 min. TEA (355 μL, 2.50 mmol) was added and the reaction mixture was concentrated to dryness. Column chromatography [silica, hexanes/CH_2Cl_2 (1:1)] afforded a purple solid (42.4 mg, 15%): ^{1}H NMR δ 1.85 (s, 6H), 2.68 (s, 3H), 7.34 (s, 2H), 7.80–7.82 (m, 3H), 8.25–8.28 (m, 2H), 9.00 (d, *J* = 4.4 Hz, 2H), 9.14 (d, *J* = 4.4 Hz, 2H), 9.41 (d, *J* = 4.4 Hz, 2H), 9.45 (d, *J* = 4.4 Hz, 2H), 10.30 (s, 2H); ^{13}C NMR δ 21.7, 22.0, 106.1, 118.7, 120.2, 126.9, 127.7, 128.0, 131.6, 131.9, 132.5, 132.7, 134.8, 137.8, 139.0, 139.6, 142.9, 149.65, 149.74, 150.17, 150.31; Anal Calcd for $C_{35}H_{26}N_4Zn$: C, 74.01; H, 4.61; N, 9.86. Found: C, 74.27; H, 4.72; N, 9.53; LD-MS obsd 565.9, Calcd 566.14 ($C_{35}H_{26}N_4Zn$); λ_{abs} 372, 392, 412, 544 nm.

REFERENCES

(4.1) Geier, G. R., III; Callinan, J. B.; Rao, P. D.; Lindsey, J. S. *J. Porphyrins Phthalocyanines* **2001**, *5*, 810–823.

(4.2) Fan, D.; Taniguchi, M.; Yao, Z.; Dhanalekshmi, S.; Lindsey, J. S. *Tetrahedron* **2005**, *61*, 10291−10302.

(4.3) Mizutani, T.; Ema, T.; Tomita, T.; Kuroda, Y.; Ogoshi, H. *J. Am. Chem. Soc*. **1994**, *116*, 4240–4250.

(4.4) Hammel, D.; Erk, P.; Schuler, B.; Heinze, J.; Müllen, K. *Adv. Mater.* **1992**, *4*,

737–739.

(4.5) Lee, C.-H.; Lindsey, J. S. *Tetrahedron* **1994**, *50*, 11427–11440.

(4.6) Lee, C.-H.; Kim, J.-Y. *Bull. Korean Chem. Soc.* **1996**, *17*, 215–217.

(4.7) Boyle, R. W.; Karunaratne, V.; Jasat, A.; Mar, E. K.; Dolphin, D. *Synlett* **1994**, 939–940.

(4.8) Oddo, B.; Cambieri, F. *Gazz. Chim. Ital.* **1940**, *70*, 559–564.

(4.9) Wang, Q. M.; Bruce, D. W. *Synlett* **1995**, 1267–1268.

(4.10) Balakumar, A.; Muthukumaran, K.; Lindsey, J. S. *J. Org. Chem.* **2004**, *69*, 5112–5115.

(4.11) Liu, Z.; Yasseri, A. A.; Loewe, R. S.; Lysenko, A. B.; Malinovskii, V. L.; Zhao, Q.; Surthi, S.; Li, Q.; Misra, V.; Lindsey, J. S.; Bocian, D. F. *J. Org. Chem.* **2004**, *69*, 5568–5577.

(4.12) Thamyongkit, P.; Speckbacher, M.; Diers, J. R.; Kee, H. L.; Kirmaier, C.; Hilten, D.; Bocian, D. F.; Lindsey, J. S. *J. Org. Chem.* **2004**, *69*, 3700–3710.

(4.13) Trova, M. P.; Gauuan, P. J. F.; Pechulis, A. D.; Bubb, S. M.; Bocckino, S. B.; Crapo, J. D.; Day, B. J. *Bioorg. Med. Chem.* **2003**, *11*, 2695–2707.

(4.14) Wilson, G. S.; Anderson, H. L. *Synlett* **1996**, 1039–1040.

(4.15) Laha, J. K.; Dhanalekshmi, S.; Taniguchi, M.; Ambroise, A.; Lindsey, J. S. *Org. Process Res. Dev.* **2003**, *7*, 799–812.

(4.16) Srinivasan, N.; Haney, C. A.; Lindsey, J. S.; Zhang, W.; Chait, B. T. *J. Porphyrins Phthalocyanines* **1999**, *3*, 283–291.

Chapter 5

Design and Synthesis of Porphyrin-Based Step-1 SPRs

5.1. General Information on Self-Assembly of Tetrapyrroles

Self-assembly by tetrapyrrolic compounds is of great interest because of the well-defined 3-dimentional architectures found within these aggregates. In photosynthetic systems, tetrapyrroles self-organize to form superstructures that perform many essential light-harvesting and energy-transfer functions. An example is provided by the light-harvesting rods of chlorosomes in green-sulfur bacteria. Chlorosomes are composed of aggregates of bacteriochlorophyll *c* (BChl *c*) without any proteinaceous scaffold.[5.1] This arrangement of highly concentrated pigments allows efficient collection of weak light and transfer of the resulting energy to the photoreaction center. Studies of the self-assembly of BChl *c* analogues (e.g., porphyrins and chlorins) revealed that the light-harvesting pigments are held together by relatively weak, non-covalent interactions such as hydrogen bonding and π-π stacking forces. The pattern of aggregation is determined by the primary chemical structure of the BChl *c* monomer. The critical interactions within the self-assembled structure include (1) coordination of the central magnesium atom of one molecule to the 3^1-hydroxyl group of a second BChl *c*; (2) hydrogen bonding of the same 3^1-hydroxyl group to the 13^1-carbonyl group of a third BChl *c* molecule; and (3) π-π interactions between the macrocycles. (Figure 5.1).[5.2]

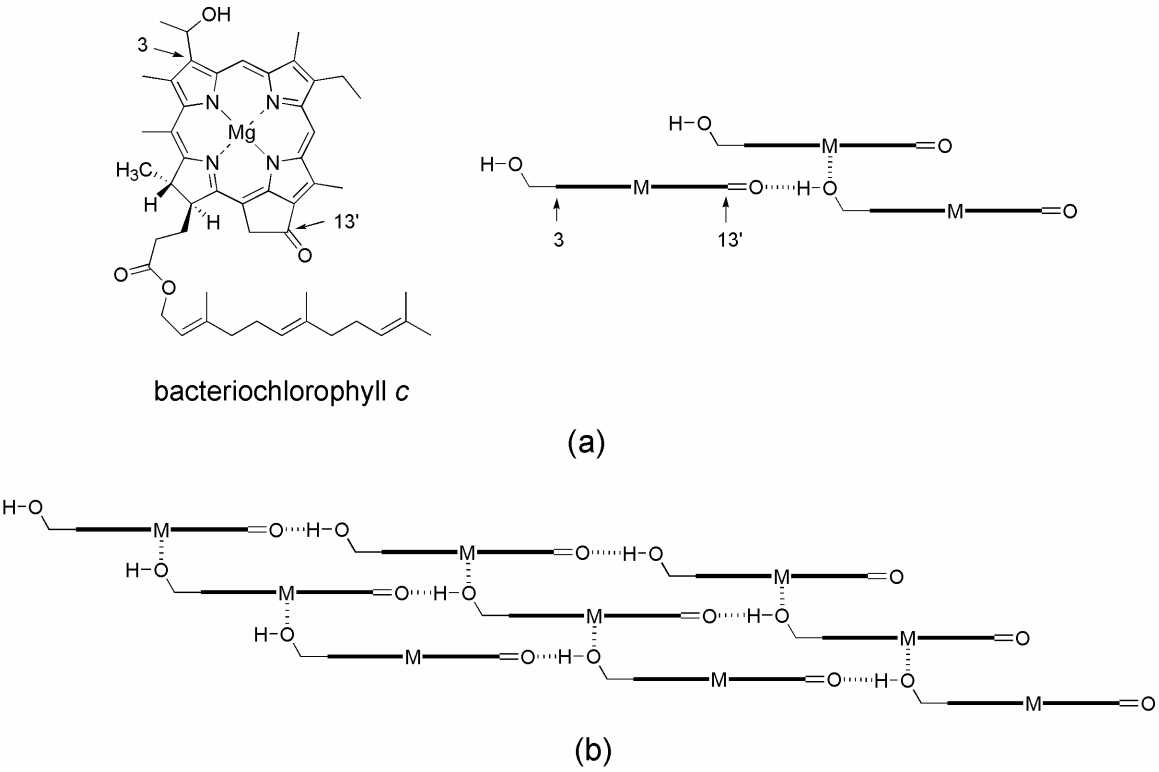

Figure 5.1. Intermolecular interactions of self-assembled bacteriochlorophyll *c* molecules: (a) a unit of cross-linkage; (b) a two-dimensional sheet of aggregates.

Tetrapyrroles with distinct structures can aggregate in organized manners other than the natural pattern described above. Because methodology is relatively well developed for preparing synthetic porphyrins, most studies of tetrapyrrole self-assembly have employed porphyrins rather than chlorins or bacteriochlorins. The self-assembled architectures of porphyrins that have been reported include but are not limited to (1) one-dimensional columns of a mixture of positively and negatively charged porphyrins;[5.3] (2) three-dimensional networks of porphyrins bearing meso 3,5-dihydroxyphenyl groups (see Chapter 5.2);[5.4] (3) cyclohexameric aggregates of zinc-porphyrin dimers bearing imidazolyl groups (see Chapter 5.4);[5.5] (4) one-dimensional columns of glucosyl-porphyrins;[5.6] (5) one-dimensional columns of cobalt or zinc porphyrins bearing pyridyl groups;[5.7] and (6) tetrameric aggregates of porphyrins bearing 2-aminopyrimidyl groups.[5.8]

We looked to those self-assembly models for guidance in our study of porphyrin-based Step-1 SPRs. This was done because in the S.T.A.R. method, the platform constructed by porphyrin aggregates with a defined architecture (wherein the handle moieties for the binding of the Step-3 agent are fully exposed) is preferred over an amorphous precipitate (where the handles may be inaccessible). The distinct structures that lead to self-assembled porphyrin architectures may be employed as intermolecular association groups, which direct the aggregation of the insoluble form of the SPR molecules (see Chapter 3.1.1). Therefore, we designed porphyrin-based SPRs by adhering to the following steps: (1) choose a known self-assembled porphyrin as the centerpiece of the SPR; (2) mask the structures required for self-assembly with enzymatically cleavable, water-solubilizing groups; and (3) place the other required components (e.g., CTA and Loracarbef) at positions on the porphyrin that are synthetically accessible. Therefore, once the water-solubilizing groups are cleaved by an enzyme, the insoluble porphyrin possessing the structure required for self-assembly can precipitate in the desired pattern. It must be noted that all self-assembled architectures reported in the literature[5.1-5.8] were observed in organic solvents. A porphyrin that self-assembles under aqueous conditions has not been reported. On the other hand, even if the insoluble porphyrin fails to self-assemble, our designs may still function to some extent in the S.T.A.R. method by forming an amorphous precipitate.

5.2. Model A: Porphyrin Self-Assembly Based on Meso 3,5-dihydroxyphenyl Groups

Porphyrins bearing four meso 3,5-dihydroxyphenyl groups are known to self-assemble to form three-dimensional networks[5.4] (Figure 5.2) while porphyrins bearing one meso 3,5-dihydroxyphenyl group can form one-dimensional columnar structure[5.9]. The

major driving force is the hydrogen-bonding between the hydroxyl groups on adjacent porphyrins. The π-π stacking interaction is considered negligible because of the distance between the macrocycles.

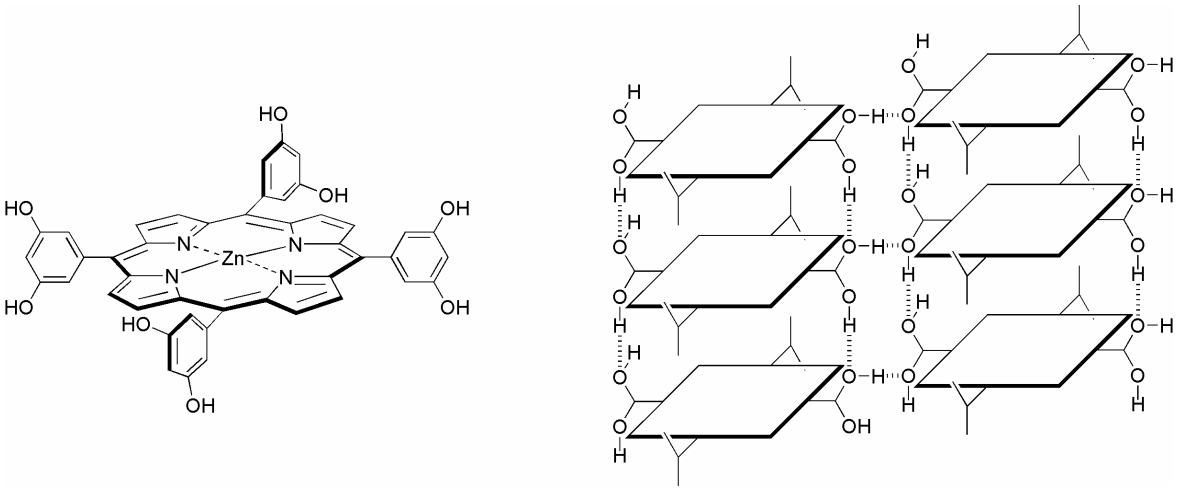

Figure 5.2. Tetrakis(3,5-dihydroxyphenyl)porphyrin and its self-assembled structure. A two-dimensional sheet is shown here while three-dimensional network was also reported.[5-4]) The proximal and distal aryl moieties are truncated, and the lateral aryl moieties are displayed in abbreviated

5.2.1. A Porphyrin-Based Step-1 SPR: Design 1.

5.2.1.1. Design and Retrosynthesis. On the basis of this self-assembly model, we designed our first porphyrin-based Step-1 SPR. The structure of Design 1 includes four glucosyl groups that are attached to two dihydroxyphenyl groups at the *trans*-meso-positions, and a Loracarbef moiety and a thiol-terminated linker at the other two meso-positions (Scheme 5.1). After the enzymatic removal of the glucosyl groups, the SPR will be converted to an insoluble form and the two meso 3,5-dihydroxyphenyl groups will be exposed to direct the self-assembly of the insoluble SPR by hydrogen-bonding. Since the conformation of the meso phenyl rings is largely perpendicular to the plane of the porphyrin macrocycle, the sugar molecules attached to the 3,5-positions on the phenyl groups project

above and below the plane of the porphyrin ring, thereby suppressing π-π stacking interactions. The Loracarbef (the binding handle for the Step-3 agent) and the thiol-terminated linker (for coupling with a maleimide-derivatized carrier or CTA) can be attached to the porphyrin via amide linkages.

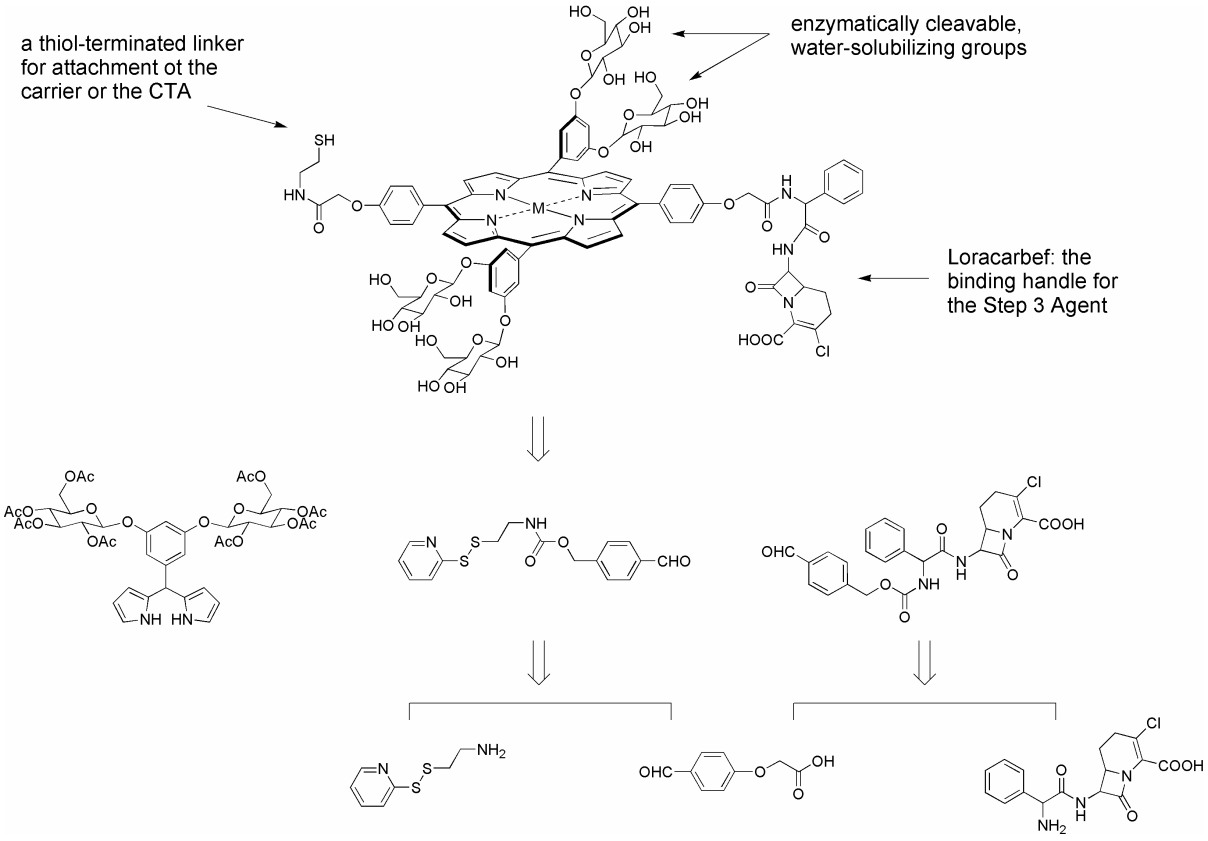

Scheme 5.1. Porphyrin-based Step-1 SPR–Design 1: Structure and retrosynthesis.

The porphyrin-based SPR in Design 1 can be synthesized in a conventional manner as shown in Scheme 5.1. The precursors (e.g., dipyrromethane and aldehyde) bearing glucosyl groups, a thiol-terminated linker or Loracarbef are synthesized; the appropriate condensation of such precursors will afford a porphyrin with all the required components. The aldehyde bearing a thiol-terminated linker or Loracarbef can be synthesized from a carboxy-

benzaldehyde and an amino-thiol or Loracarbef by amide-bond formation. Alternatively, the synthesis of a glucosyl-porphyrin bearing carboxylate moieties can be carried out first and both the linker and Loracarbef can be introduced after porphyrin formation.

5.2.1.2. Synthesis of Glycosylated Porphyrins. I carried out the synthesis of several glycosylated porphyrins to examine their water-solubility and possible utility as motifs in porphyrin-containing SPRs. Following a literature procedure,[5.10] 3,5-bis(acetylglucosyl)benzaldehyde **1** was synthesized by the condensation of 3,5-dihydroxybenzaldehyde and acetylglucosyl bromide in the presence of silver oxide. Condensation of **1** with excess pyrrole catalyzed by TFA[5.11] afforded dipyrromethane **2** bearing two sugar moieties (Scheme 5.2). A model *trans*-A_2B_2-porphyrin **3**, which bears two meso 3,5-bis(glucosyl)phenyl groups (with acetyl protection) and two phenyl groups (instead of Loracarbef and the thiol-terminated linker in the SPR molecule), was synthesized from dipyrromethane **2** and benzaldehyde. Only insignificant scrambling (see Chapter 3.2) in the reaction mixture was observed upon examination by LD-MS analysis despite the low yield (7%). On the other hand, free-base octakis(acetylglucosyl)porphyrin **4** was synthesized as reported from benzaldehyde **1** and pyrrole in 14% yield.[5.12] Metalation of **4** with zinc acetate[3.5] afforded the corresponding metalloporphyrin **4Zn**.

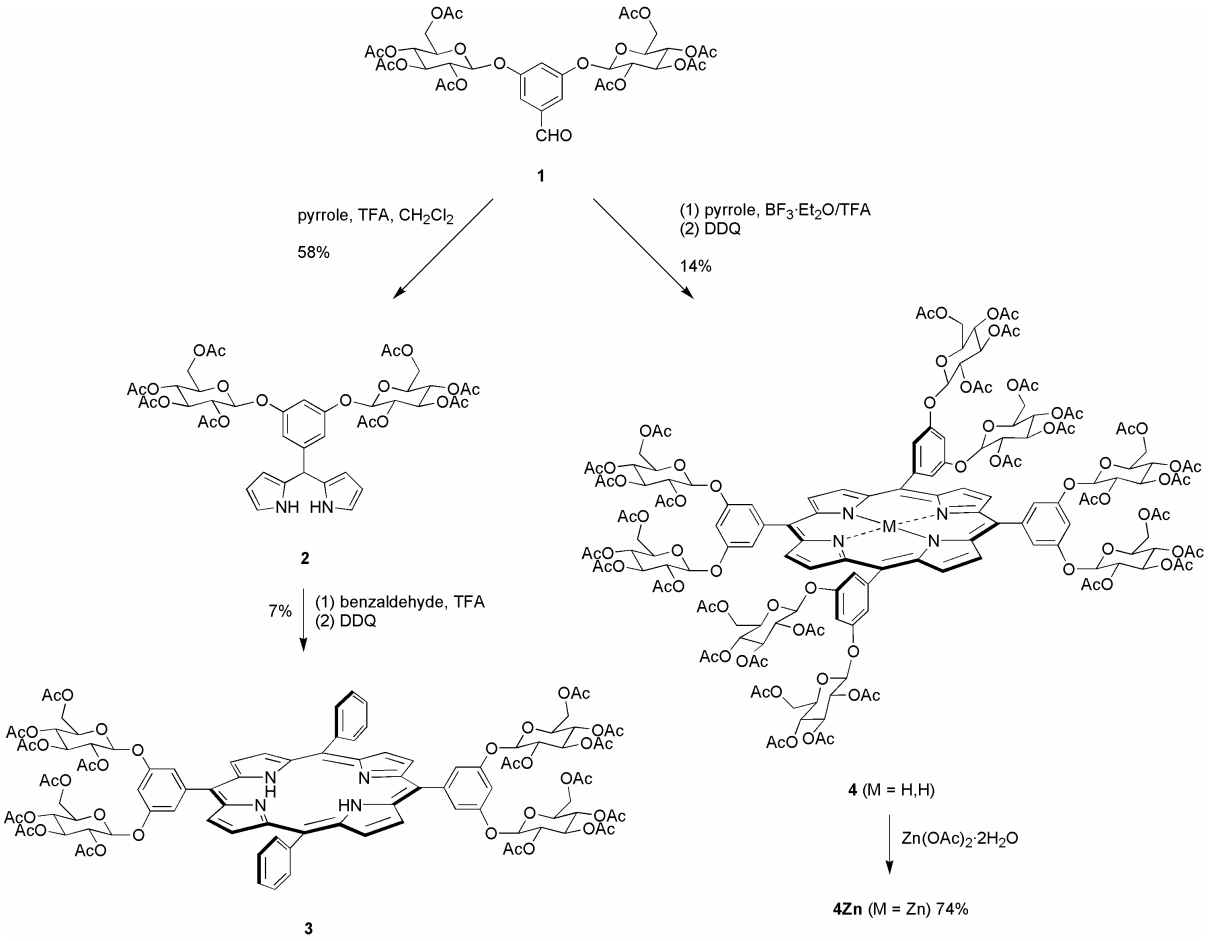

Scheme 5.2. Synthesis of porphyrins bearing meso bis(acetylglucosyl)phenyl groups.

Glucuronic acid was also employed in the synthesis of glycosylated porphyrins. Benzaldehyde **5** bearing two glucuronyl moieties was synthesized from 3,5-dihydroxybenzaldehyde and methyl acetylglucuronate in the presence of silver oxide in 54% yield (Scheme 5.3). The condensation of **5** with pyrrole was catalyzed by a mixture of TFA and $BF_3{\cdot}O(Et)_2$. In this manner,[5.13] octakis(methyl acetylglucuronate)porphyrin **6** was obtained in 22% yield after DDQ oxidation.

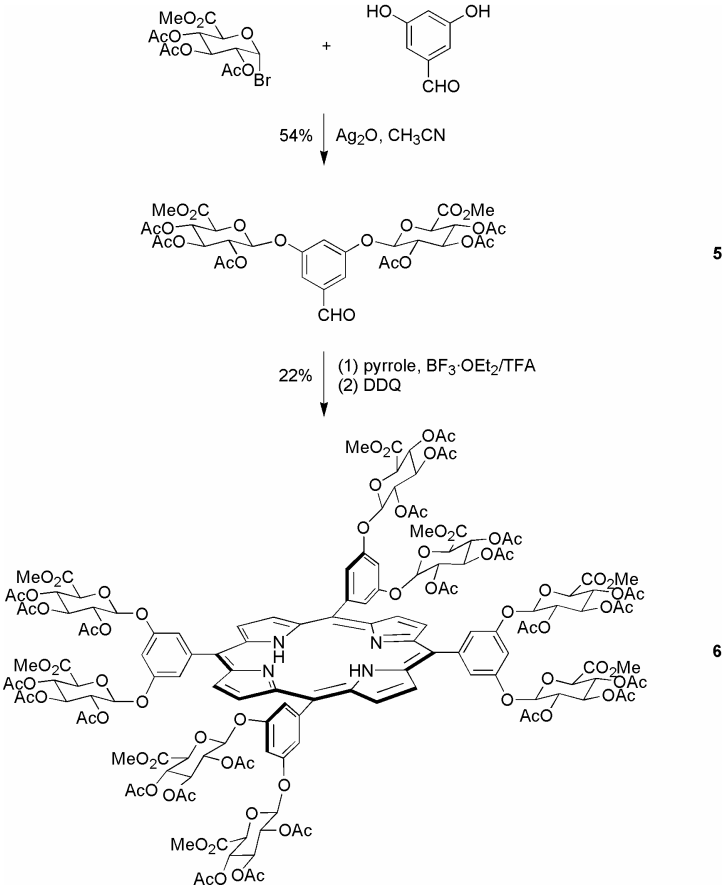

Scheme 5.3. Synthesis of a porphyrin bearing eight glucuronyl moieties.

5.2.1.3. Synthesis of Precursors Bearing a Carboxylate Moiety. As shown in the retrosynthesis (Scheme 5.1), Loracarbef and the thiol-terminated linker are each attached to the porphyrin by an amide bond. Therefore, the porphyrin needs to carry carboxylate moieties that can undergo amide formation with the amino groups on Loracarbef and the thiol-terminated linker. We synthesized the corresponding dipyrromethanes and aldehydes bearing carboxyl groups (Scheme 5.4). The reaction of 4-hydroxybenzaldehyde and ethyl bromoacetate afforded 4-(ethoxycarbonylmethoxy)benzaldehyde (**7**) in 78% yield. Condensation of **7** with excess pyrrole afforded 5-[4-(ethoxycarbonylmethoxy)phenyl]dipyrromethane (**8**). The ester group on compound **8** can be converted to the free acid by basic hydrolysis. However, the purification of the

dipyrromethane bearing a carboxylic acid was not successful due to the complexity of the reaction mixture. Alternatively, aldehyde **9** bearing a free acid was obtained quantitatively upon hydrolysis of **8**. The reaction of **9** with pyrrole yielded dipyrromethane **10** in 35% yield. Dipyrromethanes **8** and **10** were reported by the Mareček group[5.14] in 2005 following similar routes as we have explored.

Compound **9** or **10** bearing a free acid group provides alternatives in the synthesis of the porphyrin-based SPRs. We may attach Loracarbef or the thiol-terminated linker to aldehyde **9** or dipyrromethane **10** and employ the product in the porphyrin synthesis. The other options are to synthesize an ester-porphyrin from compound **7** or **8**, hydrolyze the ester to recover the free acid and then perform a coupling reaction with Loracarbef or the linker.

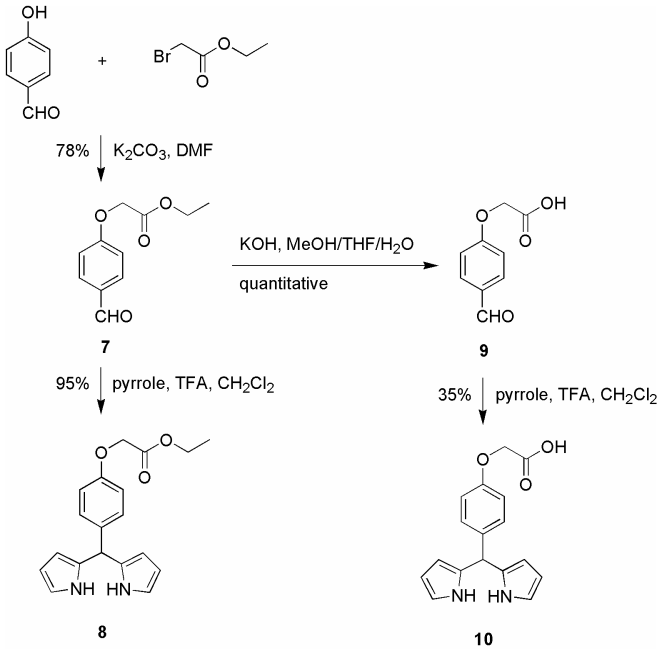

Scheme 5.4. Syntheses of aldehydes and dipyrromethanes bearing a carboxylic acid group.

I investigated new, simple approaches for preparing porphyrins bearing carboxylic acid moieties. I found that a carboxylic acid moiety may also be introduced in the acylation of a dipyrromethane with succinic anhydride (Scheme 5.5). The nucleophilic attack at the

carbonyl carbon of succinic anhydride opens the five-membered ring and unveils a carboxylic acid group. I synthesized two 1-acyldipyrromethanes: the acyldipyrromethane bearing a free carboxylic acid and the acyldipyrromethane bearing a protected carboxylic acid. The acyldipyrromethanes were reduced and the resulting carbinols were used for porphyrin formation catalyzed by TFA or $Yb(OTf)_3$[4.1]. Following a literature procedure,[3.6] 5-phenyldipyrromethane (**11**) was treated with EtMgBr and succinic anhydride to afford 1-acyldipyrromethane **12** bearing a carboxylic acid group in 40% yield (Scheme 5.5). Compound **12** was reduced by $NaBH_4$ and the resulting carbinol was treated with TFA (Table 5.1, Entry 1) or $Yb(OTf)_3$ (Entry 2). A trace amount of dicarboxyporphyrin **13** was observed in the reaction mixture (by LD-MS analysis) when TFA was employed as the acid catalyst. On the other hand, the reaction with $Yb(OTf)_3$ did not yield any porphyrin (by absorption spectroscopy). The presence of the free carboxylic acid in the porphyrin-forming reaction may cause the failure of the condensation reaction. Therefore, the carboxylic acid group in **12** was converted to a 2-(trimethylsilyl)ethyl ester by a carbodiimide-mediated coupling reaction. Following a literature procedure,[5.15] the crude **12** from the acylation reaction was treated with 1,3-dicyclohexylcarbodiimide (DCC) and 2-(trimethylsilyl)ethanol (TMSE) (Scheme 5.5). The overnight reaction yielded 1-acyldipyrromethane **14** in 56% yield. The improvement in yield is attributed to the fact that **14** is less polar than **13**, thus facilitating purification by chromatography. 1-Acyldipyrromethane **14** was reduced and the self-condensation reaction with TFA catalysis yielded three different porphyrins (Table 5.1, Entry 3). *Trans*-A_2B_2-porphyrin **15** bearing two 2-(trimethylsilyl)ethyl propionate groups was isolated in 5% yield. A porphyrin bearing one protected acid and one free acid, and dicarboxyporphyrin **13** were also observed in the reaction mixture by LD-MS analysis. The

ratio among three porphyrins was approximately 1:1:1 on the basis of the intensities of the corresponding mass peaks. The condensation catalyzed by $Yb(OTf)_3$ (Table 5.1, Entry 4) again failed to afford any porphyrin. The removal of the silyl-protecting group may occur during the reduction of the acyldipyrromethane or during the condensation process. Therefore, we performed the reduction of **14** at 0 °C (instead of room temperature) followed by the self-condensation. Although the reaction yielded exclusively porphyrin **15**, the yield (5%) was not improved.

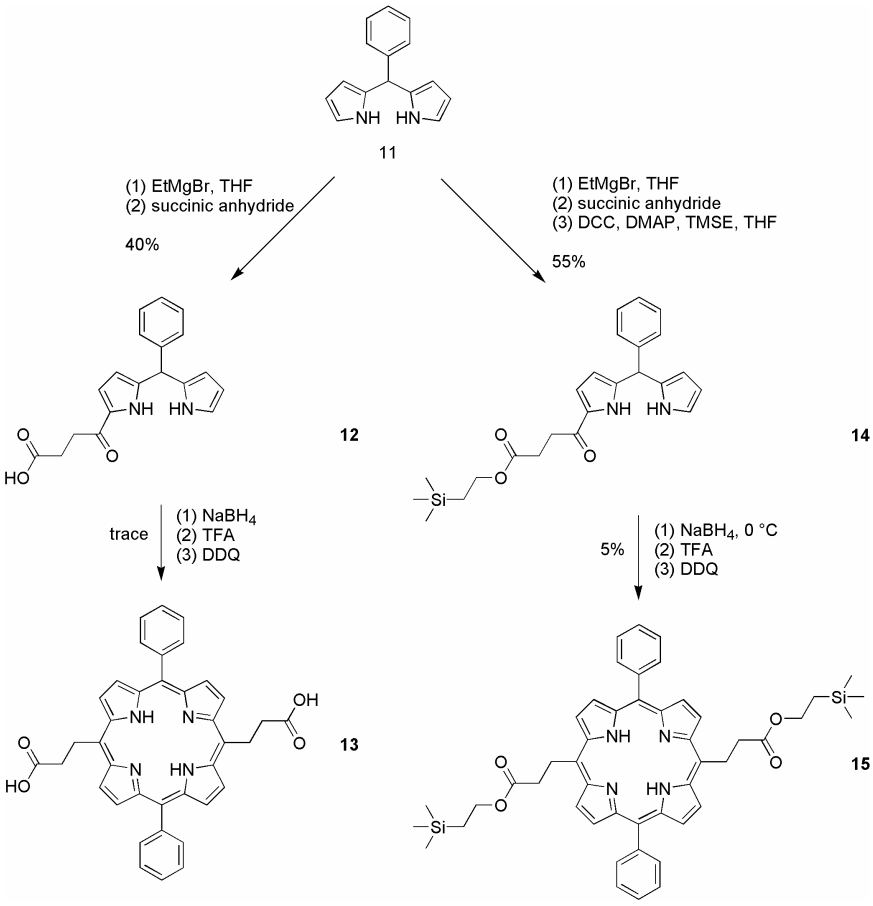

Scheme 5.5. Synthesis of porphyrins bearing carboxylic acids via acylation with succinic anhydride.

Table 5.1. Synthesis of porphyrins bearing carboxy moieties from 1-acyldipyrromethanes.

Entry	1-acyl dipyrromethane	Reduction temperature	Acid	Observation
1	**12**	RT	TFA	Trace amount of **13**
2	**12**	RT	$Yb(OTf)_3$	No porphyrin
3	**14**	RT	TFA	Three porphyrinic products were observed: porphyrin **15** and two deprotected products.
4	**14**	RT	$Yb(OTf)_3$	No porphyrin
5	**14**	0 °C	TFA	Porphyrin **15** as the only porphyrinic product

5.2.1.4. Synthesis of Glycosylated Porphyrins Bearing Carboxylate Moieties. We employed the precursors (i.e., aldehydes and dipyrromethanes) described in Chapter 5.2.1.2 and 5.2.1.3 in the synthesis of glycosylated porphyrins bearing carboxylate moieties. *Trans*-A_2B_2-porphyrin **19** bearing two carboxylate moieties was synthesized from dipyrromethane **2** and aldehyde **7** with $BF_3{\cdot}O(Et)_2$ catalysis[3-8] (Equation 5.1a). Scrambling was observed, and porphyrin **19** was isolated in 23% yield from a mixture containing the A_3B-porphyrin and the *cis*-A_2B_2-porphyrins. We also synthesized a porphyrin bearing six glucosyl groups in a statistical manner (Equation 5.1b). Condensation of dipyrromethane **2** with a mixture of aldehydes **1** and **7** (**2**:**1**:**7** = 2:1:1) afforded a mixture of porphyrins, from which porphyrin **20** was isolated in 10% yield.

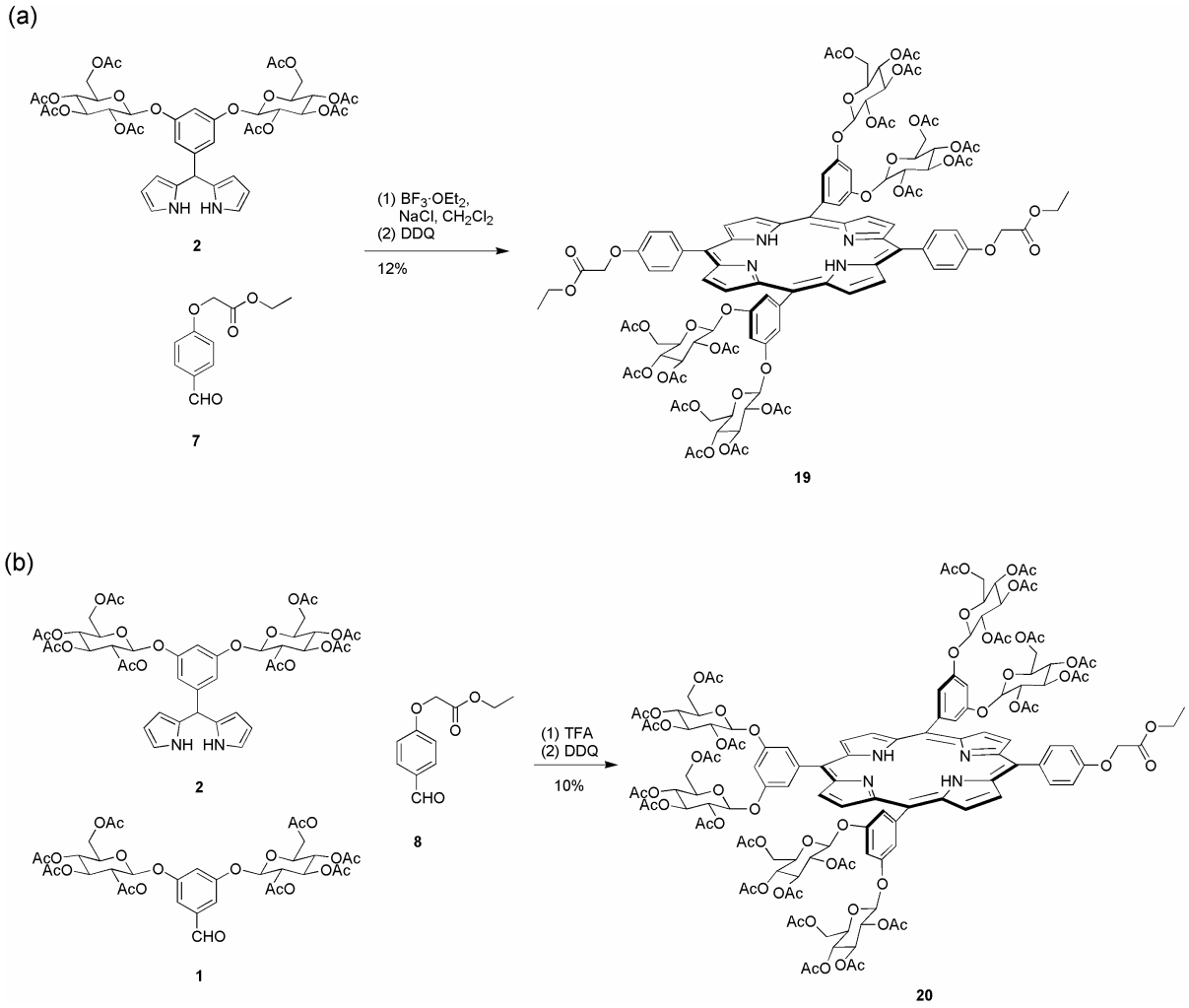

Equation 5.1. Synthesis of porphyrins bearing both glucosyl and carboxylate moieties.

5.2.1.5. Deprotection of Glycosylated Porphyrins. According to the literature,[5.12] acetyl groups on sugar units can be easily removed by treatment with sodium methoxide in MeOH or MeOH/THF in 10 min. However, the attempted deprotection of octakis(acetylglucosyl)porphyrins (**4**, **4Zn**, **4Cu**) under such conditions did not afford the corresponding glucosylporphyrins. Alternatively, overnight treatment of porphyrin **4** with triethylamine (TEA) at 40 °C[5.16] yielded octaglucosyl porphyrin **21** (Table 5.2, Entry 1). Deacetylation of **19** or **20** under the same conditions yielded glucosyl-porphyrin **22** or **23**, respectively (Entry 2 and 3). Porphyrin **22** bears four glucosyl groups, one ester and one

carboxylic acid group whereas **23** bears six glucosyl groups and one carboxylic acid group.

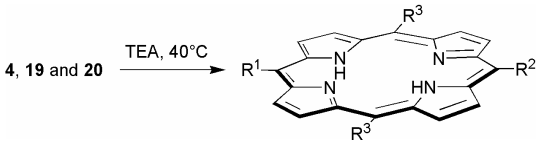

Table 5.2. Deacetylation of glycosylated porphyrins.

Entry	Acetyl-porphyrin	Reaction condition	Glucosyl-porphyrin	R^1	R^2	R^3
1	**4**	TEA, 40 °C, overnight	**21**	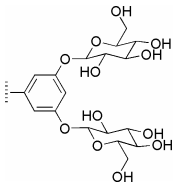	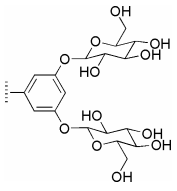	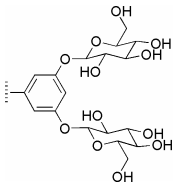
2	**19**		**22**	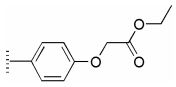	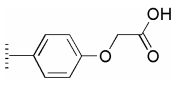	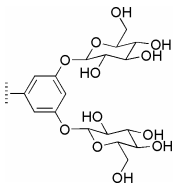
3	**20**		**23**	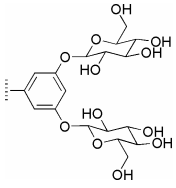	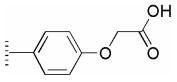	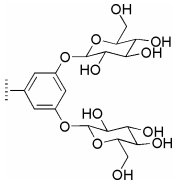

5.2.1.6. Aqueous Solubility Test for Glucosyl-Porphyrins. The deacetylation reactions were monitored by LD-MS. After the starting porphyrin **4**, **19** or **20** was totally consumed, the reaction mixture was concentrated and used for a water-solubility test without purification. All three glucosyl-porphyrins (**21**, **22** and **23**) were found to be soluble to some degree both in MeOH and in H_2O. While a solution of **21** in each solvent is purple-colored, a MeOH solution of **22** or **23** is purple but an aqueous solution is green. The absorption spectrum of **21**, **22** or **23** in MeOH showed a sharp absorption around 417 nm. On the other hand, the absorption spectrum of **21** in H_2O displayed a broadened Soret band shifted to 384 nm (Figure 5.3). Although the Soret band for an aqueous solution of **22** or **23**

also became broader, no significant blue shift was observed. Both the blue shift of the Soret band and the broadened absorption pattern indicate aggregation of porphyrin molecules. The concentrated reaction mixture of each glucosyl-porphyrin was dissolved in H_2O (HPLC grade). Centrifugation yielded a precipitate and a clear supernatant for each porphyrin (Figure 5.4). The saturated aqueous solution (i.e., the clear supernatant) was isolated and the absorption spectrum in water was obtained. The concentration was calculated from the absorption intensity of the Soret band (384 nm for **21**, 419 nm for **22**, and 416 nm for **23**; assumed ε_{Soret} = 500,000 $M^{-1}cm^{-1}$). The result shows that the concentrations of **21** (0.21 mM) and **22** (0.20 mM) are similar while the saturated solution of **23** is approximately half as concentrated (97 μM). On the basis of these data, porphyrin **22** is as aqueous-soluble as **21**, which bears twice as many glucosyl groups, probably because of the charged moiety (i.e., the carboxylate) on **22**. On the other hand, we do not have an explanation for the fact that **22**, which bears four glucosyl groups and one carboxylic acid group is more aqueous-soluble than **23**, which bears six glucosyl groups and one carboxylic acid group.

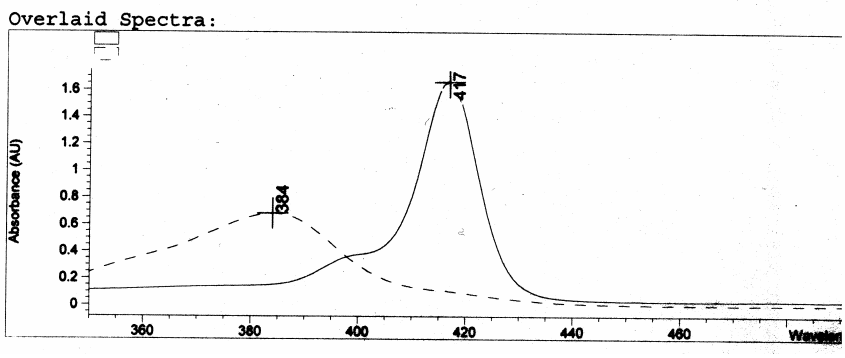

Figure 5.3. Absorption spectra of octaglucosyl porphyrin **21** in MeOH (solid line) and water (dotted line).

After each saturated solution stood at room temperature for 72 hours, tiny purple flocculants were observed with **21** or **23**. After centrifugation, the flocculants were deposited

in the tube containing **21** or **23** while no visible precipitate was observed in the tube containing **22** (Figure 5.4). The concentration of the supernatant of **21**, **22** or **23** was 21 μM, 0.20 mM or 0.54 mM, respectively. A fraction of suspended mixture was taken out from each tube and dissolved in DMF. LD-MS analysis showed that **21**, **22** or **23** was the only porphyrin species. Therefore, in each case, the decrease in concentration was due to aggregation of the porphyrins (instead of chemical modifications) during the 72 h incubation. The Shinkai group reported self-aggregation of a sugar-appended porphyrin driven by (1) π-π stacking interaction between the macrocycles, and (2) hydrogen-bonding between the glucosyl groups.[5.6a] In our case, the most extensive aggregation was observed in the solution of **21** (~90% of solubility loss upon aggregation), which is attributed to the presence of glucosyl groups at all four meso-positions. Such an architecture enables aggregation in a three-dimensional pattern by hydrogen-bonding. The solubility of **23** dropped approximately 50% while **22**, which only allows two-dimensional aggregation, did not show a significant decline in solubility. The presence of the charge on the carboxylate group may also prevent aggregation of **22** and **23**.

(a) (b) (c)

Figure 5.4. Formation of precipitate by glucosylated porphyrins: (a) **21**, (b) **22**, and (c) **23**. Each sample was dissolved in water and centrifuged (the left tube in each picture). The supernatant was transferred to another tube, stood for 72 h and centrifuged again (the right tube in each picture).

Porphyrin **6** bearing protected glucuronyl groups was also deacetylated upon treatment with TEA. The reaction mixture was concentrated and dissolved in water to yield a purple solution. Although the product octaglucuronyl porphyrin has not yet been identified, the aqueous solution did not yield a precipitate after standing for several days. The porphyrin concentration (~ 570 μM) calculated from the absorption spectrum showed no significant change during the period of observation.

In Design 1, we expected that the glucosyl groups positioned on both sides of the macrocycle would prevent two porphyrins from approaching each other in a "face-to-face" arrangement and thereby diminish the π-π stacking interactions. However, the results from the water-solubility experiments indicate that either the distance between the porphyrins was not large enough to preclude the π-π stacking interactions, or the hydrogen-bonding alone was sufficient to cause aggregation. On the other hand, the glucuronyl group appeared to be a promising candidate for the water-solubilizing group for the porphyrin-based SPRs. The negative charges on glucuronide moieties will repel porphyrins from each other by electrostatic effects.

5.2.2. A Porphyrin-based Step-1 SPR: Design 2.

5.2.2.1.Design and Retrosynthesis. While studying synthetic routes towards the first design of the porphyrin-based SPR, we pursued other possible structures based on the same model of self-assembly. In Design 1, Loracarbef is attached to the porphyrin via an amide bond (Scheme 5.1). In Design 2, Loracarbef is attached to the meso-position of the porphyrin via a reductive amination reaction between the amino group on Loracarbef and a

formyl group on the porphyrin (Scheme 5.6). The reductive amination will form a secondary amine that can potentially be thiolated to yield a thiol-terminated linker. The glycosylated porphyrin bearing three meso diglucosylphenyl groups and a meso 4-formylphenyl group can be synthesized in a similar manner as described for porphyrin **19**, which bears the same number of glucosyl groups and a carboxylic acid moiety. Compared to Design 1, the major advantage of Design 2 resides in the synthetic approach, wherein Loracarbef can be attached to the porphyrin without any protecting groups or purification of intermediates as required in the amide-forming strategy. Loracarbef is a very reactive molecule on account of the multiple functional groups it carries, including a β-lactam, α,β-unsaturated carboxylic acid, vinyl chloride, primary amine, and chiral amino acid. Thus the simplicity and the mild conditions of reductive amination are potentially very attractive for the coupling reaction with Loracarbef.

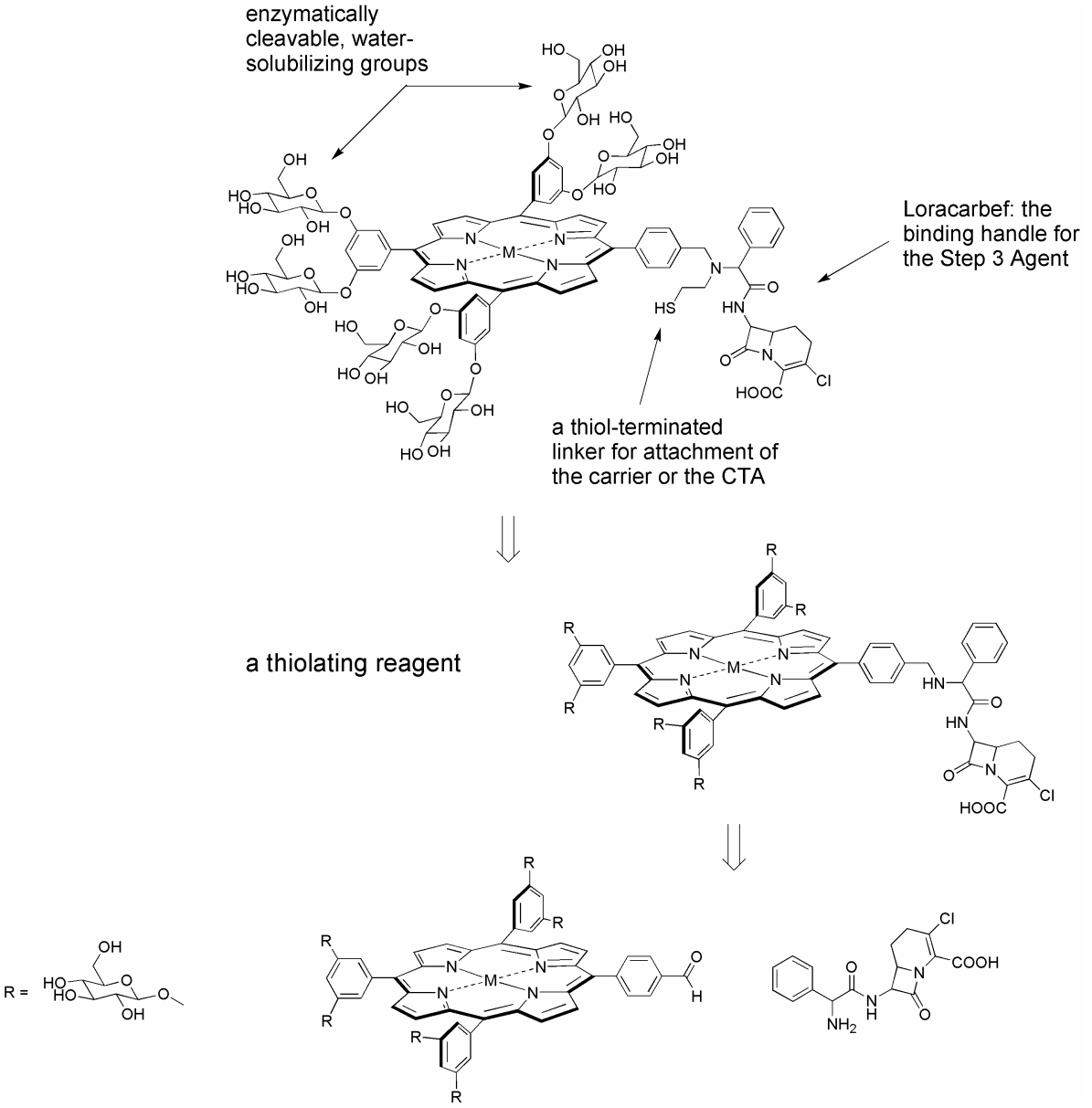

Scheme 5.6. Porphyrin-based Step-1 SPR–Design 2: Structure and retrosynthesis.

5.2.2.2. A Model Study: Reductive Amination of Loracarbef and benzaldehyde. The key step in the retrosynthesis for Design 2 is the reductive amination between Loracarbef and an aldehyde on the glycosylated porphyrin. Although we have not yet synthesized the porphyrin bearing a meso 4-formylphenyl group, we instead carried out a model study by using benzaldehyde (Equation 5.2). Following a literature procedure,[5.17]

Loracarbef was dissolved in an aqueous acetate buffer (pH = 5.0) and treated with a solution of benzaldehyde in THF and $NaBH_3CN$. The concentrations of Loracarbef and benzaldehyde were both 10 mM. The formation of the product benzylamine **24** was observed by ESI-MS analysis of the reaction mixture. Therefore, we conclude that Loracarbef can undergo reductive amination with an aryl aldehyde in aqueous media. A similar reaction is expected to occur when an aldehyde-bearing porphyrin is employed in the SPR synthesis.

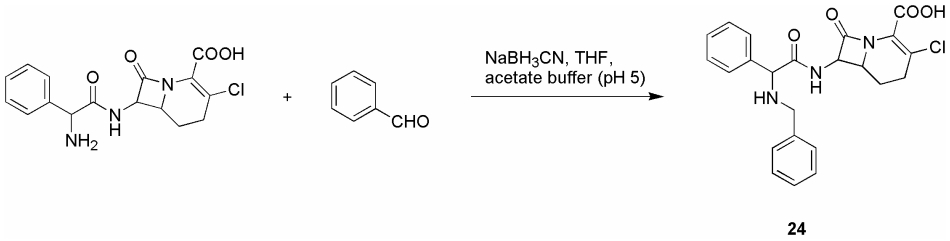

Equation 5.2. A model study for reductive amination between Loracarbef and benzaldehyde.

5.2.3 Conclusions for Design 1 and 2.

Our study towards Design 1 for a porphyrin-based SPR started from the syntheses of precursors bearing glucosyl moieties for providing water-solubility and carboxylate moieties for coupling with other components (i.e., Loracarbef and a linker that binds to the CTA). While there are several possible routes towards the target molecule, we synthesized a glucosyl-porphyrin bearing two carboxylate handles as the precursor of the final SPR. Unfortunately, the precursor porphyrin as well as other glucosyl-porphyrins slowly precipitated in water despite showing acceptable water-solubility in freshly prepared aqueous solutions. On the other hand, a preliminary result showed glucuronyl groups imparted lasting water-solubility to the porphyrin.

While we focused our research on the first design, we explored a key step for Design 2. A reductive amination reaction between Loracarbef and benzaldehyde (as an analogue of a porphyrin-aldehyde) was carried out. This model study showed that reductive amination in

aqueous solution is a promising method for the attachment of Loracarbef to the porphyrin.

A necessary alteration to Designs 1 and 2 is to replace glucosyl with glucuronyl groups so that the target porphyrins exhibit greater water-solubility and do not precipitate. However, we still lack efficient synthetic routes towards those target molecules. As a result, some of our key steps (e.g., porphyrin formation) rely on statistical reactions and the yields are generally low. Therefore, we proposed a new design (Design 3) based on a different model of porphyrin self-assembly, as described in the next section.

5.3. Model B: Porphyrin Self-assembly via a Hydroxymethyl Group, a Carbonyl Group and a Central Metal

As described in Chapter 5.1, bacteriochlorophyll *c* (BChl *c*) molecules in green photosynthetic bacteria self-assemble to form a light-harvesting apparatus in the absence of any proteinaceous scaffolding. Extensive studies on the self-assembled architectures of BChl *c* analogues have been reported by Balaban and by Tamiaki.[5.1,5.2] Three structural elements were found to be required for self-assembly in the same pattern as BChl *c*: a hydroxymethyl group, a carbonyl group and a 5- or 6-coordinate central metal (Figure 5.5a and b). The carbonyl group does not need to be coplanar with the macrocycle, as in BChl *c*, and can be incorporated as a keto moiety that has rotational freedom and can project perpendicular to the macrocycle plane. A linear alignment of the three elements (e.g., the hydroxymethyl group at C^3, the central magnesium, and the carbonyl group at C^{13} in the BChl *c* molecule) leads to extensive overlap of the macrocycles and give strong π-π interaction, while certain non-linear alignments also caused aggregation, such as the combination of a hydroxymethyl group at C^3, a central metal, and a carbonyl group at C^{15} or at C^{17} (Figure 5.5c).[5.2a]

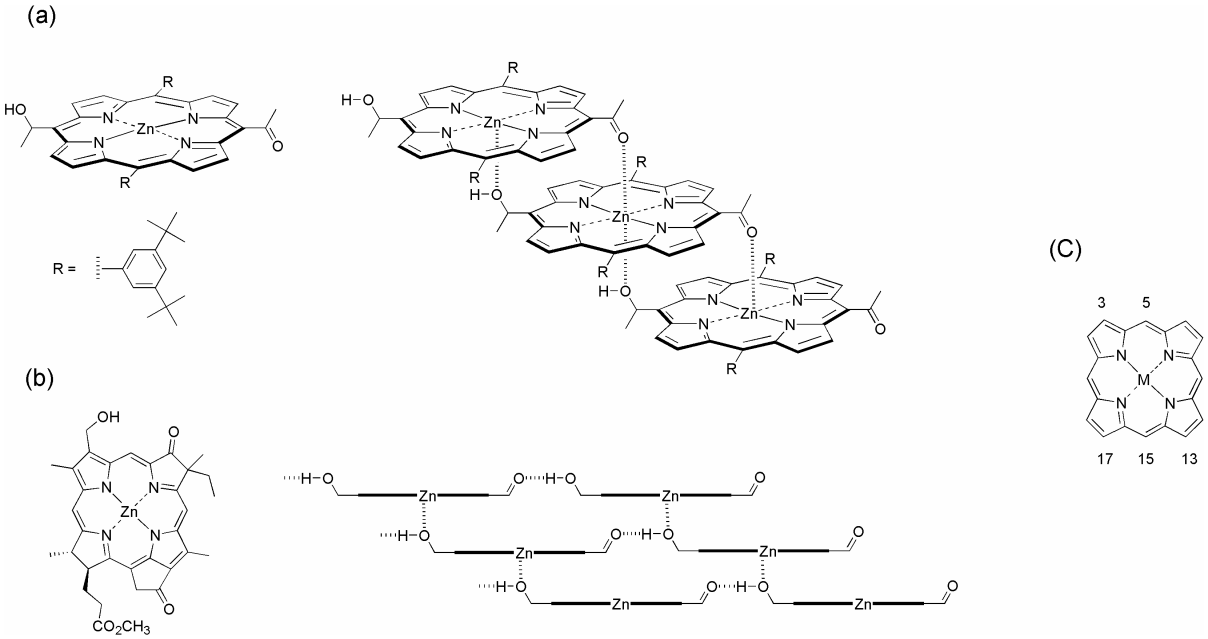

Figure 5.5. Self-assembled bacteriochlorophyll *c* analogues: (a) a self-assembled porphyrin, (b) a self-assembled chlorine, and (c) the numbering system of a porphyrin macrocycle.

5.3.1. A Porphyrin-Based Step-1 SPR: Design 3

5.3.1.1. Design and Retrosynthesis. In the third design of a Step-1 SPR, the target molecule carries a hydroxymethyl group masked by a glucuronide moiety and an acetyl group at *trans*-meso-positions (Scheme 5.7). The removal of the water-solubilizing moiety (i.e., glucuronide) reveals the hydroxymethyl group that will participate in the self-assembly process. Direct attachment of the glucuronic acid to the hydroxymethyl group may pose synthetic challenges. Therefore, a self-immolative linker will be introduced between the sugar and the hydroxymethyl group. The cleavage of the glucuronyl group is expected to cause spontaneous decomposition of the self-immolative linker and recovery of the meso-hydroxymethyl group. The Loracarbef moiety and the thiol-terminated linker are attached to the other two meso-positions. Owing to synthetic considerations, a linker will be employed to attach Loracarbef to the porphyrin meso-position.

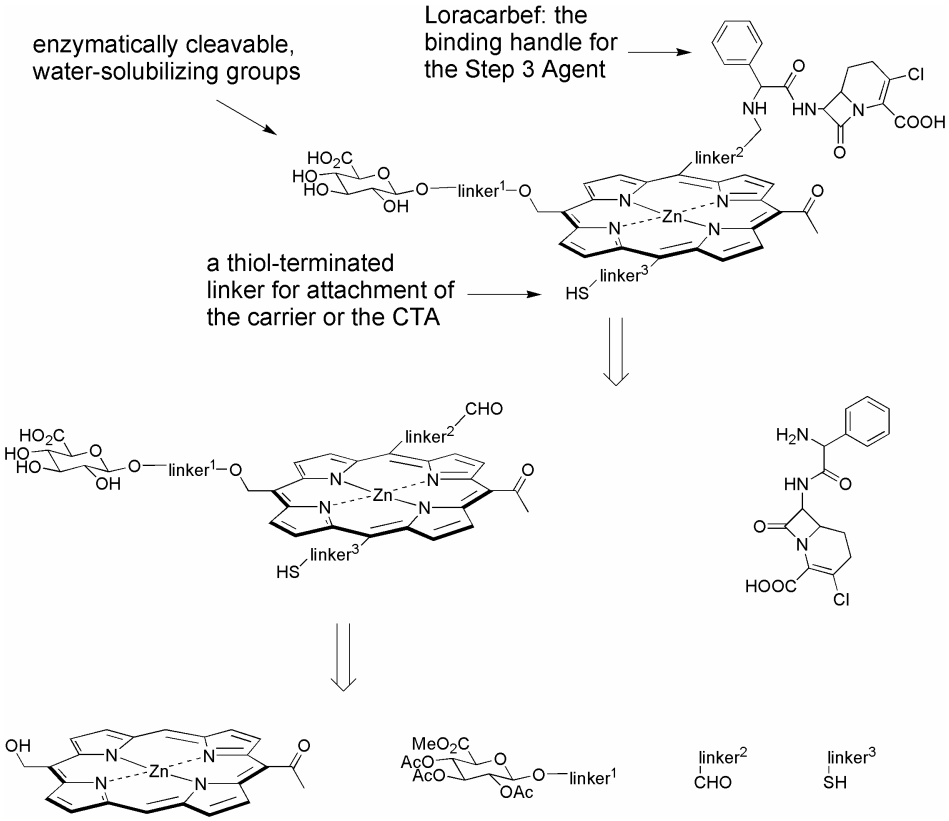

Scheme 5.7. Porphyrin-based Step-1 SPR–Design 3: Structure and retrosynthesis.

The target molecule of Design 3 can be synthesized from a porphyrin bearing an aldehyde-terminated linker and Loracarbef via the reductive amination described previously (see Chapter 5.2.2.2). The aldehyde-terminated linker, as well as the thiol-terminated linker and the self-immolative linker with a glucuronyl group, can be attached to the centerpiece of the target molecule, which is a porphyrin bearing all three elements for self-assembly: the hydroxymethyl group, the acetyl group and central zinc atom.

5.3.1.2. Synthesis of Self-immolative Linkers Bearing a Glucuronyl Group.

The advantages of self-immolative linkers in prodrug synthesis were discussed in Chapter 3.3. In Design 3, the purpose of the self-immolative linker is to mask the meso-hydroxymethyl

group and thus prevent hydrogen-bond formation that leads to self-assembly. In principle, all of the self-immolative linkers that have been found to be stable and easily cleavable during the course of research on enzyme-prodrug systems[3.10-3.16] are candidate structures for our SPR designs.

We synthesized two self-immolative linkers with a glucuronyl terminus. The first linker can be cleaved by a cyclization mechanism and the second one can be cleaved by an electron-cascade mechanism (see Chapter 3.3). The corresponding prodrugs containing these two linkers were reportedly stable, and the drug molecules were efficiently released upon treatment of β-glucuronidase.[3.15d,5.18]

Compound **28** and **30** are both known compounds,[3.15d,5.18] and were prepared as described in the literature (Scheme 5.8). The methylation of 2-amino-4-nitrophenol afforded **25**, which then was treated with di-*tert*-butyl dicarbonate to afford **26**. The hydroxyl group on **26** was derivatized with a bromo glucuronide reagent. The subsequent acidic deprotection of the Boc group yielded the self-immolative linker **28**. Linker **30** was synthesized from the reduction of **29**, which was obtained from 4-hydroxy-3-nitrobenzaldehyde and a bromo glucuronide.

Linker **28** was activated *in situ* before reacting with porphyrins as described in a later section. On the other hand, linker **30** was derivatized with *p*-nitrophenyl chloroformate to afford carbonate **31** in 64% yield. Carbonate **31** is a stable compound, and was employed in pure form in the acylation of porphyrins. Acylation of porphyrins with linker **28** and **31** will be described in Chapter 5.3.1.5, 5.3.1.6 and 5.4.1.2.

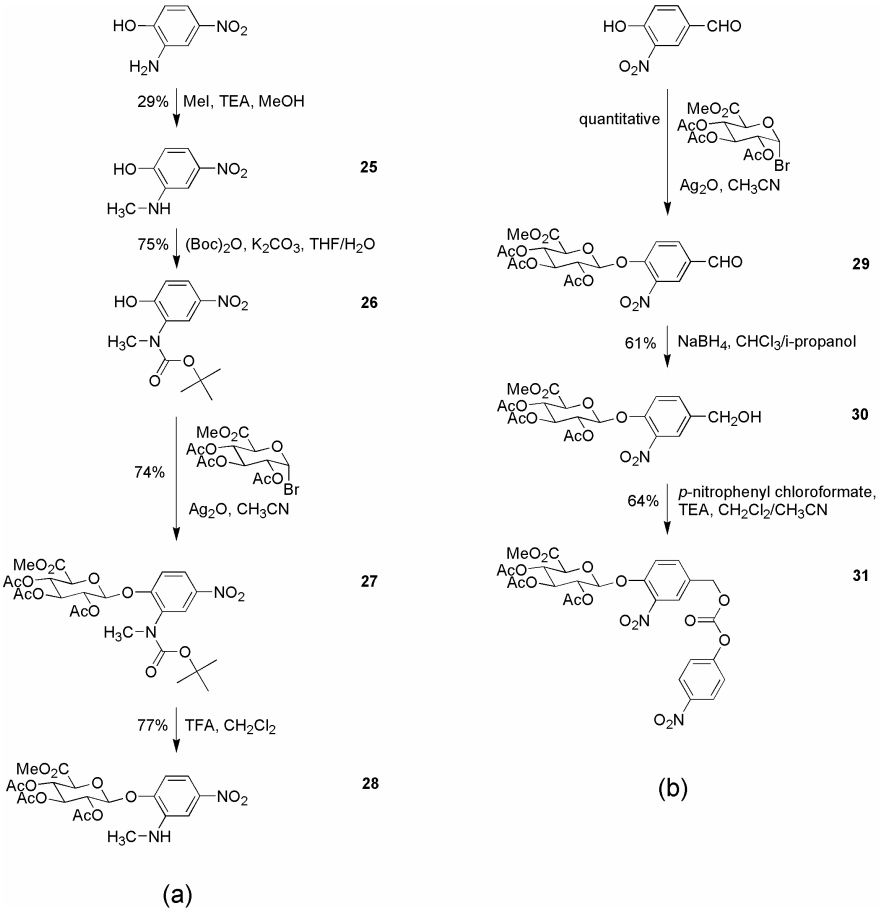

Scheme 5.8. Two self-immolative linkers with a glucuronyl terminus for masking the meso-hydroxymethyl group.

5.3.1.3. Introducing the Aldehyde and the Thiol Linker to the Porphyrin.

A porphyrin bearing an aldehyde and a thiol linker at *trans*-meso-positions can be synthesized by two different methods. The first method follows the synthetic route for an ABCD-porphyrin starting from a dipyrromethane as described in Chapter 3.2. Two separate acylation steps with corresponding Mukaiyama reagents introduce two different substituents that will appear at the *trans*-meso-positions on the porphyrin (Scheme 5.9a).[3.6] The other method is to selectively brominate one free meso-position on a *trans*-AB-porphyrin followed by Pd-mediated coupling with an ethynyl compound.[5.19] The second bromination and Pd-coupling will introduce the second ethynyl group to the opposite meso-position (Scheme

5.9b). Mukaiyama reagents (Chart 5.1a) and ethynyl compounds (Chart 5.1b) bearing an aldehyde group, an acetal, or a protected thiol group have been prepared in our group by Dr. Marcin Ptaszek and Dr. Dhanalekshmi Savithri. All of those reagents can be used in either synthetic route described above.

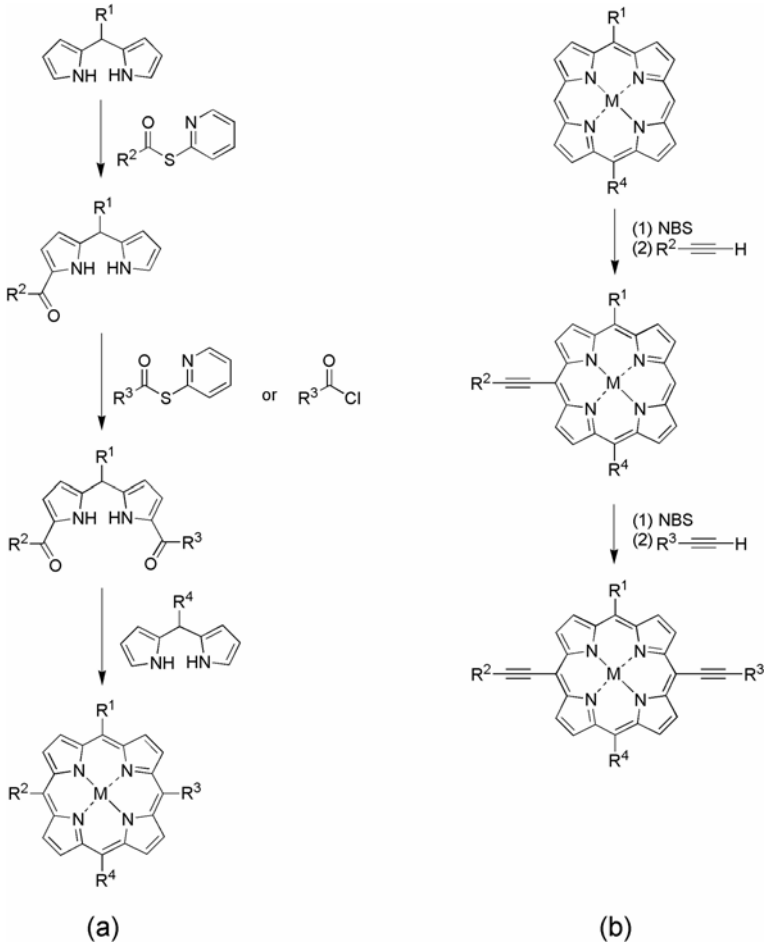

Scheme 5.9. Introducing an aldehyde and a thiol linker to the porphyrin via (a) acylation of a dipyrromethane, and (b) bromination of a free meso-position followed by Sonogashira coupling.

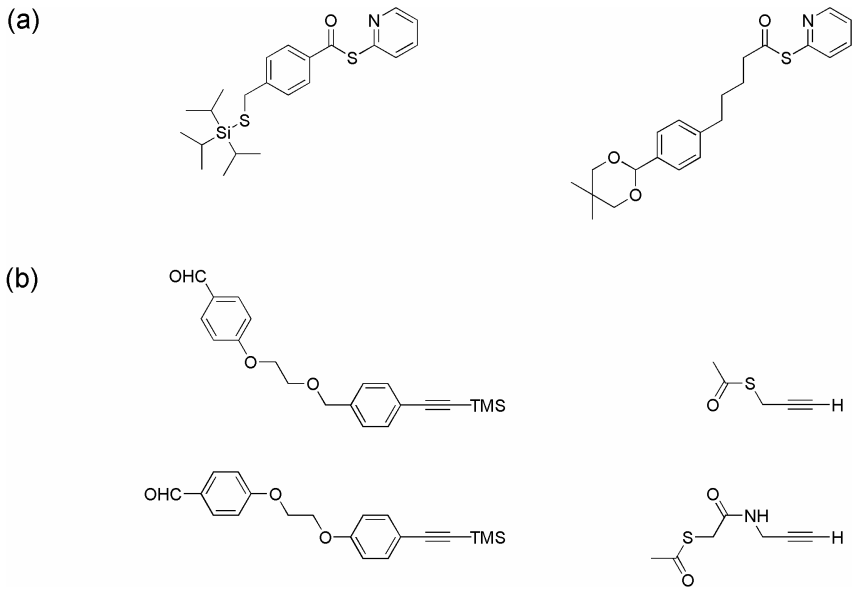

Chart 5.1. Mukaiyama reagents and ethynyl compounds with an aldehyde or thiol terminus.

5.3.1.4. Synthesis of a *Trans*-AB-Porphyrin Bearing a Hydroxymethyl Group and an Acetyl Group. The centerpiece for the porphyrin-based Step-1 SPR in Design 3 is a zinc *trans*-AB-porphyrin bearing a hydroxymethyl group and an acetyl group (Scheme 5.7). Such a *trans*-AB-porphyrin can be synthesized from a hydroxymethyl-dipyrromethane and an acetyl-dipyrromethane by following the newly developed methodology described in Chapter 4.

The synthesis of a *tert*-butyldimethylsilyl (TBDMS)-protected hydroxymethyl dipyrromethane started from the protection of glycolaldehyde diethyl acetal by TBDMS chloride. The protection reaction yielded diethyl acetal **32** quantitatively. The reaction of acetal **32** and pyrrole was carried out under literature conditions[4.15] with modification. A sample of **32** was treated with pyrrole and $InCl_3$ at 60 °C to afford 5-(*tert*-butyldimethylsiloxymethyl)dipyrromethane (**33**) as a colorless liquid in 52% yield (Scheme 5.10). Compound **33** was employed in the syntheses of meso-hydroxyl porphyrins (see Chapter 5.3.1.5).

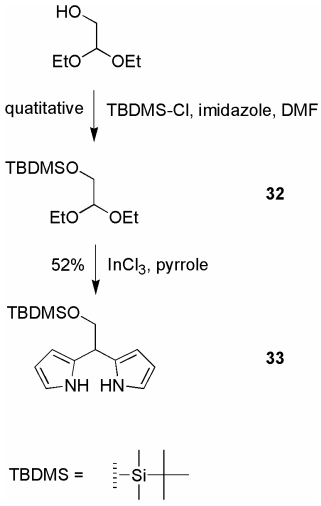

Scheme 5.10. Synthesis of a dipyrromethane bearing a hydroxymethyl group.

We attempted several different routes to access the acetyl-dipyrromethane. The condensation of methylglyoxal 1,1-dimethyl acetal and pyrrole occurred at the carbonyl position instead of the desired acetal position and yielded 5-dimethoxymethyl-5-methyldipyrromethane (**34**) (Equation 5.3a). In another route, the carbonyl group on ethyl pyruvate was converted to diethyl acetal by treatment with triethyl orthoformate (Equation 5.3b). However, attempted reduction of the ester moiety on acetal **35** did not yield the corresponding aldehyde bearing an acetal moiety.

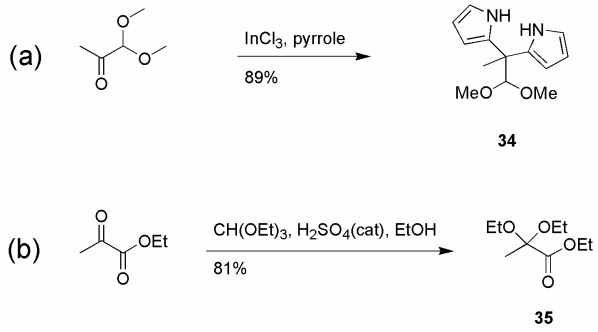

Equation 5.3. Failed attempts toward an acetyl-dipyrromethane.

Another approach for introducing an acetal group entails mercury hydration of a triple

bond. Accordingly, we first synthesized an ethynyl-dipyrromethane. The condensation of 3-trimethylsilyl propargyl aldehyde and pyrrole afforded 5-[2-(trimethylsilyl)ethynyl]dipyrromethane (**36**) in 74% yield (Scheme 5.11). After removing the TMS group by treatment with TBAF, the subsequent treatment with $Hg(OAc)_2$ did not yield the desired acetyl-dipyrromethane. Following a literature procedure,[5.20] **37** was treated with di-*tert*-butyl dicarbonate to afford the *N*-protected dipyrromethane **37** in 90% yield. The TMS group was removed upon treatment with TBAF to yield the corresponding ethynyl-dipyrromethane **38**, which was converted to acetyl-dipyrromethane **39** by mercury hydration[5.21] in 31% yield. Because dipyrromethanes can polymerize under acidic conditions, the cleavage of the Boc group needs to be carried out under neutral or basic conditions. Treatment of **39** with CuI failed to yield the desired product. On the other hand, we could perform the hydration reaction on the zinc porphyrin bearing the ethynyl group rather than on the dipyrromethane.

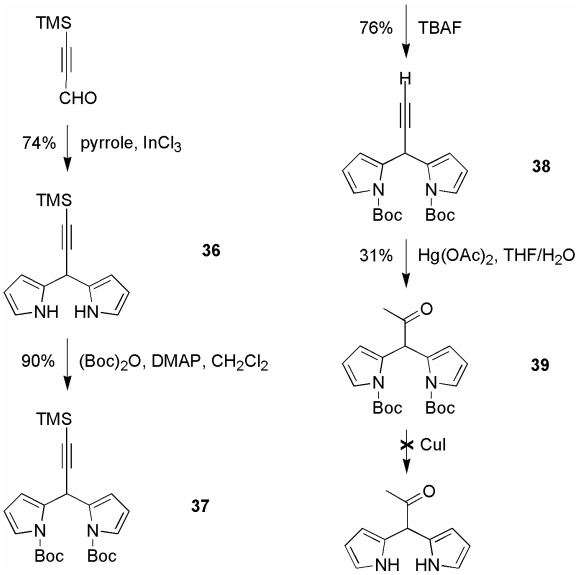

Scheme 5.11. Synthesis of an acetyl-dipyrromethane by mercury hydration.

The synthesis of an ethynyl-porphyrin started by treating **36** with Eschenmoser's salt

to yield the corresponding bis(*N*,*N*-dimethylamino)dipyrromethane **40** (Scheme 5.12).[4.2] Condensation of **40** with dipyrromethane **41** bearing an acetal group afforded *trans*-AB-porphyrin **42** in 9% yield. Removal of the TMS group by treatment with TBAF gave **43** in 75% yield. Porphyrin **43** can be converted to the porphyrin bearing a hydroxymethyl group and an acetyl group by the following steps: (1) ethyne hydration to form the acetyl group, (2) acidic hydrolysis of the acetal to recover the formyl group (possible demetalation may occur), and (3) reduction of the aldehyde to the hydroxymethyl group. However, due to the results from a model study (see Chapter 5.3.1.5), we decided not to carry out those reactions.

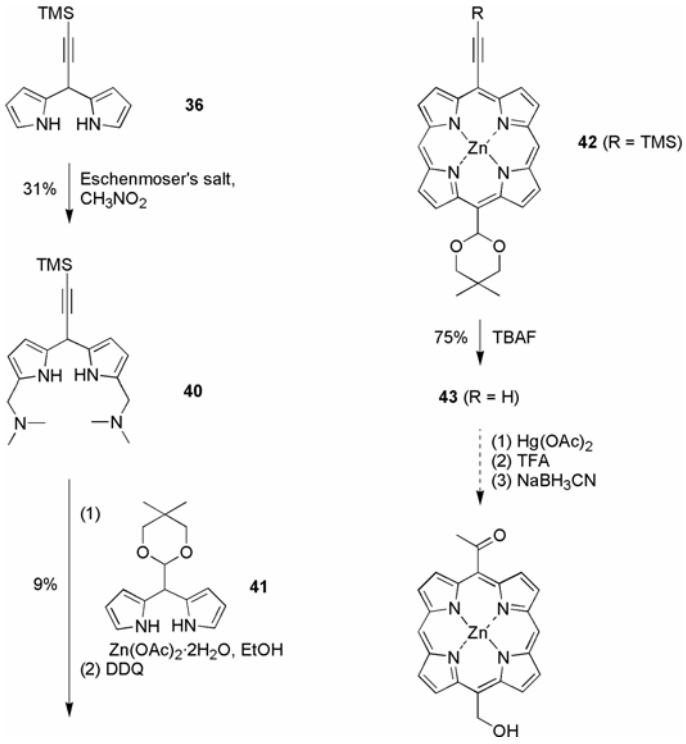

Scheme 5.12. Synthesis of an ethynyl porphyrin as the precursor to an acetyl porphyrin.

5.3.1.5. A Model Study: Synthesis and Acylation of a Meso-Hydroxymethyl Porphyrin. The synthesis of a porphyrin bearing one meso hydroxymethyl group and three meso aryl groups has been reported by the condensation of a hydroxymethyldipyrromethane and a diacyldipyrromethane.[5.22] We first employed a TBMDS-protected 5-

hydroxymethyldipyrromethane (**33**, see Chapter 5.3.1.4) in the same synthetic route to examine the stability of the silyl protection in the porphyrin-forming process. The tin complex of a diacyldipyrromethane (**44**)[5.23] was reduced by $NaBH_4$ and the resulting dipyrromethane-diol was condensed with dipyrromethane **33** to afford free base porphyrin **45** in 12% yield (Scheme 5.13). Treatment of **45** with $Zn(OAc)_2{\cdot}2H_2O$ under standard conditions[3.5] afforded the corresponding Zn-porphyrin **45Zn** in 95% yield. The TBDMS group was removed[5.24] by TBAF to yield hydroxymethyl porphyrin **46** or **46Zn** in 60% or 81% yield, respectively.

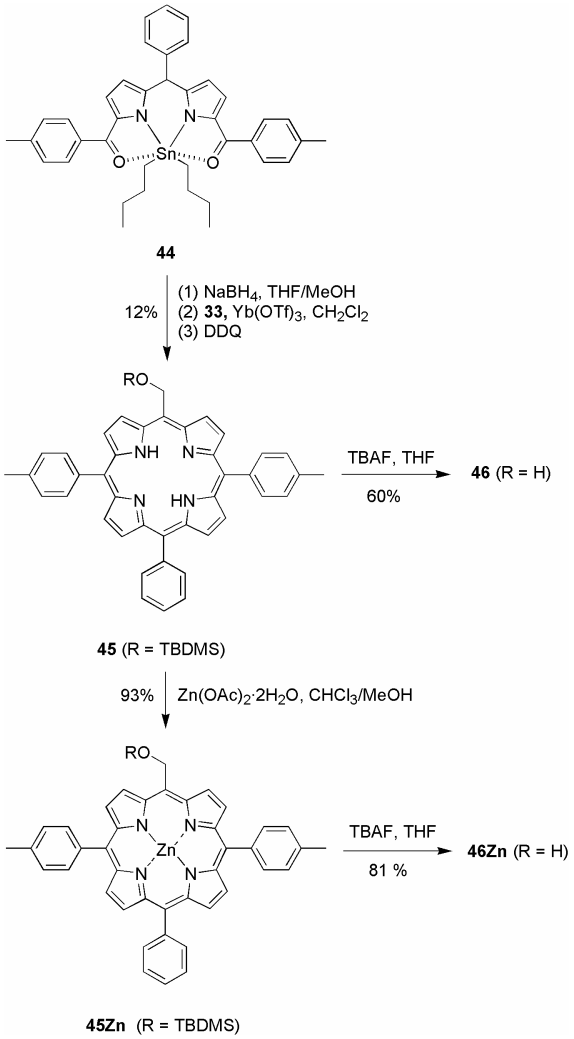

Scheme 5.13. Synthesis of mono-hydroxymethyl porphyrins.

A model porphyrin bearing a hydroxymethyl group and an ester group at *trans*-meso-positions was then synthesized following standard procedures[3.5,3.6,5.23,5.24]. Dipyrromethane **33** (see Chapter 5.3.1.4) was treated with EtMgBr and *p*-toluoyl chloride, and the resulting diacyldipyrromethane was isolated as the corresponding dibutyltin complex **47** in 41% yield (Scheme 5.14). Diacyldipyrromethane **47** was reduced by $NaBH_4$ and then condensed with 5-ethoxycarbonyldipyrromethane (**48**)[4.13] in the presence of $InCl_3$ followed by DDQ oxidation to afford the free base porphyrin **49** in 10% yield. Treatment of **50** with TBAF afforded the hydroxymethyl porphyrin **50** in 20% yield. The other major product (8%) isolated from the reaction mixture was a porphyrin bearing an aldehyde and an ester at opposite meso-positions. The free base porphyrin **50** was treated with $Zn(OAc)_2$ to yield zinc porphyrin **50Zn** quantitatively.

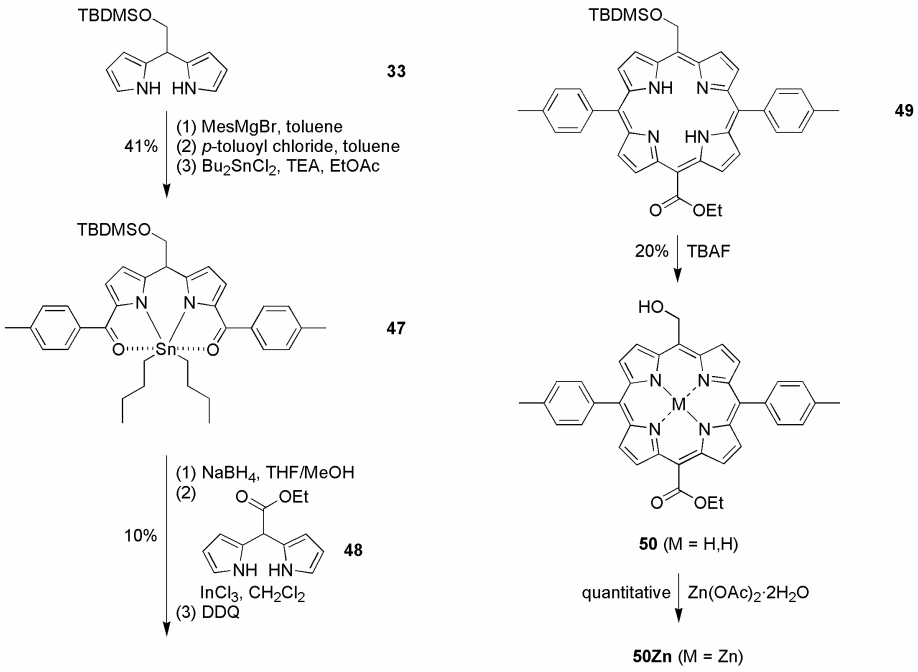

Scheme 5.14. A model compound: A zinc porphyrin bearing meso-hydroxymethyl and ester groups.

We then explored the acylation reactions of model porphyrins (**50**, **50Zn**) with self-immolative linkers (**28**, **31**, see Chapter 5.3.1.2). Linker **31** was employed directly in the reaction whereas **28** was first converted to the corresponding active carbamoyl chloride **28′** by triphosgene and TEA[5.25] (Equation 5.4), and the crude **28′** was used for acylation. Unfortunately, after more than a dozen acylation attempts with different conditions (Table 5.3, Entry 1.14), the formation of the expected glucuronide porphyrin was not observed. Acylation of **50Zn** with *p*-nitrophenyl chloroformate also was not successful (Entry 15). In each case (Entry 1.15), TLC analysis showed that no starting porphyrin (**50** or **50Zn**) remained in the reaction mixture. However, multiple porphyrinic species were observed on TLC, and one of the products was identified as 5-ethoxycarbonyl-15-formyl-10,20-di-*p*-tolylporphyrin (**51** or **51Zn**, Chart 5.2) by TLC and LD-MS analysis.

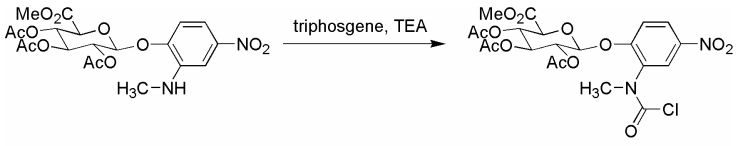

28 **28'**

Equation 5.4. Activation of self-immolative linker **28** (the reaction mixture was used in acylation reactions directly).

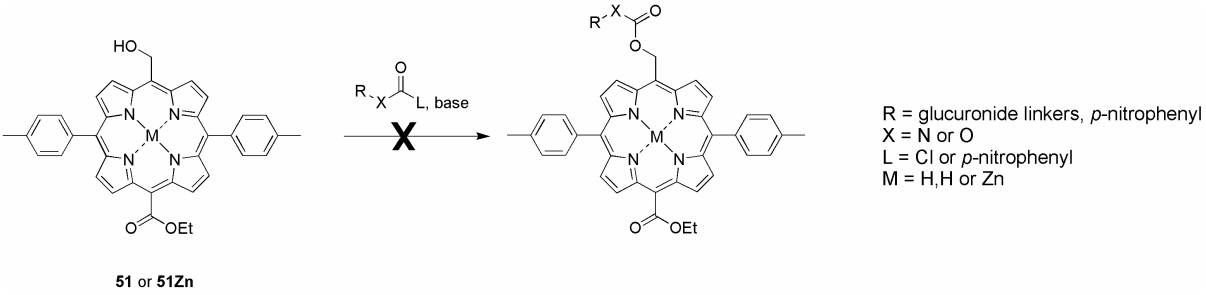

Table 5.3. Acylation of meso-hydroxymethyl porphyrins **51** and **51Zn**.

Entry	Porphyrin (concentration)	Acylating agent (concentration)	Base	Other conditions
1	**50Zn** (24 mM)	**28′** (22 mM)	TEA, DMAP	THF, RT, 24 h
2	**50Zn** (24 mM)	**28′** (22 mM)	TEA, DMAP	THF, Reflux, 17 h
3	**50Zn** (12 mM)	**28′** (20 mM)	TEA	THF, AgCN, reflux, 24 h
4	**50Zn** (12 mM)	**28′** (20 mM)	TEA	THF, AgCN, reflux, 3 days
5	**50Zn** (12 mM)	**28′** (50 mM)	NaH	THF, RT
6	**50Zn** (10 mM)	**28′** (50 mM)	TEA	THF, AgCN, reflux, 3 days
7	**50Zn** (10 mM)	**28′** (50 mM)	$(i\text{-}Pr)_2EtN$	DMF, 60 °C, 2 days
8	**50Zn** (10 mM)	**28′** (50 mM)	K_2CO_3	DMF, 60 °C, 2 days
9	**50Zn** (10 mM)	**28′** (50 mM)	*t*-BuLi	THF, RT, 28 h
10	**50** (36 mM)	**31** (90 mM)	TEA	THF, RT, 18 h
11	**50** (28 mM)	**31** (280 mM)	pyridine	Neat, 60 °C, 18 h
12	**50Zn** (20 mM)	**31** (50 mM)	TEA	THF/DMF, 60 °C, 18 h
13	**50Zn** (20 mM)	**31** (50 mM)	pyridine	THF/DMF, 60 °C, 18 h
14	**50Zn** (20 mM)	**31** (50 mM)	*t*-BuLi	THF/DMF, 60 °C, 18 h
15	**50Zn** (14 mM)	*p*-nitrophenyl chloroformate (2 M)	pyridine	Neat, 60 °C, 18 h

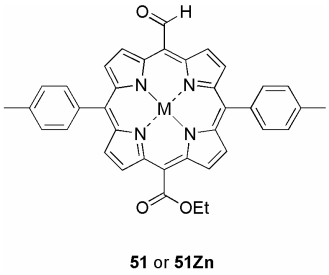

Chart 5.2. Formyl-porphyrins isolated from the acylation reaction of **50** or **50Zn**.

A possible cause for the conversion from the hydroxymethyl porphyrin to the formyl

porphyrin is arial oxidation. A stability test of the hydroxymethyl porphyrin was carried out (Table 5.4). A sample of **50** or **50Zn** in THF solution or in dry form was exposed to air at room temperature for 7 days. LD-MS analysis showed the presence of a small amount of formyl porphyrin **51Zn** in the samples of **50Zn** (Table 5.3, Entry 5 and 6). The instability of the meso-hydroxymethyl group might stem from the high electron density at the meso-position of the porphyrin.

Table 5.4. Stability tests for hydroxymethyl porphyrins **50** and **50Zn**.

Entry	Porphyrin	Conditions	LD-MS analysis
1	**50**	after chromatography	592.4 (M^+)
2	**50**	solution in CH_2Cl_2 kept at RT for a week	592.2 (M^+), 575.1 [$(M - OH)^+$]
3	**50**	solid kept at RT for a week	592.2 (M^+), 575.1 [$(M - OH)^+$]
4	**50Zn**	after chromatography	654.2 (M^+), 637.2 [$(M - OH)^+$]
5	**50Zn**	solution in THF kept at RT for a week	654.2, a small signal at 652.2 for **51Zn**
6	**50Zn**	solid kept at RT for a week	654.2, a small signal at 652.1 for **51Zn**, 637.2 [$(M - OH)^+$]

5.3.1.6. A Model Study: Synthesis and Acylation of β-Hydroxymethyl and β-*N*-methylaminomethyl Porphyrins. It is know that *meso*-tetraarylporphyrins bearing electron-rich aryl groups have lower electron density at the β-positions than the meso-positions.[5.26] Therefore, we expected the hydroxymethyl group at a β-position would be more stable during the acylation reaction.

The current methodologies for preparing porphyrins bearing one β-substituent include (1) condensation of an aldehyde and a mixture of a β-substituted pyrrole and an unsubstituted pyrrole,[5.27] and (2) derivatization at one β-position following porphyrin formation.[5.28-5.32] Similar to meso-derivatization, both methods rely on statistical reactions and thus require the

target product to be isolated from a mixture of porphyrins. The substituents that can be introduced by the latter method include formyl,[5.28] nitro,[5.29] alkyl,[5.30] and bromo[5.31]. Although high yields (up to 88% for nitration[5.29a]) have been reported, β-derivatization typically is limited to porphyrins bearing the same substituent at all four meso-positions (because the statistical reaction will afford regioisomers when a porphyrin carries different meso-substituents). Moreover, β-derivatization typically is not applicable for porphyrins with free meso-positions due to possible competing meso-substitution.[5.33]

In the rational synthesis of β-substituted porphyrins, the key precursor for a β-substituted porphyrin is the corresponding 3-substituted dipyrromethane. The synthesis of a 3-aryldipyrromethane from a β-aryl-β′-ethoxycarbonylpyrrole and an *N*-protected pyrrole[5.34] or from an *N*-protected-2-hydroxymethyl-3-arylpyrrole and pyrrole[5.35] have been reported. A 3,7-dibromoporphyrin was synthesized from a 1,9-diacyl-3,7-dibromodipyrromethane followed by Stille coupling to introduce vinyl groups at the 3,7-positions of the porphyrin.[4.11] The porphyrin bearing a synthetic handle (e.g., the bromo group) rather than any specific substituent at the β-position is an attractive platform because porphyrins with a wide variety of β-substituents can be introduced via Pd-mediated coupling reactions. Therefore, we developed a rational method to synthesize a 3-bromoporphyrin that also carries three meso-substituents (two different groups). Porphyrins bearing three different C1 β-substituents (hydroxymethyl, formyl and *N*-methylaminomethyl) were synthesized from the bromoporphyrin.

The synthesis of a 3-bromoporphyrin started from the synthesis of the dibutyltin complex of a 1,9-di-*p*-toluoyldipyrromethane (**52**)[5.23] following literature conditions. The acyl groups at the 1- and 9-positions direct electrophilic substitution (such as bromination) to

the 3- and 7-positions.[5.36] Thus, the treatment of **52** with 1 equivalent of NBS at –78 °C yielded a mixture of the desired 3-bromo-1,9-diacydipyrromethane-Sn-complex (**53**), the dibromo product and the starting material in a ratio of 10:1:1.5 (determined by ^{1}H NMR analysis of the reaction mixture) (Scheme 5.15). Compound **53** was isolated by chromatography in 54% yield. The regiochemistry of the bromo substituent was established by NOESY and COSY spectroscopy. Diacyldipyrromethane **53** was reduced by $NaBH_4$ and condensed with 5-(ethoxycarbonyl)dipyrromethane (**48**) followed by oxidation, affording 3-bromo-15-(ethoxycarbonyl)-10,20-di-*p*-tolylporphyrin (**54**) in 7% yield. LD-MS analysis of the crude mixture did not reveal any scrambling. The free base porphyrin **54** was converted to the corresponding Zn porphyrin **54Zn** in 98% yield. We chose a Stille coupling reaction to convert β-bromo porphyrin **54** to the corresponding β-hydroxymethyl porphyrin because hydroxymethyl tributyltin (**55**)[5.37] can be conveniently prepared following literature conditions. The Pd-mediated coupling[5.38] between **54Zn** and the tin reagent **55** was then carried out in a Schlenk flask in THF containing $Pd(PPh_3)_4$. The reaction mixture was refluxed at 80 °C for 48 h and the β-hydroxymethyl porphyrin **56Zn** was isolated in 55% yield. LD-MS analysis of the reaction mixture did not reveal the formation of any Pd-porphyrin, despite the prolonged reaction at elevated temperature.

However, the acylation of β-hydroxymethyl porphyrin **56Zn** with self-immolative linker **31** did not yield the expected product. The starting porphyrin was recovered instead of being converted to the corresponding formyl porphyrin (as in the acylation reaction with the meso-hydroxymethyl porphyrin **51**). A possible explanation is that the lower electron density at the β-position leads to a more stable but less reactive hydroxymethyl group. Therefore, we turned to synthesize a porphyrin bearing a more reactive aminomethyl group at the β-position.

The target β-aminomethyl porphyrin can be synthesized directly form the β-hydroxymethyl porphyrin **56Zn**. Treatment of **56Zn** with pyridinium chlorochromate[5.39] at room temperature afforded β-formyl porphyrin **57Zn** in 43% yield. Reductive amination[5.2d] of **57Zn** with methylamine hydrochloride, triethylamine and $NaBH_3CN$ at room temperature for 3 days gave β-*N*-methylaminomethylporphyrin **58Zn** in 49% yield. The acylation of **58Zn** with linker **31** (see Chapter 5.3.1.2) yielded porphyrin **59Zn** bearing a glucuronyl group with an intervening self-immolative linker.

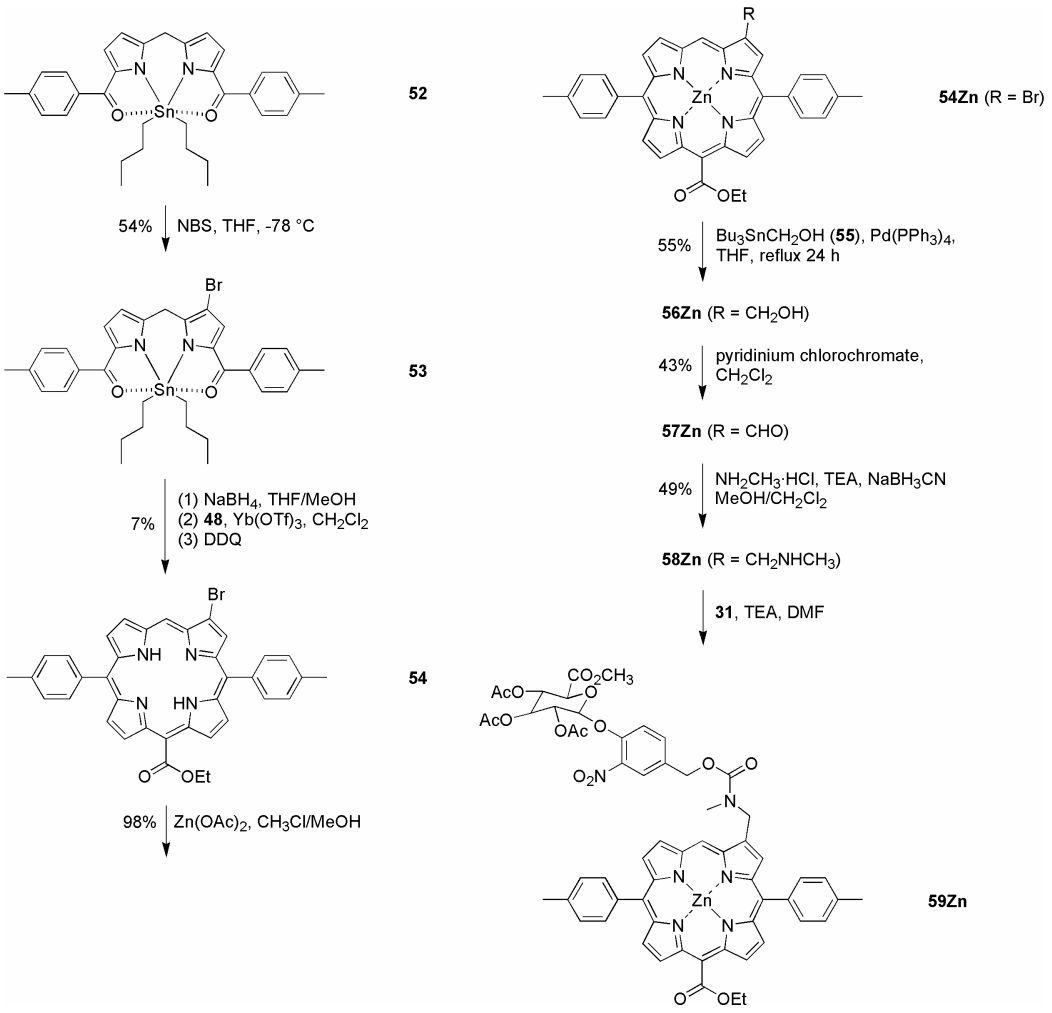

Scheme 5.15. Synthesis and acylation of a β-*N*-methylaminomethyl porphyrin.

5.3.1.7. Synthesis of a Tributyltin Reagent Bearing an Aminomethyl

Group. As shown in Scheme 5.18, the synthesis of the β-aminomethyl porphyrin **59Zn** via the corresponding β-hydroxymethyl porphyrin **58Zn** was lengthy and the overall yield was low (12% for three steps: Pd coupling, oxidation and amination). An alternative route entails the coupling reaction of the β-bromo porphyrin **56Zn** directly with a tributyltin reagent bearing an aminomethyl group. Such a tin reagent can be synthesized from the known compound iodomethyl tributyltin (**61**)[5.37], which was conveniently synthesized from tributyltin hydride in two steps as described in the literature (Scheme 5.16). Treatment of **61** with methylamine hydrochloride in the presence of a base (TEA or NaOH) did not yield the expected product. On the other hand, the reaction with propylamine under standard conditions[5.40] yielded tin reagent **62** bearing an *N*-propylaminomethyl group in 83% yield. The Pd-coupling reaction between **62** and β-bromo porphyrin **54Zn** has not yet been explored.

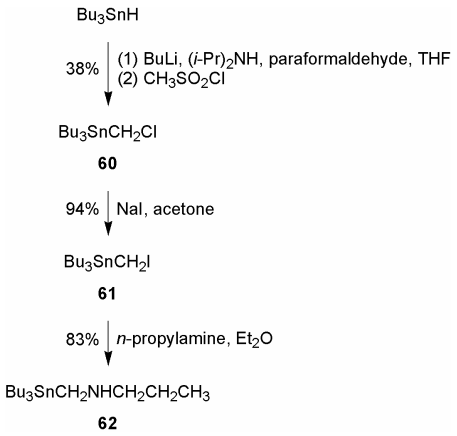

Scheme 5.16. Synthesis of a tributyltin reagent bearing an aminomethyl group.

5.3.2. Synthesis of Meso-Formyl Porphyrins

During the study of Design 2 for a porphyrin-based SPR, we also explored the synthesis of meso-formyl porphyrins. A meso-formyl group on a porphyrin can be converted

to a hydroxymethyl group by reduction,[5.2a,5.41] a carboxylic acid by oxidation,[5.42] an *N*-alkylaminomethyl group by reductive amination,[5.2d] or an oxime by imine formation[5.43]. Such functional groups provide alternative ways to construct the porphyrin-based Step-1 SPR other than the designs that we demonstrate in this thesis. Therefore, the versatility of meso-formyl porphyrins is potentially valuable to our research.

Porphyrins bearing meso-formyl groups can be synthesized from the corresponding porphyrin-acetals. Precursors of porphyrin-acetals such as 5-(5,5-dimethyl-1,3-dioxan-2-yl)dipyrromethane,[4.10] 1-acyl-5-(5,5-dimethyl-1,3-dioxan-2-yl)dipyrromethane,[4.10] (5,5-dimethyl-1,3-dioxan-2-yl)-*S*-pyridyl thioester (Mukaiyama reagent)[4.10] and 1,9-bis(*N*,*N*-dimethylaminomethyl)-5-(5,5-dimethyl-1,3-dioxan-2-yl)dipyrromethane[4.2] have been reported. The porphyrin-acetals synthesized from such precursors are shown in Chart 5.3.

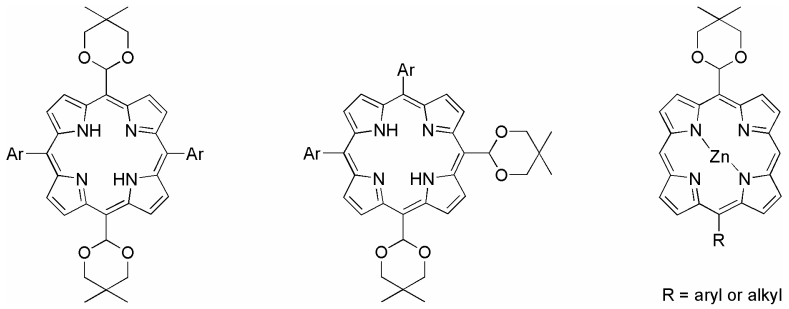

Chart 5.3. Porphyrins-acetals reported in the literature.

5.3.2.1. Synthesis of a *Trans*-AB$_2$C-Porphyrin Bearing a Formyl Group and an Ester Group. As described in previous sections, a *trans*-AB$_2$C-porphyrin can be synthesized via the condensation of a dipyrromethane and a 1,9-diacyldipyrromethane. Because the ester moiety may be labile during the synthesis of the diacyldipyrromethane, we used the combination of a diacyldipyrromethane bearing an acetal group and a dipyrromethane bearing an ester for the porphyrin synthesis.

A porphyrin bearing a formyl group and an ester group at *trans*-meso-positions was synthesized from a 1,9-diacyl-5-(acetal)dipyrromethane and an ester-dipyrromethane (Scheme 5.17). The direct diacylation of the acetal dipyrromethane **41**[4.10] with EtMgBr and *p*-toluoyl chloride was not successful. We then carried out the two acylations (1-acylation and 9-acylation) in separate steps. Following known procedures,[4.10,5.44] 1-*p*-toluoyl-5-(5,5-dimethyl-1,3-dioxan-2-yl)dipyrromethane was synthesized from **41** and Mukaiyama reagent **63**[3.6], and treated with Bu_2B-OTf to form the boron complex **64** in 34% yield. The boron complex **64** was treated under standard conditions[5.45] with MesMgBr and *p*-toluoyl chloride to form the corresponding diacyldipyrromethane **65** in 56% yield. Compound **65** was reduced by $NaBH_4$ and the resulting dipyrromethane dicarbinol was condensed with ester-dipyrromethane **48** to afford acetal-ester porphyrin **66** in 14% yield. A small amount (~1%) of a formyl-porphyrin (from deprotection of **66**) was also observed in the reaction mixture by LD-MS analysis. Acetal-ester porphyrin **66** was treated with TFA/H_2O to afford *trans*-AB_2C-porphyrin **67** in 85% yield.

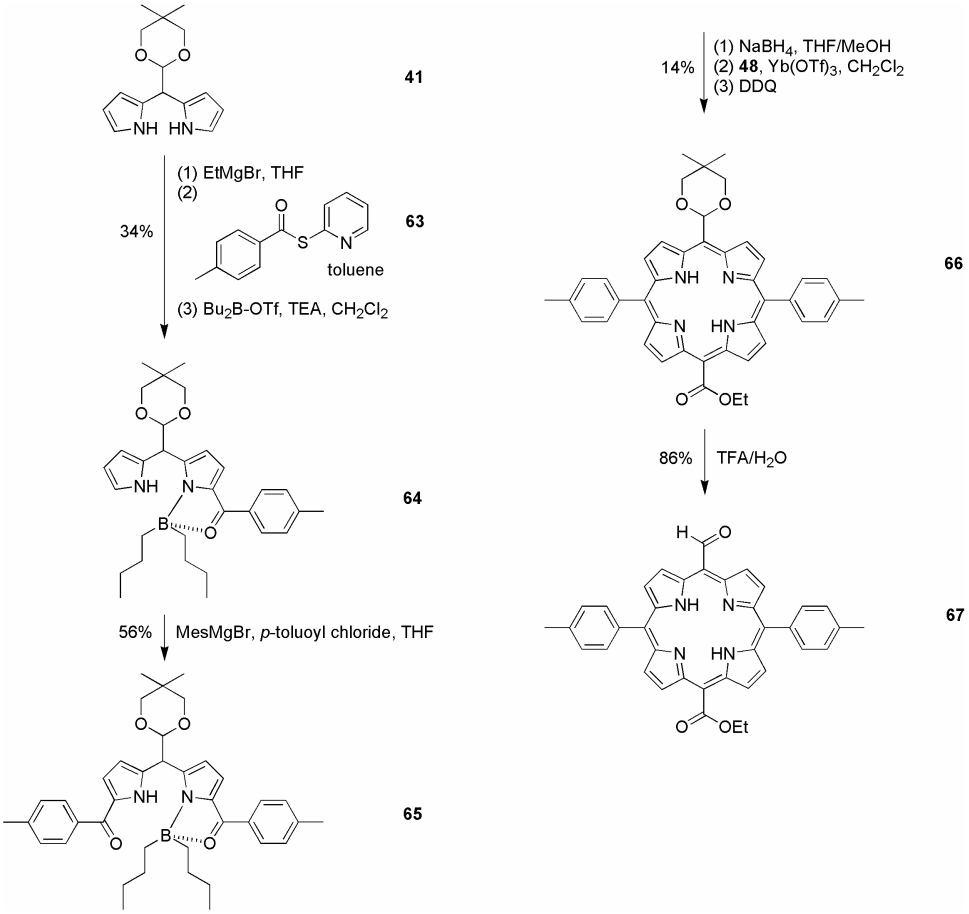

Scheme 5.17. Synthesis of a *trans*-AB_2C-porphyrin bearing a formyl group and an ester group.

5.3.2.2. Synthesis of *Trans*-AB-Porphyrins bearing an Acetal Group and an Ester Group. *Trans*-AB-porphyrins can be synthesized via the newly developed methodology discussed in Chapter 4. However, as previous results indicate, the yields of porphyrins are typically low with certain moieties present such as an ethoxycarbonyl group or a 2-(trimethylsilyl)ethynyl group. Therefore, we compared the synthesis of a *trans*-AB-porphyrin bearing an acetal group and an ester group via three different condensation reactions. A 1,9-disubstituted dipyrromethane bearing an acetal group and a 5-ethoxycarbonyldipyrromethane (**48**) were employed in all three routes. The results are shown in Table 5.5.

Route 1 [condensation of a 1,9-bis(hydroxymethyl)dipyrromethane and a dipyrromethane][4.1]: 1,9-Diformyl-5-(acetal)dipyrromethane **68** was previously synthesized in our group upon Vilsmeier formylation of acetal-dipyrromethane **41**. Diformyldipyrromethane **68** was reduced by $NaBH_4$ followed by condensation with **48** in the presence of $Yb(OTf)_3$ to yield the free-base porphyrin **70** in 10% yield. LD-MS analysis of the reaction mixture did not show any scrambling, or any loss of the acetal group.

Route 2 (condensation of a 1,9-bis[(*n*-propylimino)methyl]dipyrromethane and a dipyrromethane)[5.46]: 1,9-Diformyl-5-(acetal)dipyrromethane **68** reacted with *n*-propylamine to form the corresponding 1,9-bis[(*N*-propylimino)methyl]dipyrromethane. After aqueous workup, the crude product was condensed with **48** in refluxing EtOH containing $Zn(OAc)_2$. LD-MS analysis of the reaction mixture showed the desired acetal-porphyrin as well as the deprotected formyl-porphyrin. The mixture of porphyrins was treated with TFA and the fully deprotected *trans*-AB-porphyrin **71Zn** bearing a formyl group and an ester group was isolated in 1% yield.

Route 3 [condensation of a 1,9-bis(*N*,*N*-dimethylaminomethyl)dipyrromethane and a dipyrromethane][4.2]: 1,9-Bis(*N*,*N*-dimethylaminomethyl)-5-(5,5-dimethyl-1,3-dioxan-2-yl)dipyrromethane (**69**)[4.2] and dipyrromethane **48** were refluxed in EtOH containing $Zn(OAc)_2$. Similar to route 2, a mixture of acetal-porphyrin and formyl-porphyrin was obtained. The mixture of porphyrins was treated with TFA to yield porphyrin **71Zn** in 2% yield.

Routes 2 and 3 employed 1,9-disubstituted dipyrromethanes bearing nitrogen-containing substituents (i.e., amine or imine) and achieved low yields in the porphyrin syntheses. Partial deprotection of the acetal group can be attributed to the somewhat acidic

reaction conditions. Toluene has been reported as an alternative solvent for zinc-mediated porphyrin-forming reactions[5.47] and can replace EtOH when acid-sensitive groups such as an acetal group are present. On the other hand, route 1, where a 1,9-diformyldipyrromethane was employed, gave a higher yield without any porphyrinic byproducts and thus appears to be the better synthetic method for preparing *trans*-AB-porphyrins with substituents of this type.

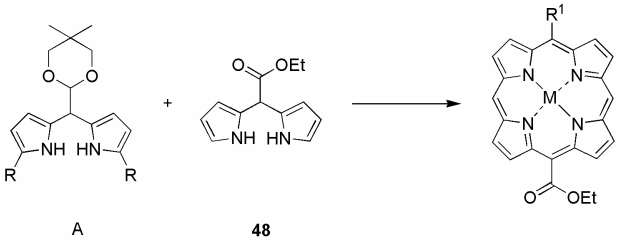

Table 5.5. Three routes to a *trans*-AB-porphyrin bearing a formyl group and an ester group.

Route	A	R	Porphyrin	R^1	M	Conditions	Yield
1	**68**	—CHO	**70**	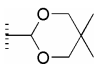	H,H	(1) $NaBH_4$, THF/MeOH (2) $Yb(OTf)_3$, CH_2Cl_2 (3) DDQ	10%
2	**68**	—CHO	**71Zn**	—CHO	Zn	(1) *n*-propylamine, THF (2) $Zn(OAc)_2$, EtOH, reflux (3) TFA, THF	<1%
3	**69**		**71Zn**	—CHO	Zn	(1) $Zn(OAc)_2$, EtOH, reflux (2) TFA, THF	2%

5.3.2.3. Synthesis of an Oxime-Porphyrin from a Formyl-Porphyrin. As mentioned previously, a formyl-porphyrin can be derivatized in a variety of ways. We attempted one of those possible derivatizations and synthesized an oxime porphyrin. The formyl-porphyrin **71Zn** was treated with hydroxylamine[5.48] to give the oxime porphyrin **72Zn** in 95% yield (Equation 5.5). The oxime moiety is not known to be compatible with any reported self-assembled porphyrin architectures. However, such a reactive functional group provides a handle to connect the porphyrin to other components (e.g., the CTA or

Loracarbef) required for a Step-1 SPR.

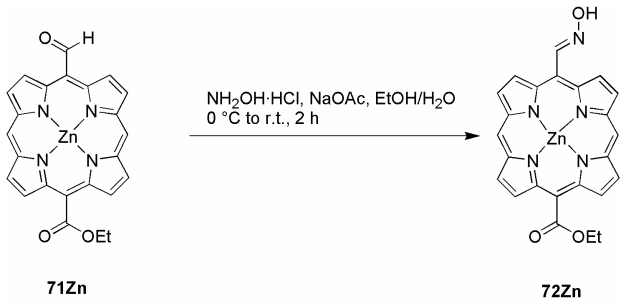

71Zn 72Zn

Equation 5.5. Synthesis of a *trans*-AB-porphyrin bearing an oxime group and an ester group.

5.3.3. Conclusions for Design 3.

Despite our efforts in search of synthetic methods for preparing a target molecule analogous to bacteriochlorophyll *c*, the original Design 3 seems limited because of the difficulties in attaching a self-immolative linker to the meso-hydroxymethyl group on the porphyrin. On the other hand, an aminomethyl group at the β-position of a model porphyrin was derivatized with a glucuronide linker. Accordingly, the original structure in Design 3 can be modified by replacing the meso-hydroxymethyl with a β-aminomethyl group. A rational approach towards a model porphyrin bearing a β-*N*-methylaminomethyl group was developed but the overall synthesis of the new target molecule (a Step-1 SPR) has not been studied.

5.4. Model C: Porphyrin Self-assembly via Meso Imidazolyl Groups and a Central Metal

Metalloporphyrins bearing heterocyclic substituents such as pyrimidyl, pyridyl and imidazolyl groups at the meso-positions have also been reported to form self-assembled structures.[5.5,5.8,5.49] In the case of imidazolyl porphyrins, there appear to be three major

driving forces that direct self-assembly: (1) coordination between the central 5- or 6-coordinate metal and the imidazole imino nitrogen; (2) hydrogen-bonding between the secondary amine of imidazole and the imino nitrogen of an imidazole on an adjacent porphyrin; (3) π-π stacking interactions. The resulting aggregates normally consist of a one-dimensional column rather than the two- or three-dimentional architectures as in the first two models. It has also been reported that porphyrins bearing 2-aminopyrimidyl groups formed tetrameric subunits upon coordination, and the subunits further aggregate driven by other weak interactions such as hydrogen-bonding (Figure 5.6a).[5.8]

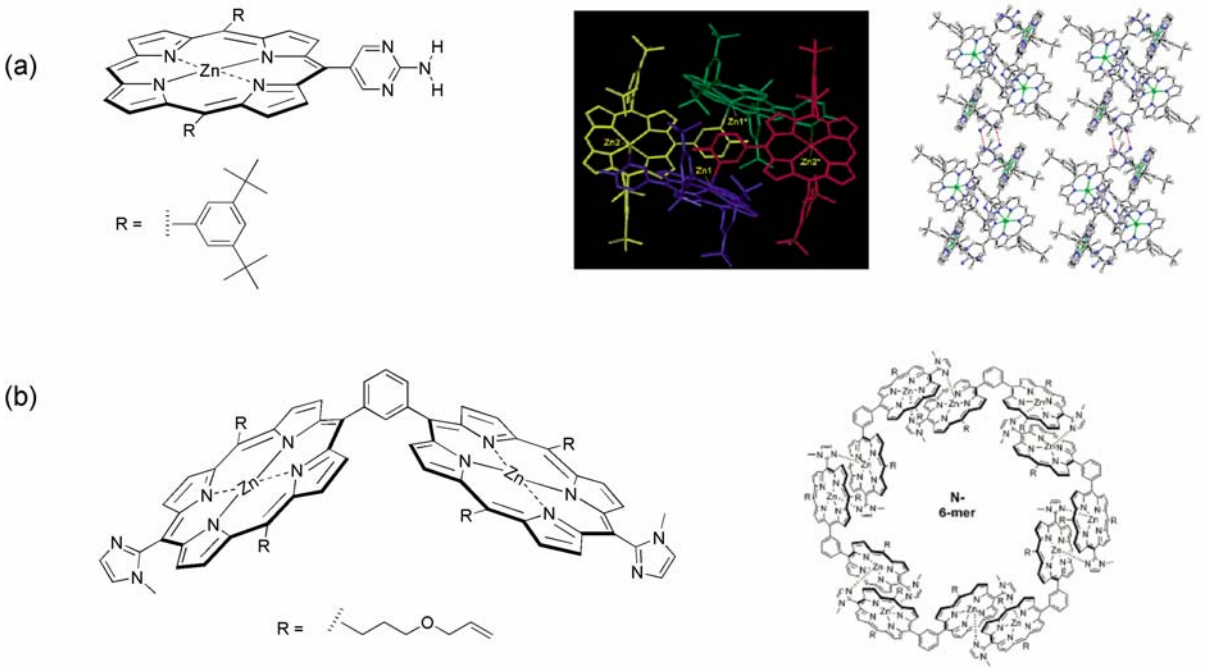

Figure 5.6. Self-assembly of porphyrins bearing heterocyclic groups: (a) an aminopyrimidyl porphyrin and its tetrameric aggregate; (b) an imidazolyl porphyrin dimer and its cyclic aggregate. Adapted from ref. 5.8 (a) and 5.5 (b).

5.4.1. A Porphyrin-Based Step-1 SPR: Design 4.

5.4.1.1. Design and Retrosynthesis. The structure and retrosynthesis for the fourth design of a Step-1 SPR are similar to those of Design 3. Instead of a hydroxymethyl

group and an acetal group, the target molecule carries two imidazolyl groups at *trans*-meso-positions (Scheme 5.18). The amino nitrogens on the imidazoles are masked by glucuronide linkers. The Loracarbef moiety and the thiol-terminated linker are attached to the other two meso-positions. The target molecule of Design 3 can be synthesized from a porphyrin bearing an aldehyde-terminated linker and Loracarbef via the reductive amination described previously. The aldehyde-terminated linker, as well as the thiol-terminated linker and the self-immolative linker with a glucuronyl group, can be attached to the centerpiece of the target molecule, which is a zinc porphyrin bearing two imidazolyl groups at *trans*-meso-positions.

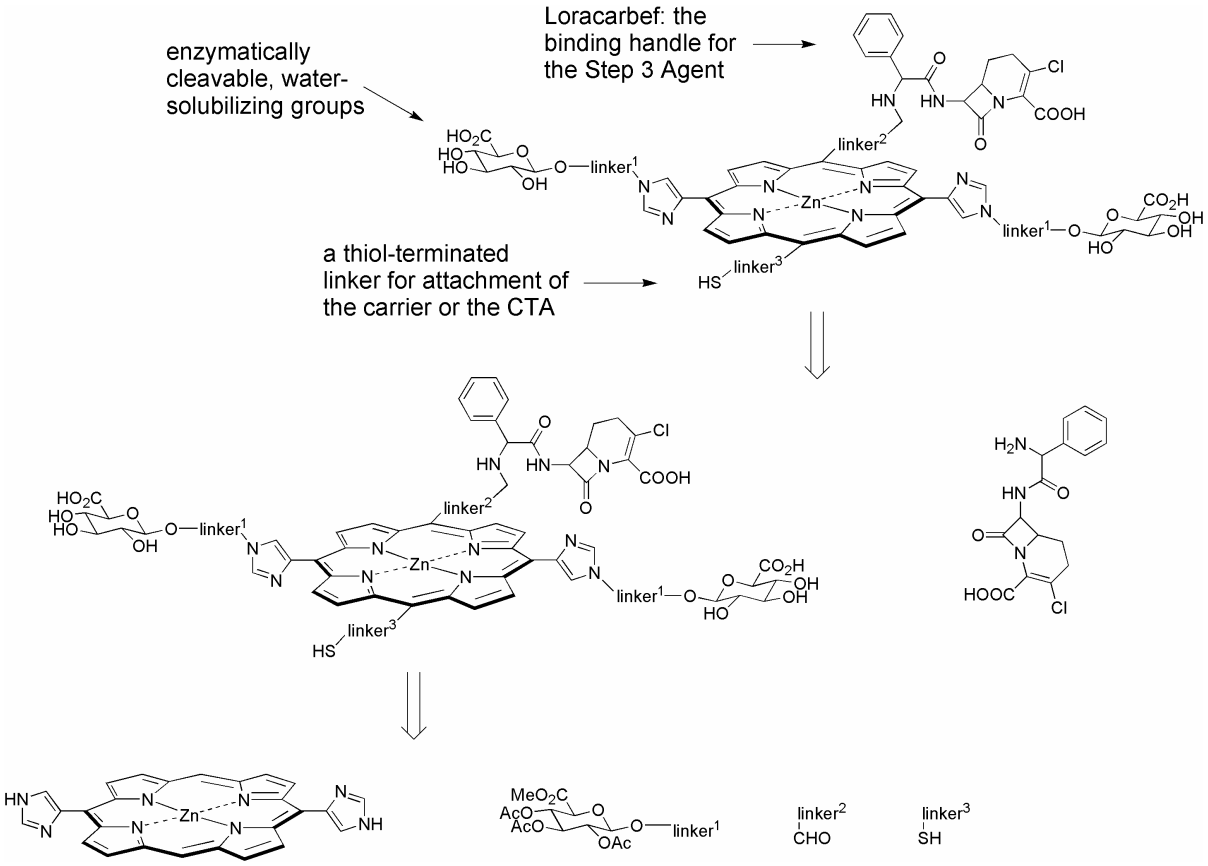

Scheme 5.18. Porphyrin-based Step-1 SPR–Design 4: structure and retrosynthesis.

5.4.1.2. Synthesis of A Model Compound: A Porphyrin Bearing Two

Imidazolyl Groups. A new rational synthetic method for preparing imidazolyl porphyrins has been developed in our group.[5.50] A dipyrromethane bearing an imidazolyl group with protection of both the amino nitrogen and the imino nitrogen was synthesized. The protection is achieved with an 2-(trimethylsilyl)ethoxymethyl (SEM) group (amino nitrogen) and a dialkylboron complex (imino nitrogen). Such a doubly protected imidazolyl moiety largely facilitates the porphyrin synthesis because (1) the protected imidazolyl compounds are less polar and easier to purify, and (2) the protection prevents interference with porphyrin formation by the weak acid (amino nitrogen) or the weak base (imino nitrogen).

A mixture of isomeric SEM-protected imidazolyldipyrromethanes (**73a** and **73b**) was previously prepared in our group by the protection of 4(5)-imidazolylcarboxaldehyde with 2-(trimethylsilyl)ethoxymethyl chloride followed by condensation with pyrrole. 5-(SEM-imidazol-4-yl)dipyrromethane was isolated in low yields (8-16%) from the mixture by extensive chromatography. Alternatively, treatment of the isomeric mixture with TEA and dibutylboron triflate yielded 10-dibutylboron-5-(SEM-imidazol-4-yl)dipyrromethane (**74**) (Scheme 5.19). The less polar **74** was easily separated from the other isomer, which does not form a boron complex. The recovery of dipyrromethane was 10% (mole percentage). The actual yield was not calculated because the original ratio of the two isomers was not known.

Dipyrromethane **74** was treated with MesMgBr and Mukaiyama reagent **63** followed by complexation with dibutylboron triflate to afford a bis(dialkylboron) complex of a diacyldipyrromethane (**75**) in 21% yield. The diacyldipyrromethane **75** can react with a dipyrromethane to afford a *trans*-AB_2C-porphyrin bearing one imidazole group.

Dipyrromethane **74** was condensed with *p*-tolualdehyde to yield bis(SEM-imidazolyl)porphyrin **76**. Level 1 scrambling[3.8] was observed in the reaction mixture by LD-

MS analysis; nevertheless, the pure *trans*-A_2B_2-porphyrin **76** was isolated in 26% yield. A different porphyrin with the same mass as **76** was also isolated by chromatography and is provisionally considered to be the *cis*-regioisomer. The synthesis of a *trans*-AB-porphyrin bearing two imidazolyl groups from a dipyrromethane and an aldehyde (imidazole on either dipyrromethane or aldehyde) has been reported in low yield (2-3%).[5.51] Therefore, the use of protected imidazolyl building blocks affords a more efficient synthesis of such porphyrins.

The SEM groups on porphyrin **76** were removed by treatment with TBAF to give the diimidazolyl-porphyrin **77** in 33% yield. The crude mixture was treated directly with self-immolative linker **31** (see Chapter 5.3.1.2) in DMF containing TEA. The formation of the bis(glucuronide)porphyrin **78** was confirmed by LD-MS analysis of the reaction mixture. However, the product decomposed in a size exclusion chromatography (SEC) column during attempted purification.

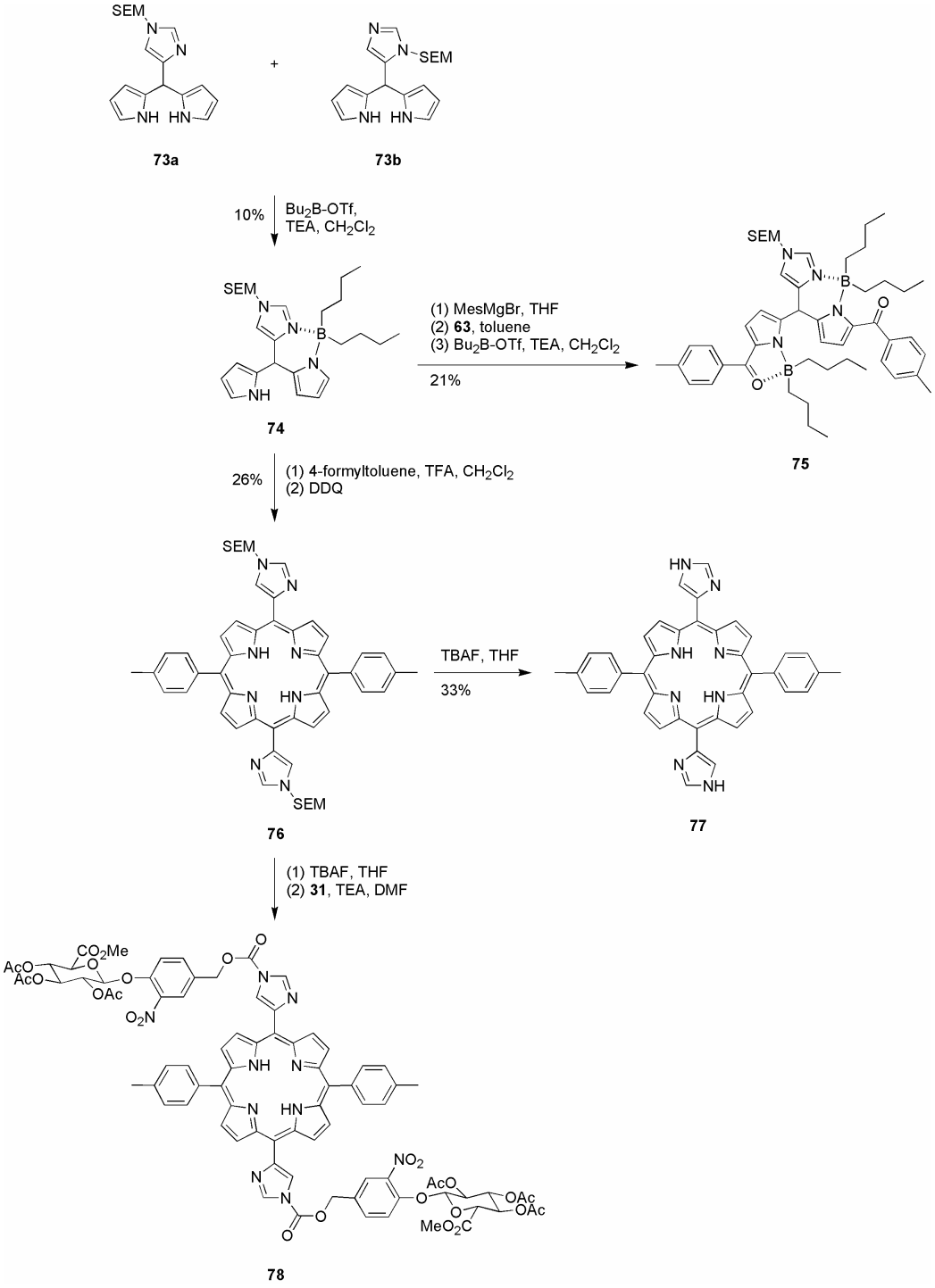

Scheme 5.19. Synthesis and acylation of a diimidazolyl porphyrin.

5.4.2. Conclusions for Design 4.

It is known that the *N*-acylimidazole moiety is quite reactive. One example is

carbonyldiimidazole (CDI), which can be used in coupling reactions to form esters or amides. On the other hand, imidazolyl compounds protected by carbamoyl esters (e.g., benzyl, *tert*-butyl) are commonly employed in organic synthesis.[5.52] In our case, the carbamoyl ester may have caused the decomposition of the acylation product **68**. Instead of acylation, the imidazole could be masked by alkylation at both nitrogen sites with water-solubilizing moieties. Although alkyl imidazole groups may not be cleaved tracelessly, in which case the porphyrin may not attain the necessary structure for self-assembly, the *N*,*N*′-dialkylimidazolyl porphyrin is expected to precipitate upon the removal of the water-solubilizing moieties.

5.5. Summary of Our Study on Porphyrin-Based Step-1 SPRs

We have proposed four designs for Step-1 SPRs on the basis of different patterns of porphyrin aggregation. The goal is to enzymatically convert the water-soluble porphyrin to a precipitate (platform), with an organized architecture so that the Step-3 agent can efficiently bind the platform.

We explored a wide variety of chemistry regarding the syntheses of those designs and synthesized several model compounds to test key steps in the proposed synthetic routes. The difficulties that we encountered include the lack of rational methodologies for preparing the desired structures, low reactivity of certain intermediates, and instability of some of the products. Due to those obstacles, the final target molecules have not yet been synthesized for the soluble-to-insoluble conversion. On the other hand, the studies provided valuable insights on various subjects such as synthesis of porphyrin-carboxylates, synthesis and water-solubility of sugar porphyrins, reductive amination with Loracarbef, and the acylation of C1

substituents (i.e., hydroxymethyl and aminomethyl) on porphyrins. As mentioned in Chapter 5.1, a well-defined architecture of the porphyrin precipitate is preferred for the S.T.A.R. method, but such an architecture may not be required. According, the future design of porphyrin-based Step-1 SPRs should not be limited to the three models of self-assembly listed here. Nevertheless, the results we have obtained from our studies provide guidance towards more promising porphyrin-based SPRs.

5.6. Experimental Section.

General. All ^{1}H NMR spectra (400 MHz) and ^{13}C NMR spectra (100 MHz) were recorded in $CDCl_3$ unless noted otherwise. Mass spectra of porphyrins were obtained by high-resolution fast atom bombardment mass spectrometry (FAB-MS) or by laser desorption mass spectrometry (LD-MS). Absorption spectra were collected in CH_2Cl_2 at room temperature unless noted otherwise. Melting points are uncorrected. Silica gel (40 μm average particle size) and alumina (80–200 mesh) were used for column chromatography. All reagents were used as received.

Noncommercial Compounds. Aldehyde **1**,[5.10] dipyrromethane **11**,[4.13] **41**,[4.10] and **48**,[4.13] tin complex **44** and **52**,[5.23] Mukaiyama reagent **63**,[3.6] and bis(*N*,*N*-dimethylaminomethyl)dipyrromethane **69**,[4.2] were prepared as described in the literature.

5-[3,5-Bis(2,3,4,6-tetra-O-acetyl-β-D-glycopyranosyloxy)phenyl]dipyrromethane (2). Following a literature procedure,[5.11] a mixture of aldehyde **1** (80 mg, 0.10 mmol) and pyrrole (2.88 mL, 40.0 mmol) was degassed with argon for 5 min. TFA (1.0 μL, 13 μmol) was added, and the reaction mixture was stirred for 40 min. TEA was added to quench the reaction. Ethyl acetate was then added, and the mixture was washed with brine. The organic

layer was separated, dried ($NaSO_4$) and concentrated. Chromatography [silica, hexanes/ethyl acetate (1:1)] afforded a yellow solid (81 mg, 89%): the product became a viscous black oil at 80 °C; ^{1}H NMR (300 MHz) δ 2.025 (s, 6H), 2.032 (s, 6H), 2.037 (s, 6H), 2.043 (s, 6H), 3.73–3.78 (m, 2H), 4.09–4.26 (m, 4H), 5.03 (d, J = 5.7 Hz, 2H), 5.11–5.30 (m, 6H), 5.41 (s, 1H), 5.91–5.94 (m, 2H), 6.13–6.17 (m, 2H), 6.50 (dd, $^1J = {}^2J$ = 1.5 Hz, 1H), 6.54 (d, J = 1.5 Hz, 2H), 6.70–6.73 (m, 2H), 8.06 (br, 2H); ^{13}C NMR δ 20.76, 20.80, 20.82, 44.06, 61.76, 68.19, 71.12, 72.13, 72.84, 98.46, 104.84, 107.57, 108.66, 111.36, 117.68, 117.77, 131.78, 145.46, 157.63, 169.50, 169.58, 170.40, 170.93; LD-MS obsd 914.40, calcd 914.2957 ($C_{43}H_{50}N_2O_{20}$); Anal. calcd for $C_{43}H_{50}N_2O_{20}$: C, 56.45; H, 5.52; N, 3.06. Found: C, 56.42; H, 5.58; N, 2.98.

5,15-Bis[3,5-bis(2,3,4,6-tetra-*O*-acetyl-β-D-glucofuranosyloxy)phenyl]-10,20-diphenylporphyrin (3). Following a literature procedure,[3.8] a solution of dipyrromethane **2** (19 mg, 21 μmol) and benzaldehyde (2.2 μL, 21 μmol) in CH_2Cl_2 (2 mL) was treated with TFA (2.9 μL, 37 μmol) at room temperature for 30 min. DDQ (5 mg, 0.02 mmol) was added, and the reaction mixture was stirred at room temperature for another 30 min. The reaction mixture was filtered through an alumina pad (ethyl acetate). The eluent was concentrated to give a green solid. The crude product was dissolved in toluene (1.5 mL) and treated with DDQ (10 mg, 0.44 mmol) under reflux for 1 h. The reaction mixture was cooled to room temperature and filtered through an alumina pad (ethyl acetate). The eluent was concentrated. Chromatography [silica, CH_2Cl_2/ethyl acetate (2:1)] afforded a dark red solid (2 mg, 7%): ^{1}H NMR δ –2.90 (br, 2H), 1.96 (s, 12H), 2.02 (s, 12H), 2.05 (s, 12H), 2.10 (s, 12H), 3.70–3.78 (m, 4H), 3.92–4.16 (m, 8H), 5.06–5.39 (m, 16H), 7.03–7.08 (m, 2H), 7.58 (d, J = 2.1 Hz, 4H), 7.75–7.84 (m, 6H), 8.16–8.23 (m, 4H), 8.84–8.96 (m, 8H); LD-MS obsd 1998.1, calcd

1998.6070 ($C_{100}H_{102}N_4O_{40}$); λ_{abs} 418, 514, 548, 589, 644 nm; FAB-MS analysis was not successful.

Zn(II)-5,10,15,20-Tetrakis[3,5-bis(2,3,4,6-tetra-*O*-acetyl-β-D-glucofuranosyloxy)phenyl]porphyrin (4Zn). Following a literature procedure,[3.5] a solution of porphyrin **4** (17 mg, 5.0 μmol) in $CHCl_3$/MeOH (5:1, 12 mL) was treated overnight with $Zn(OAc)_2 \cdot 2H_2O$ (17 mg, 75 μmol) at room temperature. The reaction mixture was filtered through a silica pad (ethyl acetate). The eluent was concentrated to afford a dark red solid (13 mg, 74%): ^{1}H NMR δ 1.98–2.10 (m, 96H), 3.80–3.83 (m, 8H), 4.02 (d, J = 10.4 Hz, 8H), 4.14–4.18 (m, 8H), 5.15–5.43 (m, 32H), 7.08 (dd, $^1J = {}^2J$ = 2.4 Hz, 4H), 7.55 (d, J = 2.4 Hz, 8H) 9.02 (s, 8H); LD-MS obsd 3444.1, calcd 3448.40 ($C_{156}H_{172}N_4O_{80}Zn$); λ_{abs} 419, 546 nm; FAB-MS analysis was not successful.

3,5-Bis(methyl 2,3,4-tri-*O*-acetyl-β-D-glucopyranosyloxyuronate)benzaldehyde (5). A solution of 1-bromo-2,3,4-tri-O-acetyl-α-D-glucopyranuronic acid methyl ester (1.00 g, 2.52 mmol) and 3,5-dihydroxybenzaldehyde (139 mg, 1.01 mmol) in acetonitrile (5 mL) was treated with silver oxide (702 mg, 3.03 mmol) at room temperature for 40 h. The reaction mixture was filtered through a silica pad (ethyl acetate). The eluent was concentrated. The resulting crude product was dissolved in hexanes/ethyl acetate (1:1) and filtered. The filtrate was concentrated. Chromatography [silica, hexanes/ethyl acetate (1:1)] afforded a light yellow solid (423 mg, 54%): ^{1}H NMR δ 2.04–2.08 (m, 18H), 3.74 (s, 6H), 4.24–4.28 (m, 2H), 5.25–5.39 (m, 8H), 6.95 (dd, $^1J = {}^2J$ = 2.4 Hz, 1H), 7.21 (d, J = 2.4 Hz, 2H), 9.90 (s, 1H).

5,10,15,20-Tetrakis[3,5-bis(methyl 2,3,4-tri-*O*-acetyl-β-D-glucopyranosyloxyuronate]phenyl]porphyrin (6). Following a literature procedure,[5.13] a

solution of aldehyde **5** (53 mg, 69 μmol) and pyrrole (4.8 μL, 69 μmol) in CH_2Cl_2 (7 mL) was charged with argon for 5 min. The mixture was treated with TFA (8.0 μL, 0.10 μmol) and $BF_3{\cdot}OEt_2$ (2.5 M solution in CH_2Cl_2, 1.0 μL, 2.5 μmol) for 1 h. DDQ (12 mg, 52 μmol) was added, and the reaction mixture was stirred for 30 min. TEA was added, and the reaction mixture was filtered through an alumina pad [hexanes/ethyl acetate (4:1)]. The eluent was concentrated. Chromatography [silica, hexanes/ethyl acetate (4:1)] afforded a purple solid (12 mg, 22%): ^{1}H NMR δ –2.97 (br, 2H), 2.02 (s, 24H), 2.04 (s, 24H), 2.05 (s, 24H), 3.72 (s, 24H), 4.23 (d, J = 8.8 Hz, 8H), 5.34–5.51 (m, 32H), 7.16 (dd, $^1J = {}^2J$ = 2.0 Hz, 4H), 7.54 (d, J = 2.0 Hz, 8H), 8.89 (s, 8H).

1-(3-Carboxypropionyl)-5-phenyldipyrromethane (12). Following a literature procedure,[3.6] a solution of 5-phenyldipyrromethane (**11**, 56 mg, 0.25 mmol) in dry toluene (1 mL) was treated with EtMgBr (1.0 M solution in THF, 1.5 mL, 1.5 mmol) at room temperature under argon for 10 min. Succinic anhydride (75 mg, 0.75 mmol) was added, and the mixture was stirred for 4.5 h. The insoluble material in the reaction mixture was dissolved by addition of MeOH and acetic acid. The reaction mixture was diluted with ethyl acetate. The mixture was washed with brine, dried (Na_2SO_4) and concentrated. Chromatography [silica, hexanes/ethyl acetate (1:1)] afforded a yellow oil (32 mg, 40%): ^{1}H NMR (THF-d_8) δ 2.57 (t, J = 7.2 Hz, 2H), 2.99 (t, J = 7.2 Hz, 2H), 5.47 (s, 1H), 5.66 (m, 1H), 5.80 (m, 1H), 5.94 (m, 1H), 6.61 (m, 1H), 6.84 (m, 1H), 7.10–7.30 (m, 5H), 9.84 (br, 1H), 10.89 (br, 1H).

1-[4-(2-(Trimethylsilyl)ethoxy)-4-oxobutanoyl]-5-phenyldipyrromethane (14). A solution of 5-phenyldipyrromethane (**11**, 1.96 g, 8.82 mmol) in dry THF (27 mL) was treated with EtMgBr (1.0 M solution in THF, 27 mL, 27 mmol) at room temperature under argon for

10 min. Succinic anhydride (2.65 g, 26.5 mmol) was added, and the mixture was stirred for 4.5 h. The insoluble material in the reaction mixture was dissolved by the addition of MeOH and acetic acid. Water and ethyl acetate were added to the reaction mixture. The organic layer was washed with brine, dried (Na_2SO_4), and concentrated. Chromatography [silica, hexanes/ethyl acetate (1:1)] afforded a yellow oil. The oil (crude 1-acyldipyrromethane), 4-dimethylaminopyridine (537 mg, 4.40 mmol) and 2-(trimethylsilyl)ethanol (2.52 mL, 17.6 mmol) were dissolved in dry THF (88 mL). The solution was treated with *N*,*N*-dicyclohexylcarbodiimide (2.2 g, 11 mmol) at 0 °C for 3 h, then allowed to warm overnight to room temperature. The reaction mixture was filtered through a Celite pad. The eluent was concentrated. Chromatography [silica, hexanes/ethyl acetate (5:1)] afforded a yellow oil (2.1 g, 56%): ^{1}H NMR (300 MHz) δ 0.01–0.05 (m, 9H), 2.63 (t, *J* = 6.9 Hz, 2H), 3.03 (t, *J* = 6.9 Hz, 2H), 3.70 (t, *J* = 8.4 Hz, 2H), 4.14 (t, *J* = 8.4 Hz, 2H), 5.47 (s, 1H), 5.91 (m, 1H), 5.99 (m, s), 6.12 (m, 1H), 6.68 (m, 1H), 6.87 (m, 1H), 7.15–7.35 (m, 5H), 8.13 (br, 1H), 9.38 (br, 2H); ^{13}C NMR (300 MHz) δ –1.36, –1.26, 17.39, 22.20, 28.81, 32.25, 44.05, 60.19, 63.08, 107.79, 108.49, 117.73, 117.84, 127.31, 128,40, 128.83, 130.88, 121.20, 141.18, 141.36, 173.29, 188.40, 204.35; LD-MS obsd 420.8; FAB-MS obsd 422.2035, calcd 422.2026 ($C_{24}H_{30}N_2O_3Si$).

5,15-Bis[4-(2-(trimethylsilyl)ethoxy)-4-oxobutanoyl]-10,20-diphenylporphyrin (15). Following a literature procedure,[3,7] a solution of **14** (150 mg, 355 μmol) in dry THF/MeOH (10:1, 17 mL) was treated with $NaBH_4$ (134 g, 3.55 mmol) at 0 °C under argon for 15 min. Saturated aqueous NH_4Cl (30 mL) was added, and the mixture was extracted with CH_2Cl_2 (60 mL). The organic layer was washed twice with H_2O, dried (Na_2SO_4) and concentrated. The resulting mono-carbinol was dissolved in acetonitrile (56 mL) and

treated with TFA (129 μL, 1.68 mmol) at room temperature under argon for 20 min. DDQ (95 mg, 0.42 mmol) was added, and the mixture was stirred for 1 h. The reaction mixture was filtered through an alumina pad (CH_2Cl_2). The filtrate was concentrated. Column chromatography [silica, hexanes/ethyl acetate (5:1)] afforded a purple solid (7 mg, 5%): ^{1}H NMR δ –2.78 (br, 2H), 1.00 (t, J = 8.4 Hz, 4H), 3.47 (t, J = 8.4 Hz, 4H), 4.25 (t, J = 8.4 Hz, 4H), 5.33 (t, J = 8.4 Hz, 4H), 7.75–7.80 (m, 6H), 8.16 (dd, ^1J = 1.4 Hz, ^2J = 8.0 Hz, 4H), 8.87 (d, J = 4.8 Hz, 4H), 9.45 (d, J = 4.8 Hz, 4H); LD-MS obsd 806.5; FAB-MS obsd 806.3715, calcd 806.3684 ($C_{48}H_{54}N_4O_4Si_2$); λ_{abs} 417, 516, 550, 593, 650 nm.

5,15-Bis[4-(ethoxycarbonylmethoxy)phenyl]-10,20-bis[3,5-bis(2,3,4,6-tetra-*O*-acetyl-β-D-glucofuranosyloxy)phenyl]porphyrin (19). Following a literature procedure,[5.13] a solution of dipyrromethane **2** (46 mg, 50 μmol) and aldehyde **7** (10 mg, 50 μmol) in $CHCl_3$ (5 mL) was treated with $BF_3{\cdot}OEt_2$ (2.5 M solution in CH_2Cl_2, 13 μL, 32 μmol) and NaCl (73 mg, 1.3 mmol) at room temperature for 2 h. DDQ (17 mg, 75 μmol) was added, and the reaction mixture was stirred at room temperature for another 30 min. TEA was added, and the reaction mixture was filtered through a silica pad (CH_2Cl_2 then ethyl acetate). The eluent was concentrated. Chromatography [silica, CH_2Cl_2/ethyl acetate (1:1)] afforded a dark red solid (13 mg, 23%): ^{1}H NMR δ –2.89 (br, 2H), 1.43 (t, J = 7.2 Hz, 6H), 1.96 (s, 12H), 2.02 (s, 12H), 2.05 (s, 12H), 2.11 (s, 12H), 3.97–4.14 (m, 12H), 4.43 (q, J = 7.2 Hz, 4H), 4.95 (s, 4H), 5.09–5.38 (m, 16H), 7.05–7.08 (m, 2H), 7.33 (d, J = 8.4 Hz, 4H), 7.58 (d, J = 2.0 Hz, 4H), 8.12 (d, J = 8.4 Hz, 4H), 8.87–8.94 (m, 8H); LD-MS obsd 2202.0, calcd 2202.6704 [$C_{108}H_{114}N_4O_{46}$, 2,5-dihydroxybenzoic acid (DHB) as matrix]; λ_{abs} 420, 515, 550, 589, 646 nm; FAB-MS analysis was not successful.

5-[4-(Ethoxycarbonylmethoxy)phenyl]-10,15,20-tris[3,5-bis(2,3,4,6-tetra-*O*-

acetyl-β-D-glucofuranosyloxy)phenyl]porphyrin (20). Following a literature procedure,[3.9] a solution of dipyrromethane **2** (88 mg, 96 μmol), aldehyde **1** (38 mg, 48 μmol) and **7** (10 mg, 48 μmol) in CH_2Cl_2 (10 mL) was treated with TFA (13 μL, 171 μmol) at room temperature for 30 min. DDQ (33 mg, 144 μmol) was added, and the reaction mixture was stirred at room temperature for another 30 min. The reaction mixture was filtered through an alumina pad (ethyl acetate). The eluent was concentrated. Chromatography [silica, CH_2Cl_2/ethyl acetate (1:3)] afforded a dark red solid (13 mg, 9.7%): ^{1}H NMR δ –2.95 (br, 2H), 1.43 (t, *J* = 7.2 Hz, 3H), 1.94–2.14 (m, 72H), 3.96–4.17 (m, 18H), 4.43 (q, *J* = 7.2 Hz, 2H), 4.95 (s, 2H), 5.09–5.31 (m, 24H), 7.05–7.09 (m, 3H), 7.33 (d, *J* = 8.4 Hz, 4H), 7.56 (d, *J* = 2.0 Hz, 6H), 8.10 (d, *J* = 8.4 Hz, 4H), 8.92 (d, *J* = 10.8 Hz, 8H); LD-MS obsd 2793.1, calcd 2792.8187 ($C_{132}H_{144}N_4O_{63}$, DHB as matrix); λ_{abs} 419, 515 nm; FAB-MS analysis was not successful.

5,10,15,20-Tetrakis[3,5-bis(β-D-glucofuranosyloxy)]phenyl]porphyrin (21). A suspension of porphyrin **4** (58 mg, 17 μmol) in MeOH (760 μL) was treated overnight with TEA (240 μL, 1.72 mmol) at 40 °C. LD-MS analysis showed that the title compound was the only porphyrinic species in the reaction mixture. The reaction mixture was concentrated and used for water-solubility tests without further purification: LD-MS obsd 2040.6, calcd 2039.6362 [$(M + H)^+$, M = $C_{92}H_{110}N_4O_{48}$, DHB as matrix]; λ_{abs} (MeOH) 417, 513, 547, 588 nm.

5-[4-(Carboxymethoxy)phenyl]-15-[4-(ethoxycarbonylmethoxy)phenyl]-10,20-bis[3,5-bis(β-D-glucofuranosyloxy)phenyl]porphyrin (22). A suspension of porphyrin **19** (9 mg, 4 μmol) in MeOH (200 μL) was treated overnight with TEA (52 μmol, 0.41 mmol) at 40 °C. LD-MS analysis showed that the title compound was the only porphyrinic species in the reaction mixture. The reaction mixture was concentrated and used for water-solubility

tests without further purification: LD-MS obsd 1503.9, calcd 1503.4774 [$(M + H)^+$, M = $C_{74}H_{78}N_4O_{30}$, DHB as matrix]; λ_{abs} (MeOH) 418, 514, 551, 591 nm.

5-[4-(Carboxymethoxy)phenyl]-10,15,20-tris[3,5-bis(β-D-glucofuranosyloxy)phenyl]porphyrin (23). A suspension of porphyrin **20** (23 mg, 8.3 μmol) in MeOH (400 μL) was treated overnight with TEA (28 μL, 0.20 mmol) at 40 °C. LD-MS analysis showed that the title compound was the only porphyrinic species in the reaction mixture. The reaction mixture was concentrated and used for water-solubility tests without further purification: LD-MS obsd 1772.6, calcd 1774.5444 [$(M + H_2O)^+$, M = $C_{82}H_{92}N_4O_{39}$, DHB as matrix]; λ_{abs} (MeOH) 417, 514, 550, 589 nm.

[(6R,7S)-7-[(R)-2-benzylamino-2-phenylacetamido]-3-chloro-8-oxo-1-azabicyclo[4.2.0]oct-2-ene-2-carboxylic acid (24). An aqueous acetate buffer was prepared by dissolving acetic acid (22 μL, 0.40 mmol) and sodium acetate (66 mg, 0.80 mmol) in distilled water (10 mL). A solution of Loracarbef (4 mg, 0.01 mmol) and benzaldehyde (1.1 μL, 10 μmol) in a mixed solvent of the acetate buffer (0.5 mL) and THF (0.5 mL) was treated with $NaBH_3CN$ (2 mg, 0.03 mmol) for 30 h. The reaction mixture (10 μL) was diluted with THF (490 μL). The mass spectrum of the diluted solution was obtained: ESI-MS obsd 462.0, calcd 462.1197 [$(M + Na)^+$, M = $C_{23}H_{22}ClN_3O_4$].

4-[3-(Methyl 2,3,4-*tri*-*O*-acetyl-β-D-glucopyranosyloxy-uronate)-2-nitro-benzoxycarbonyloxy]-1-nitro-benzene (31). Following a literature method,[5.18] a solution of **30** (97 mg, 0.20 mmol) and triethylamine (279 μL, 2.00 mmol) in CH_2Cl_2 (7 mL) was treated with a solution of 4-nitrophenyl chloroformate (80 mg, 0.40 mmol) in acetonitrile (4 mL) at 0 °C under argon for 1.5 h. The reaction mixture was diluted with CH_2Cl_2 and washed with water. The organic layer was dried (Na_2SO_4) and concentrated. Chromatography [silica,

CH_2Cl_2/ethyl acetate (19:1)] afforded a white solid (83 mg, 64%): ^{1}H NMR δ 2.07 (s, 3H), 2.08 (s, 3H), 2.14 (s, 3H), 3.75 (s, 3H), 4.24 (d, *J* = 8.8 Hz, 2H), 5.26–5.41 (m, 5H), 7.39 (d, *J* = 9.2 Hz, 2H), 7.42 (d, *J* = 8.8 Hz, 1H), 7.63 (dd, ^1J = 1.6 Hz, ^2J = 8.8 Hz, 1H), 7.92 (d, *J* = 1.6 Hz, 1H), 8.29 (d, *J* = 9.2 Hz, 2H).

1-(*tert*-Butyldimethylsiloxy)-2,2-diethoxyethane (32). A solution of glycolaldehyde diethyl acetal (6.70 g, 50.0 mmol) in DMF (150 mL) was treated with *tert*-butyldimethylsilyl chloride (18.8 g, 125 mmol) and imidazole (17.0 g, 250 mmol) at room temperature under argon for 14 h. The reaction was quenched with water (5 mL), and the mixture was extracted with ethyl acetate. The organic layer was washed (water and brine), dried (Na_2SO_4) and concentrated to afford a light yellow liquid (12 g, quantitative): ^{1}H NMR δ 0.07 (s, 6H), 0.90 (s, 9H), 1.22 (t, *J* = 7.2 Hz, 6H), 3.56–3.76 (m, 4H), 3.63 (d, *J* = 5.2 Hz, 2H), 4.49 (t, *J* = 5.2 Hz, 1H); ^{13}C NMR δ –5.1, 15.6, 18.6, 26.1, 63.0, 64.8, 103.2.

5-(*tert*-Butyldimethylsiloxymethyl)dipyrromethane (33). Following a literature procedure[4.15] with modification, a mixture of **32** (12.4 g, 50.0 mmol) and pyrrole (347 mL, 5.00 mol) was treated with $InCl_3$ (1.11 g, 5.00 mmol) at 60 °C under argon for 2 h. The reaction was quenched by addition of TEA (5 mL). The reaction mixture was stirred for another 15 min at room temperature. The reaction mixture was concentrated. Chromatography [silica, hexanes/ethyl acetate (4:1)] afforded a light yellow oil (7.5 g, 52%): ^{1}H NMR δ 0.04 (s, 6H), 0.91 (s, 9H), 4.06 (d, *J* = 5.2 Hz, 2H), 4.24 (t, *J* = 5.2 Hz, 1H), 5.99 (m, 2H), 6.12–6.17 (m, 2H), 6.69 (m, 2H), 8.40–8.60 (br, 2H); ^{13}C NMR δ –5.3, 18.4, 26.2, 40.1, 67.7, 106.1, 108.3, 117.0, 131.8.

5-(Dimethoxymethyl)-5-methyldipyrromethane (34). A mixture of pyruvic aldehyde dimethyl acetal (346 μL, 2.86 mmol) and pyrrole (20.0 mL, 286 mmol) was treated

with $InCl_3$ (63 mg, 0.29 mmol) at room temperature under argon for 1.5 h. NaOH (beads, 343 mg, 8.56 mmol) was added. The mixture was stirred for 45 min. The mixture was filtered. The filtrate was concentrated to dryness. Chromatography [silica, hexanes/ethyl acetate (4:1)] afforded a dark solid (0.60 g, 89%): mp 58–60 °C; ^{1}H NMR δ 1.66 (s, 3H), 3.46 (s, 6H), 4.35 (s, 1H), 5.93–5.95 (m, 2H), 6.11–6.13 (m, 2H), 6.68–6.70 (m, 2H), 8.75 (br, 2H); ^{13}C NMR δ 134.85, 116.94, 113.74, 107.70, 106.05, 58.48, 45.16, 24.47; FAB-MS obsd 234.1373, calcd 234.1368 ($C_{13}H_{18}N_2O_2$); Anal. calcd for $C_{13}H_{18}N_2O_2$: C, 66.64, H, 7.74, N, 11.96. Found: C, 66.80, H, 7.72, N, 12.18.

***N,N′*-Bis(*tert*-butoxycarbonyl)-5-[2-(trimethylsilyl)ethynyl]dipyrromethane (37).** A solution of **36** (611 mg, 2.52 mmol) in CH_2Cl_2 (25 mL) was treated overnight with di-*tert*-butyl dicarbonate (2.20 g, 10.1 mmol) and 4-dimethylaminopyridine (31 mg, 0.25 mmol) at room temperature under argon. The reaction mixture was washed (water and brine), dried (Na_2SO_4) and concentrated under reduced pressure. The resulting residue was chromatographed [silica, hexanes/ethyl acetate (4:1)] to afford a white solid (1.0 g, 90%): mp 86–88 °C; ^{1}H NMR (300 MHz) δ 0.15 (s, 9H), 1.05 (s, 18H), 5.95–5.99 (m, 2H), 6.00 (s, 1H), 6.07–6.10 (m, 2H), 7.28–7.31 (m, 2H); ^{13}C NMR (300 MHz) δ 0.26, 27.99, 32.88, 84.17, 86.01, 105.26, 110.08, 113.34, 122.15, 132.94, 149.36; Anal. calcd for $C_{24}H_{34}N_2O_4Si$: C, 65.12; H, 7.74; N, 6.33. Found: C, 65.28; H, 7.71; N, 6.31.

***N,N′*-(*tert*-Butoxycarbonyl)-5-ethynyldipyrromethane (38).** A solution of **37** (320 mg, 864 μmol) in THF (30 mL) was treated overnight with TBAF (15 wt % on alumina, 3.0 g, 1.7 mmol) under reflux. The reaction mixture was filtered. The filtrate was concentrated. Chromatography [silica, hexanes/ethyl acetate (9:1)] gave a yellow solid. Recrystallization (CH_2Cl_2/MeOH) yielded a colorless oil (0.64 g, 76%): ^{1}H NMR (300 MHz) δ 1.51 (s, 18H),

2.31 (d, 1H, J = 2.7 Hz), 6.01–6.04 (m, 2H), 6.06 (d, 1H, J = 2.7 Hz), 6.08–6.10 (m, 2H), 7.27–7.29 (m, 2H); ^{13}C NMR (300 MHz) δ 27.58, 27.98, 31.47, 70.32, 83.33, 84.18, 85.35, 110.07, 113.24, 122.15, 132.75, 146.92, 149.27; FAB-MS obsd 371.3122, calcd 371.1985 ($C_{21}H_{26}N_2O_4$).

***N,N′*-Bis(*tert*-butoxycarbonyl)-5-acetyldipyrromethane (39).** A solution of **38** (1.01 g, 2.28 mmol) in CH_2Cl_2 (25 mL) was treated with a solution of $Hg(OAc)_2$ (551 mg, 1.73 mmol) in H_2O (200 μL) under argon under reflux for 5 h. $Na_2S{\cdot}9H_2O$ (416 mg, 1.73 mmol) was added to the reaction mixture in small fractions, whereupon formation of a black precipitate was observed. The reaction mixture was filtered through a Celite pad. The filtrate was washed (water and brine), dried (Na_2SO_4) and concentrated. Chromatography [silica, hexanes/ethyl acetate (2:1)] afforded a white solid (0.10 g, 31%): ^{1}H NMR δ 1.48 (s, 18H), 2.32 (s, 3H), 5.74–5.78 (m, 2H), 6.09–6.11 (m, 2H), 6.25 (s, 1H), 7.27–7.30 (m, 2H); ^{13}C NMR δ 28.05, 29.31, 52.01, 84.02, 110.41, 114.15, 122.18, 131.12, 149.54, 204.79; FAB-MS obsd 388.2003, calcd 388.1998 ($C_{21}H_{28}N_2O_5$); Anal. calcd for $C_{21}H_{28}N_2O_5$: C, 64.93, H, 7.27, N, 7.21. Found: C, 64.58, H, 7.39, N, 6.68.

Zn(II)-5-(5,5-Dimethyl-1,3-dioxan-2-yl)-15-[2-(trimethylsilyl)ethynyl]porphyrin (42). A solution of **40** (11 mg, 30 μmol) and **41** (7.8 mg, 30 μmol) in EtOH (3 mL) was treated overnight with $Zn(OAc)_2{\cdot}2H_2O$ (66 mg, 0.30 mmol) under reflux. DDQ (20 mg, 90 μmol) was added, and the reaction mixture was stirred for 30 min. The reaction mixture was concentrated. Chromatography [silica, hexanes/ethyl acetate (3:1)] afforded a purple solid (2 mg, 9%): ^{1}H NMR δ 0.68 (s, 9H), 1.16 (s, 3H), 1.98 (s, 3H), 4.26–4.38 (m, 4H), 7.97 (s, 1H), 9.33 (d, J = 4.4, 2H), 9.41 (d, J = 4.8 Hz, 2H), 9.77 (d, J = 4.4 Hz, 2H), 10.08 (d, J = 4.8 Hz, 2H), 10.13 (s, 2H); LD-MS obsd 583.406; FAB-MS obsd 582.1473, calcd 582.1430

($C_{31}H_{30}N_4O_2SiZn$); λ_{abs} 417, 550, 589 nm.

Zn(II)-5-(5,5-Dimethyl-1,3-dioxan-2-yl)-15-ethynylporphyrin (43). A solution of porphyrin **42** (13 mg, 22 μmol) in THF (10 mL) was treated with TBAF (1 M solution in THF, 50 μL, 50 μmol). The reaction mixture was concentrated. Chromatography [silica, hexanes/ethyl acetate (3:1)] afforded a purple solid (yield to be determined): LD-MS obsd 511.238; FAB-MS obsd 510.1077, calcd 510.1034 ($C_{28}H_{22}N_4O_2Zn$).

Synthesis of *Trans*-AB$_2$C-Porphyrins from 1,9-Diacyldipyrromethane and Dipyrromethane, Exemplified for 5-(*tert*-Butyldimethylsiloxymethyl)-15-phenyl-10,20-di-*p*-tolylporphyrin (45). A solution of **44** (588 mg, 852 μmol) in dry THF/MeOH (10:1, 33 mL) was treated with $NaBH_4$ (642 mg, 17.0 mmol) for 2 h. A second batch of $NaBH_4$ (642 mg, 17.0 mmol) was added and the reaction mixture was stirred for another 2 h. Saturated aqueous NH_4Cl was added, and the mixture was extracted with CH_2Cl_2. The organic layer was separated, dried (K_2CO_3) and concentrated. The resulting dicarbinol was dissolved in CH_2Cl_2 (340 mL) and treated with **33** (247 mg, 852 μmol) and $Yb(OTf)_3$ (675 mg, 1.09 mmol) under argon for 30 min. DDQ (579 mg, 2.55 mmol) was added, and the mixture was stirred for 1 h. TEA was added, and the reaction mixture was concentrated. Chromatography [silica, hexanes/CH_2Cl_2 (1:3)] afforded a purple solid (77 mg, 12%): ^{1}H NMR δ –2.83 (br, 2H), 0.20 (s, 6H), 0.95 (s, 9H), 2.72 (s, 6H), 7.01 (s, 2H), 7.56 (d, J = 8.0 Hz, 4H), 7.71–7.78 (m, 3H), 8.10 (d, J = 8.0 Hz, 4H), 8.19 (dd, ^1J = 7.6 Hz, ^2J = 1.6 Hz, 2H), 8.80 (d, J = 4.8 Hz, 2H), 8.83 (d, J = 4.8 Hz, 2H), 8.98 (d, J = 4.8 Hz, 2H), 9.59 (d, J = 4.8 Hz, 2H); LD-MS obsd 710.7; FAB-MS obsd 710.3429, calcd 710.3441 ($C_{47}H_{46}N_4OSi$); λ_{abs} 417, 515, 549, 590, 646 nm.

Zinc Metalation of a Free Base Porphyrin, Exemplified for Zn(II)-5-(*tert*-

Butyldimethylsiloxymethyl)-15-phenyl-10,20-di-*p*-tolylporphyrin (45Zn). A solution of **45** (70 mg, 99 μmol) in CH_2Cl_2 (25 mL) was treated overnight with $Zn(OAc)_2 \cdot 2H_2O$ (107 mg, 492 μmol) at room temperature. The reaction mixture was concentrated. Chromatography (silica, CH_2Cl_2) afforded a purple solid (72 mg, 95%): ^{1}H NMR δ 0.18 (s, 6H), 0.96 (s, 9H), 2.71 (s, 6H), 6.87 (s, 2H), 7.54 (d, *J* = 8.0 Hz, 4H), 7.69–7.78 (m, 3H), 8.07 (d, *J* = 8.0 Hz, 4H), 8.16–8.22 (m, 2H), 8.90 (d, *J* = 4.0 Hz, 2H), 8.93 (d, *J* = 4.0 Hz, 2H), 8.99 (d, *J* = 4.8 Hz, 2H), 9.55 (d, *J* = 4.8 Hz, 2H); LD-MS obsd 772.8; FAB-MS obsd 772.2573, calcd 772.2576 ($C_{47}H_{44}N_4OSiZn$); λ_{abs} 419, 548 nm.

Deprotecting the TBDMS Group with TBAF, Exemplified for 5-Hydroxymethyl-15-phenyl-10,20-di-*p*-tolylporphyrin (46). A solution of **45** (50 mg, 71 μmol) in THF (5 mL) was treated with TBAF (1.0 M in THF, 0.35 mL, 0.35 mmol) at room temperature under argon for 9 h. The reaction was quenched by addition of water. The mixture was extracted with CH_2Cl_2 and ethyl acetate. The combined organic extraction was dried (Na_2SO_4) and concentrated to afford the crude product as a solid. Chromatography [silica, CH_2Cl_2/ethyl acetate (4:1)] afforded a purple solid (25 mg, 60%): ^{1}H NMR δ (THF-d_8) δ –2.76 (br, 2H), 2.68 (s, 6H), 5.35 (t, *J* = 5.6 Hz, 1H), 6.86 (d, *J* = 5.6 Hz, 2H), 7.57 (d, *J* = 7.6 Hz, 4H), 7.68–7.78 (m, 3H), 8.07 (d, *J* = 7.6 Hz, 4H), 8.14–8.22 (m, 2H), 8.74–8.84 (m, 4H), 8.92 (d, *J* = 4.0 Hz, 2H), 9.73 (d, *J* = 4.0 Hz, 2H); LD-MS obsd 596.8; FAB-MS obsd 596.2570, calcd 596.2576 ($C_{41}H_{32}N_4O$); λ_{abs} 417, 515, 549, 590, 646 nm.

Zn(II)-5-Hydroxymethyl-15-phenyl-10,20-di-*p*-tolylporphyrin (46Zn). Following the general deprotection procedure for **46** with modification, the reaction of **45Zn** (10.8 mg, 14.0 μmol) followed by chromatography [silica, CH_2Cl_2/ethyl acetate (4:1)] afforded a red purple solid (7.5 mg, 81%): ^{1}H NMR (THF-d_8) δ 2.70 (s, 6H), 5.15 (t, *J* = 6.0 Hz, 1H), 6.94

(d, J = 6.0 Hz, 2H), 7.57 (d, J = 8.0 Hz, 4H), 7.69–7.75 (m, 3H), 8.08 (d, J = 8.0 Hz, 4H), 8.14–8.19 (m, 2H), 8.79 (d, J = 4.8 Hz, 2H), 8.83 (d, J = 4.8 Hz, 2H), 8.95 (d, J = 4.8 Hz, 2H), 9.76 (d, J = 4.8 Hz, 2H); LD-MS obsd 658.4; FAB-MS obsd 658.1736, calcd 658.1711 ($C_{41}H_{30}N_4OZn$); λ_{abs} 419, 548 nm.

Dibutyl[5-(*tert*-butyldimethylsiloxymethyl)-5,10-dihydro-1,9-di-*p*-tolyl-dipyrrinato]tin(IV) (47). Following a literature procedure[5.24] with modification, EtMgBr (1.0 M in THF, 13 mL, 13 mmol) was added dropwise to a solution of **33** (936 mg, 3.22 mmol) in toluene (65 mL) in an ice bath. The reaction was stirred at 0 °C for 30 min. *p*-Toluoyl chloride (1.06 mL, 8.05 mmol) was added dropwise, and the mixture was stirred at 0 °C for 1 h. The reaction mixture was poured into saturated aqueous NH_4Cl solution and ethyl acetate. The organic layer was separated, washed with brine, dried (Na_2SO_4) and concentrated. The resulting yellow oil was dissolved in ethyl acetate (20 mL) and treated with TEA (1.35 mL, 9.66 mmol) and Bu_2SnCl_2 (978 mg, 3.22 mmol) at room temperature for 30 min. The reaction mixture was washed (water and brine), dried (Na_2SO_4) and concentrated. Chromatography (silica, CH_2Cl_2) afforded a light yellow solid (1.0 g, 41%): mp 81–83 °C; ^{1}H NMR δ –0.15 (s, 6H), 0.60 (t, J = 7.2 Hz, 3H), 0.81 (t, J = 7.2 Hz, 3H), 0.94–1.80 (m, 12H), 2.44 (s, 6H), 3.77 (d, J = 7.2 Hz, 2H), 4.44 (d, J = 7.2 Hz, 1H), 6.43 (d, J = 4.0 Hz, 2H), 7.11 (d, J = 4.0 Hz, 2H), 7.31 (d, J = 8.0 Hz, 4H), 7.82 (d, J = 8.0 Hz, 4H); ^{13}C NMR δ –5.59, 13.71, 13.86, 18.7, 21.8, 23.2, 25.6, 26.0, 26.1, 26.8, 27.2, 27.8, 43.7, 71.4, 115.9, 123.5, 129.3, 129.4, 135.3, 136.4, 142.3, 149.7, 184.5; Anal. calcd for $C_{40}H_{54}N_2O_3Sn$: C, 63.41, H, 7.18, N, 3.70. Found: C, 63.43, H, 7.21, N, 3.69.

5-(*tert*-Butyldimethylsiloxymethyl)-15-(ethoxycarbonyl)-10,20-di-*p*-tolyporphyrin (49). Following the general procedure for **45** with modification, the reaction

of **47** (841 mg, 1.11 mmol) and **48** (242 mg, 1.11 mmol) followed by chromatography [silica, hexanes/CH_2Cl_2 (1:3)] afforded a purple solid (77 mg, 9.8%): ^{1}H NMR δ –2.55 (br, 2H), –0.03–0.01 (s, 6H, overlapping with the TMS peak at 0.0 ppm), 1.54 (s, 9H), 1.77 (t, *J* = 7.2 Hz, 3H), 2.72 (s, 6H), 5.04 (q, *J* = 7.2 Hz, 2H), 7.57 (d, *J* = 10.0 Hz, 4H), 8.06 (d, *J* = 10.0 Hz, 4H), 8.87 (d, *J* = 4.8 Hz, 2H), 8.90 (d, *J* = 5.2 Hz, 2H), 9.35 (d, *J* = 5.2 Hz, 2H), 9.48 (d, *J* = 4.8 Hz, 2H); LD-MS obsd 576.3, calcd 706.3339 [(M – TMDMSO), M = $C_{44}H_{46}N_4O_3Si$); λ_{abs} 417, 515, 550, 590 nm.

5-(Ethoxycarbonyl)-15-hydroxymethyl-10,20-di-*p*-tolylporphyrin (50). Following the general deprotection procedure for **46**, the reaction of **49** (77 mg, 0.11 mmol) followed by chromatography [silica, CH_2Cl_2/ethyl acetate (9:1)] afforded a purple solid (13 mg, 20%): ^{1}H NMR δ –2.98 (br, 2H), 1.76 (t, *J* = 9.6 Hz, 3H), 2.72 (s, 6H), 5.05 (q, *J* = 9.6 Hz, 2H), 6.88 (s, 2H), 7.56 (d, *J* = 10.4 Hz, 4H), 8.04 (d, *J* = 10.4 Hz, 4H), 8.94–8.96 (m, 4H), 9.39 (d, *J* = 6.4 Hz, 2H), 9.54 (d, *J* = 6.4 Hz, 2H); LD-MS obsd 592.4; FAB-MS obsd 592.2471, calcd 592.2474 ($C_{38}H_{32}N_4O_3$); λ_{abs} 415, 512, 548, 592 nm.

Zn(II)-5-(Ethoxycarbonyl)-15-hydroxymethyl-10,20-di-*p*-tolylporphyrin (50Zn). Following the general procedure for **45Zn**, the reaction of **50** (12 mg, 20 μmol) followed by chromatography [silica, CH_2Cl_2/ethyl acetate (19:1)] afforded a purple solid (13 mg, 95%): ^{1}H NMR (THF-d_8) δ 1.71–1.76 (t, 3H, overlapping with the THF peak at 1.73 ppm), 2.72 (s, 6H), 5.00 (q, *J* = 7.2 Hz, 2H), 5.20 (t, *J* = 6.0 Hz, 1H), 6.93 (d, *J* = 6.0 Hz, 2H), 7.59 (d, *J* = 7.6 Hz, 4H), 8.07 (d, *J* = 7.6 Hz, 4H), 8.90–8.97 (m, 4H), 9.41 (d, *J* = 4.4 Hz, 2H), 9.78 (d, *J* = 4.4 Hz, 2H); LD-MS obsd 654.5; FAB-MS obsd 654.1636, calcd 654.1609 ($C_{38}H_{30}N_4O_3Zn$); λ_{abs} 417, 547 nm.

5-(Ethoxycarbonyl)-15-formyl-10,20-di-*p*-tolylporphyrin (51). Porphyrin **51** was

obtained as a byproduct from the acylation of porphyrin **50**: ^{1}H NMR δ –2.53 (br, 2H), 1.78 (t, *J* = 9.6 Hz, 3H), 2.73 (s, 6H), 5.07 (q, *J* = 9.6 Hz, 2H), 7.59 (d, *J* = 10.8 Hz, 4H), 8.05 (d, *J* = 10.8 Hz, 4H), 8.89 (d, *J* = 6.8 Hz, 2H), 9.02 (d, *J* = 6.8 Hz, 2H), 9.35 (d, *J* = 6.8 Hz, 2H), 10.01 (d, *J* = 6.8 Hz, 2H), 12.52 (s, 1H); LD-MS obsd 590.1; FAB-MS obsd 590.2307, calcd 590.2318 ($C_{38}H_{30}N_4O_3$); λ_{abs} 422, 525, 566, 661 nm.

Zn(II)-5-(Ethoxycarbonyl)-15-formyl-10,20-di-*p*-tolylporphyrin (51Zn). Porphyrin **51Zn** was obtained as a byproduct from the acylation of porphyrin **50Zn**: LD-MS obsd 652.2; FAB-MS obsd 652.1479, calcd 652.1453 ($C_{38}H_{28}N_4O_3Zn$); λ_{abs} 427, 563, 607 nm.

Dibutyl-(3-bromo-5,10-dihydro-1,9-di-*p*-toluoyldipyrrinato)tin(IV) (53). Following a literature procedure,[5.53] a solution of 1,9-diacyldipyromethane **52** (10.8 g, 17.0 mmol) in dry THF (75 mL) at –78 °C under argon was treated with NBS (3.10 g, 17.0 mmol) in one portion. The reaction mixture was stirred for 1 h at –78 °C. Hexanes/H_2O (1:1) was added, and the mixture was allowed to warm to room temperature. The organic layer was washed with H_2O, dried (K_2CO_3) and concentrated. Chromatography (silica, CH_2Cl_2 dried over K_2CO_3) afforded a yellow solid (7.3 g, 62%): mp 139-140 °C; ^{1}H NMR δ 0.70 (t, *J* = 6.85 Hz, 6H), 1.10–1.20 (m, 5H), 1.30–1.39 (m, 5H), 1.50–1.60 (m, 2H), 2.45 (s, 6H), 4.30 (s, 2H), 6.41 (d, *J* = 4.0 Hz, 1H), 7.17–7.18 (m, 3H), 7.31 (d, *J* = 8.0 Hz, 4H), 7.78–7.87 (m, 4H); ^{13}C NMR δ 13.8, 21.9 (two methyl carbons on the *p*-toluoyl groups overlapped), 24.6, 26.3, 27.1, 27.4, 100.5, 114.7, 124.09, 124.15, 129.28, 129.35 (two of the four signals for C2/C3 of the *p*-toluoyl groups overlapped), 129.40, 134.3, 134.8, 134.9, 135.8, 142.6, 142.8, 144.3, 147.2, 184.2, 184.4; Anal. Calcd. for ($C_{33}H_{37}BrN_2O_2Sn$): C, 57.03; H, 5.40; N, 3.95. Found: C, 57.25; H, 5.40; N, 4.05.

3-Bromo-15-(ethoxycarbonyl)-10,20-di-*p*-tolylporphyrin (54). Following the

general procedure for **45**, the reaction of **53** (286 mg, 413 μmol) and **48** (90 mg, 0.41 μmol) followed by chromatography [silica, hexanes/CH_2Cl_2 (1:4)] afforded a purple solid (36 mg, 14%): ^{1}H NMR δ –3.07 (br, 2H), 1.78 (t, *J* = 6.8 Hz, 3H), 2.73 (s, 6H), 5.08 (q, *J* = 7.1 Hz, 2H), 7.60 (d, *J* = 7.6 Hz, 4H), 8.06–8.11 (m, 4H), 8.94 (s, 1H), 8.95 (d, *J* = 4.8 Hz, 1H), 9.09 (d, *J* = 4.8 Hz, 1H), 9.10 (d, *J* = 4.8 Hz, 1H), 9.32 (d, *J* = 5.2 Hz, 1H), 9.46 (d, *J* = 4.8 Hz, 1H), 9.51 (d, *J* = 5.2 Hz, 1H), 10.44 (s, 1H); LD-MS obsd 640.3; FAB-MS obsd 640.1470, calcd 640.1474 ($C_{37}H_{29}BrN_4O_2$); λ_{abs} 415, 511, 583, 638 nm.

Zn(II)-3-Bromo-15-(ethoxycarbonyl)-10,20-di-*p*-tolylporphyrin (54Zn). Following the general procedure for **45**, the reaction of **54** (39 mg, 60 μmol) followed by chromatography (silica, CH_2Cl_2) afforded a red purple solid (41 mg, 98%): ^{1}H NMR δ 1.24 (t, *J* = 8.0 Hz, 3H), 2.79 (s, 6H), 4.12 (q, *J* = 7.5 Hz, 2H), 7.62 (d, *J* = 7.5 Hz, 1H), 8.10–8.17 (m, 4H), 8.36–8.42 (m, 2H), 8.83–8.89 (m, 2H), 9.07–9.12 (m, 3H), 9.46 (d, *J* = 4.5 Hz, 1H), 10.5 (s, 1H); LD-MS obsd 701.8; FAB-MS obsd 702.0661, calcd 702.0609 ($C_{37}H_{27}BrN_4O_2Zn$); λ_{abs} 416, 544, 574, 656 nm.

Zn(II)-5-(Ethoxycarbonyl)-13-hydroxymethyl-10,20-di-*p*-tolylporphyrin (56Zn). Following a literature procedure,[5.39a] a mixture of **54Zn** (41 mg, 59 μmol), (hydroxymethyl)tributyltin (**55**) (42 mg, 0.13 mmol) and $Pd(PPh_3)_4$ (10 mg, 8.0 μmol) was refluxed in THF (2.5 mL) for 48 h in a Schlenk flask. The crude mixture was concentrated. Chromatography [silica, CH_2Cl_2/ethyl acetate (19:1)] afforded a red purple solid (21 mg, 55%): ^{1}H NMR (THF-d_8, 300 MHz) δ 1.71–1.76 (t, 3H, overlapping with the THF peak at 1.73 ppm), 2.73 (s, 6H), 4.90–5.17 (q, *J* = 10.2 Hz, 2H), 6.07 (d, *J* = 7.2 Hz, 2H), 7.60 (d, *J* = 9.2 Hz, 4H), 8.03–8.12 (m, 4H), 8.86 (s, 1H), 8.94–9.00 (m, 3H), 9.37 (d, *J* = 4.2 Hz, 1H), 9.45 (d, *J* = 4.8 Hz, 2H), 10.4 (s, 1H); LD-MS obsd 654.9; FAB-MS obsd 654.1644, calcd

654.1609 ($C_{38}H_{30}N_4O_3Zn$); λ_{abs} 416, 545, 575, 656 nm.

Zn(II)-5-(Ethoxycarbonyl)-13-formyl-10,20-di-*p*-tolylporphyrin (57Zn). Following a literature procedure,[5.40] a solution of porphyrin **56Zn** (21.3 mg, 32.6 μmol) in THF (4 mL) was treated with pyridinium chlorochromate (10 mg, 46 μmol) at room temperature under argon for 6 h. The mixture was diluted with CH_2Cl_2 and washed (saturated NH_4Cl solution and water). The organic layer was dried (Na_2SO_4) and concentrated. Chromatography [silica, CH_2Cl_2/ethyl acetate (97:3)] afforded a purple solid (6.7 mg, 32%): ^{1}H NMR δ 0.79 (t, *J* = 7.2 Hz, 3H), 2.83 (d, *J* = 4.8 Hz, 6H), 3.33 (q, *J* = 7.2 Hz, 2H), 7.41–7.49 (m, 2H), 7.60–7.68 (m, 4H), 8.10–8.18 (m, 4H), 8.58–8.66 (m, 2H), 9.02 (d, *J* = 4.5 Hz, 1H), 9.44 (d, *J* = 4.5 Hz, 1H), 9.54 (s, 1H), 11.1 (s, 1H), 11.3 (s, 1H); LD-MS obsd 652.6; FAB-MS obsd 652.1467, calcd 652.1453 ($C_{387}H_{28}BrN_4O_3Zn$); λ_{abs} 426, 554, 594, 656 nm.

Zn(II)-5-(Ethoxycarbonyl)-13-(*N*-methylaminomethyl)-10,20-di-*p*-tolylporphyrin (58Zn). Following a literature procedure,[5.2d] $NaBH_3CN$ (12 mg, 0.98 mmol) was added to a mixture of **57Zn** (6.4 mg, 9.8 μmol) in CH_2Cl_2 (4 mL) containing molecular sieves 4Å (50 mg). A solution of methylamine hydrochloride (66 mg, 0.98 mmol) and TEA (91 μL, 0.66 mmol) in MeOH (20 mL) was added to the reaction mixture. The mixture was stirred at room temperature under argon in the dark for 24 h. The reaction mixture was poured into ice/CH_2Cl_2. The organic layer was separated and concentrated. The organic layer was washed (5% aqueous $NaHCO_3$ solution and brine), dried (Na_2SO_4) and concentrated. Chromatography [alumina, CH_2Cl_2/MeOH (4:1)] afforded a red purple solid (yield to be determined): LD-MS obsd 667.5, calcd 667.1926 ($C_{39}H_{33}N_5O_2Zn$); λ_{abs} 419, 550 nm.

Zn(II)-15-ethoxycarbonyl-3-(*N*-methyl-{3-nitro-4-*O*-[methyl (2,3,4-tri-*O*-acetyl-

β-D-glucopyranoside)uronate]benzyloxycarbonyl}aminomethyl)-10,20-di-*p*-tolylporphyrin (59Zn). A solution of porphyrin **58Zn** (6 mg, 9 μmol) in DMF (1 mL) under argon was treated with TEA (13 μL, 90 μmol). A solution of **31** (14 mg, 22 μmol) in DMF (1 mL) was then slowly added, and the reaction mixture was stirred at room temperature for 3 d. Ethyl acetate was added, and the mixture was washed (water and brine), dried (Na_2SO_4) and concentrated. Chromatography [silica, CH_2Cl_2/MeOH (50:1)] afforded a purple solid (yield to be determined): LD-MS obsd 1178.5; calcd 1178.2888 ($C_{60}H_{54}N_6O_{16}Zn$).

***n*-Propylaminomethyltributyltin (62).** Following a general precedure,[5.40] a solution of **61** (200 mg, 464 μmol) in Et_2O (2 mL) was treated with *n*-propylamine (381 μL, 4.64 mmol) at room temperature in the dark for 48 h. The reaction mixture was concentrated. Chromatography [silica, hexanes/ethyl acetate (4:1)] afforded a colorless liquid (0.14 g, 83%): ^{1}H NMR δ 0.89–0.96 (m, 12H), 1.10–1.70 (m, 24H); GC-MS obsd 361, calcd 363.1948 ($C_{16}H_{37}NSn$).

10-(Dibutylboryl)-5-(5,5-dimethyl-1,3-dioxan-2-yl)-1-*p*-toluoyl-dipyrromethane (64). Following a general precedure,[5.45] a solution of **41** (260 mg, 1.00 mmol) in THF (1 mL) was treated with EtMgBr (1.0 M in THF, 2.5 mL, 2.5 mmol) at –78 °C for 10 min. A solution of Mukaiyama reagent **63** (230 mg, 1.00 mmol) in THF (1 mL) was added dropwise to the reaction mixture. The mixture was stirred at room temperature for 10 min. Saturated aqueous NH_4Cl solution was added, and the reaction mixture was extracted with ethyl acetate. The organic layer was washed with brine, dried (Na_2SO_4) and concentrated. The resulting solid was dissolved in CH_2Cl_2 (2 mL) and treated with TEA (335 μL, 2.40 mmol) and Bu_2B-OTf (2.00 mL, 2.00 mmol) at room temperature for 30 min. The solvent was removed under reduced pressure. Chromatography [silica, hexanes/CH_2Cl_2 (1:4)] afforded a yellow-greenish

oil (0.17 g, 34%): ^{1}H NMR δ 0.50–1.30 (m, 24H), 2.43 (s, 3H), 3.40–3.48 (m, 2H), 3.63–3.69 (m, 2H), 4.54 (d, *J* = 3.6 Hz, 1H), 4.79 (d, *J* = 3.6 Hz, 1H), 5.88–5.93 (m, 1H), 6.07–6.12 (m, 1H), 6.64 (d, *J* = 4.4 Hz, 1H), 6.70–6.74 (m, 1H), 7.22 (d, *J* = 4.4 Hz, 1H), 7.32 (d, *J* = 8.0 Hz, 2H), 8.09 (d, *J* = 8.0 Hz, 2H), 8.95 (br, 1H); ^{13}C NMR δ 14.3, 14.5, 21.9, 22.0, 22.8 (br), 23.2 (br), 23.28, 26.2, 26.4, 27.0, 27.2, 30.4, 42.9, 77.51, 77.56, 103.1, 108.03, 108.07, 117.3, 117.6, 119.8, 128.1, 128.4, 129.86, 129.90, 133.8, 145.1, 147.1, 175.4; FAB-MS 503.3426, calcd 503.3445 [$(M + H)^+$, M = $C_{31}H_{43}BN_2O_3$].

10-(Dibutylboryl)-1,9-di-*p*-toluoyl-5-(5,5-dimethyl-1,3-dioxan-2-yl)dipyrromethane (65). Following a general precedure,[5.46] a solution of **64** (172 mg, 343 μmol) in THF (343 μL) was treated with MesMgBr (1.0 M in THF, 0.69 mL, 0.69 mmol) at room temperature for 5 min. A solution of *p*-toluoyl chloride (99.7 μL, 754 μmol) in THF was added dropwise to the mixture. The reaction was stirred at room temperature for 10 min. Saturated aqueous NH_4Cl solution was added, and the reaction mixture was extracted with ethyl acetate. The organic layer was washed with brine, dried (Na_2SO_4) and concentrated. Chromatography (silica, CH_2Cl_2) afforded an orange solid (0.12 g, 56%): ^{1}H NMR δ 0.50–1.30 (m, 24H), 2.41 (s, 3H), 2.47 (s, 3H), 3.40–3.52 (m, 2H), 3.68–3.78 (m, 2H), 4.59 (d, *J* = 4.0 Hz, 1H), 4.83 (d, *J* = 4.0 Hz, 1H), 6.00–6.06 (m, 1H), 6.70 (d, *J* = 4.0 Hz, 1H), 6.73–6.78 (m, 1H), 7.22–7.28 (m, 3H), 7.35 (d, *J* = 8.0 Hz, 2H), 7.80 (d, *J* = 8.0 Hz, 2H), 8.12 (d, *J* = 8.0 Hz, 2H), 10.1 (br, 1H); ^{13}C NMR δ 14.3, 14,5, 21,8, 21.9, 22.1, 22.7 (br), 23.1 (br), 23,3, 26.2, 26.4, 27.14, 27.21, 30.4, 43.0, 77.67, 77.76, 102.4, 111,4, 117.7, 119.3, 119.8, 128.0, 129.11, 129.24, 130.02, 130.04, 131.1, 134.1, 126.1, 136.4, 142.3, 145.1, 145.5, 176.4, 184.3; FAB-MS obsd 621.3864, calcd 621.3864 [$(M + H)^+$, M = $C_{39}H_{49}BN_2O_4$].

5-Ethoxycarbonyl-15-(5,5-dimethyl-1,3-dioxan-2-yl)-10,20-di-*p*-tolylporphyrin

(66). Following the general procedure for **45**, the reaction of **65** (119 mg, 192 μmol) and **48** (41.9 mg, 192 μmol) followed by chromatography (silica, CH_2Cl_2) afforded a purple solid (18 mg, 14%): ^{1}H NMR δ –2.98 (br, 2H), 1.11 (s, 3H), 1.77 (t, *J* = 7.2 Hz, 3H), 1.91 (s, 3H), 2.72 (s, 6H), 4.27–4.36 (m, 4H), 5.05 (q, *J* = 7.2 Hz, 2H), 7.57 (d, *J* = 8.0 Hz, 4H), 7.94 (s, 1H), 8.06 (d, *J* = 8.0 Hz, 4H), 8.91–8.99 (m, 4H), 9.42 (d, *J* = 4.8 Hz, 2H), 9.93 (d, *J* = 4.8 Hz, 2H); LD-MS obsd 676.4; FAB-MS obsd 676.3049, calcd 676.3050 ($C_{43}H_{40}N_4O_4$); λ_{abs} 415, 512, 546, 588, 642 nm.

5-Ethoxycarbonyl-15-formyl-10,20-di-*p*-tolylporphyrin (67). A solution of **66** (7.2 mg, 11 μmol) in CH_2Cl_2 (1 mL) was treated with a mixture of TFA (0.80 mL, 10 mmol) and H_2O (100 μL) at room temperature for 28 h. The reaction mixture was diluted in CH_2Cl_2, washed (saturated aqueous $NaHCO_3$ and water), dried (Na_2SO_4) and concentrated. Chromatography (silica, CH_2Cl_2) afforded a purple solid (5.5 mg, 85%): ^{1}H NMR δ –2.54 (br, 2H), 1.77 (t, *J* = 7.2 Hz, 3H), 2.73 (s, 6H), 5.07 (q, *J* = 7.2 Hz, 2H), 7.58 (d, *J* = 7.6 Hz, 4H), 8.04 (d, *J* = 7.6 Hz, 4H), 8.88 (d, *J* = 4.8 Hz, 2H), 9.01(d, *J* = 4.8 Hz, 2H), 9.35 (d, *J* = 4.8 Hz, 2H), 10.00 (d, *J* = 4.8 Hz, 2H), 12.51 (s, 1H); LD-MS obsd 590.4; FAB-MS obsd 590.2321, calcd 590.2318 ($C_{38}H_{30}N_4O_3$); λ_{abs} 422, 525, 567, 604, 661 nm.

5-Ethoxycarbonyl-15-(5,5-dimethyl-1,3-dioxan-2-yl)porphyrin (70). Following the general procedure for **45**, the reaction of 1,9-diformyldipyrromethane **68** (32 mg, 0.10 mmol) and dipyrromethane **48** (22 mg, 0.10 mmol) followed by chromatography (silica, CH_2Cl_2) afforded a purple solid (5.1 mg, 10%): ^{1}H NMR δ –3.21 (s, 1H), –3.15 (s, 1H), 1.16 (s, 3H), 1.85 (t, *J* = 7.2 Hz, 3H), 1.99 (s, 3H), 4.36 (d, *J* = 4.0 Hz, 4H), 5.11 (q, *J* = 7.2 Hz, 2H), 7.97 (s, 1H), 9.42–9.42 (m, 4H), 9.69 (d, *J* = 4.4 Hz, 2H), 10.05 (d, *J* = 4.4 Hz, 2H), 10.30 (s, 2H); FAB-MS obsd 497.2200, calcd 497.2189 [$(M + H)^+$, M = $C_{29}H_{28}N_4O_4$]; λ_{abs}

401, 500, 536 nm.

Zn(II)-5-Ethoxycarbonyl-15-formylporphyrin by Route 2 (71Zn). Following a literature procedure,[5.47] a solution of dipyrromethane **68** (316 mg, 1.00 mmol) in THF (4 mL) was treated with *n*-propylamine (205 μL, 2.50 mmol) at room temperature for 1 h. The reaction mixture was concentrated and then dissolved in EtOH (100 mL). Dipyrromethane **48** (218 mg, 1.00 mmol) and $Zn(OAc)_2$ (1.83 g, 10.0 mmol) were added, and the mixture was refluxed for 16 h. The reaction mixture was filtered through a Celite pad. The eluent was concentrated. Chromatography [silica, CH_2Cl_2/ethyl acetate (9:1)] afforded a purple solid (5 mg, 1%): ^{1}H NMR δ 1.82 (t, *J* = 7.2 Hz, 3H), 5.09 (q, *J* = 7.2 Hz, 2H), 9.44 (d, *J* = 4.5 Hz, 2H), 9.55 (d, *J* = 4.5 Hz, 2H), 9.60 (d, *J* = 4.5 Hz, 2H), 10.32–10.36 (m, 4H), 12.68 (s, 1H); LD-MS obsd 471.8; FAB-MS obsd 472.0532, calcd 472.0514 ($C_{24}H_{16}N_4O_3Zn$); λ_{abs} 413, 548, 598 nm.

Zn(II)-5-Ethoxycarbonyl-15-formylporphyrin by Route 3 (71Zn). Following literature procedures[4.2,5.44] with modification, a solution of dipyrromethane **68** (390 mg, 1.50 mmol) in CH_2Cl_2 (15 mL) was treated with Eschenmoser's salt (611 mg, 3.30 mmol) at room temperature for 1 h. The reaction mixture was washed with saturated aqueous $NaHCO_3$, dried (Na_2SO_4) and concentrated. The resulting crude 1,9-bis(*N*,*N*-dimethylaminomethyl)dipyrromethane (**69**) and dipyrromethane **48** (310 mg, 1.42 mmol) were dissolved in EtOH (140 mL) and treated with $Zn(OAc)_2$ (2.60 g, 14.2 mmol) under reflux for 2 h. DDQ (967 mg, 4.26 mmol) was added, and the mixture was stirred for 15 min. TEA was added, and the mixture was concentrated. The resulting dark solid was dissolved in CH_2Cl_2/THF (4:1, 25 mL) and treated with TFA (1.42 mL, 18.4 mmol) and water (1.42 mL) at room temperature for 2.5 h. The reaction mixture was concentrated. Chromatography

(silica, CH_2Cl_2) afforded a purple solid (12 mg, 2%). Characterization data (^{1}H NMR and LD-MS) were consistent with the value reported above.

Zinc(II)-5-(Ethoxycarbonyl)-15-(*N*-hydroxyiminomethyl)-10,20-di-*p*-tolylporphyrin (72Zn). A solution of hydroxylamine hydrochloride (1.2 mg, 17 μmol) in H_2O/EtOH (1:2, 300 μL) was cooled to 0 °C in an ice bath. Sodium acetate (2.1 mg, 25 μmol) and a solution of porphyrin **71Zn** (4.0 mg, 8.4 μmol) in EtOH (300 μL) were added to the hydroxylamine solution. The mixture was warmed to room temperature and stirred for 2 h. The mixture was concentrated. Chromatography [silica, CH_2Cl_2/MeOH (9:1)] afforded a purple solid (3.9 mg, 95%): ^{1}H NMR δ (THF-d_8, 300 MHz) 1.83 (t, J = 5.6 Hz, 3H), 5.10 (q, J = 5.6 Hz, 2H), 9.41–9.49 (m, 6H), 9.58–9.65 (m, 2H), 12.63 (s, 1H); LD-MS obsd 487.0; FAB-MS obsd487.0607, calcd 487.0623 ($C_{24}H_{17}N_5O_3Zn$); λ_{abs} 410, 548, 593 nm.

10-Dibutylboryl-5-{1-[2-(trimethylsilyl)ethoxymethyl]imidazol-4-yl}dipyrromethane (74). A solution of regioisomers **73a** and **73b** (343 mg, 1.00 mmol) in CH_2Cl_2 (2 mL) was treated with TEA (335 μL, 2.40 mmol) and Bu_2B-OTf (1.0 M solution in CH_2Cl_2, 2.0 mL, 2.0 mmol) under argon for 30 min. The reaction mixture was concentrated. Chromatography [silica, hexanes/CH_2Cl_2 (1:1)] afforded a dark oil (45 mg, 9.6%): ^{1}H NMR δ 0.50–0.65 (m, 4H), 0.80 (t, J = 7.2 Hz, 6H), 0.88–1.28 (m, 10H), 3.50 (t, J = 8.0 Hz, 2H), 5.30 (s, 2H), 5.50 (s, 1H), 5.91 (m, 1H), 6.18 (m, 3H), 6.71 (m, 1H), 6.75 (m, 1H), 6.83 (m, 1H), 7.83 (d, J = 1.6 Hz, 1H), 8.23 (br, 1H); ^{13}C NMR δ 15.69, 19.16, 27.96, 29.23, 29.61, 35.51, 69.01, 79.05, 105.88, 108.05, 108.73, 109.55, 117.31, 118.77, 123.02, 129.87, 131.43, 133.45, 141.17; FAB-MS obsd 467.3377, calcd 467.3374 ($C_{26}H_{43}N_4OSiB$).

10,11-Bis(dibutylboryl)-1,9-di-*p*-tolyl-5-{1-[2-(trimethylsilyl)ethoxymethyl]imidazol-4-yl}dipyrromethane (75). A solution of **74** (340

mg, 729 μmol) in THF (1 mL) was treated with MesMgBr (1 M solution in THF, 1.5 mL, 1.5 mmol) at room temperature under argon for 10 min. The reaction mixture was cooled to –78 °C, and a solution of **63** (341 mg, 1.50 mmol) in THF (1.5 mL) was added dropwise. The reaction mixture was stirred at –78 °C for another 10 min. Saturated aqueous NH_4Cl was added, and the mixture was extracted with ethyl acetate. The organic layer was washed (water and brine), dried (Na_2SO_4) and concentrated. The resulting yellow solid was dissolved in CH_2Cl_2 (1.5 mL) and treated with TEA (209 μL, 1.50 mmol) and Bu_2B-OTf (1.50 mL, 1.50 mmol, 1 M solution in CH_2Cl_2) at room temperature for 30 min. The solvent was removed under reduced pressure. Chromatography (silica, CH_2Cl_2) afforded a yellow liquid (0.13 g, 21%): ^{1}H NMR δ (300 MHz) 3.49 (t, *J* = 8.0 Hz, 2H), 5.30 (s, 2H), 5.58 (s, 1H), 6.26 (m, 1H), 6.53 (d, *J* = 4.4 Hz, 1H), 6.61 (m, 1H), 7.19 (d, *J* = 8.0 Hz, 2H), 7.31 (d, *J* = 4.4 Hz, 1H), 7.35 (d, *J* = 1.6 Hz, 1H), 7.40 (d, *J* = 8.0 Hz, 2H), 7.74 (d, *J* = 8.0 Hz, 2H), 7.87 (d, *J* = 1.6 Hz, 1H), 8.16 (d, *J* = 8.0 Hz, 2H); LD-MS obsd 825.5; calcd 826.5560 ($C_{50}H_{72}N_4O_3SiB_2$)..

5,15-Bis{1-[2-(trimethylsilyl)ethoxymethyl]imidazol-4-yl}-10,20-di-*p*-tolylporphyrin (76). A solution of **74** (615 mg, 1.32 mmol) and *p*-tolualdehyde (156 μL, 1.32 mmol) in CH_2Cl_2 (132 mL) was treated with TFA (362 μL, 4.70 mmol) at room temperature under argon for 1 h. DDQ (449 mg, 1.98 mmol) was added. The solvent was removed under reduced pressure. Chromatography [silica, CH_2Cl_2/ethyl acetate (1:1) then ethyl acetate] afforded a purple solid (0.15 g, 26%): ^{1}H NMR δ –2.73 (s, 2H), 0.10 (s, 18H), 1.11 (t, *J* = 8.0 Hz, 4H), 2.72 (s, 6H), 3.86 (t, *J* = 8.0 Hz, 4H), 5.67 (s, 4H), 7.70 (d, *J* = 7.2 Hz, 4H), 7.82 (d, *J* = 1.6 Hz, 2H), 8.11 (d, *J* = 7.8 Hz, 4H), 8.16 (d, *J* = 1.6 Hz, 2H), 8.87 (d, *J* = 4.4 Hz, 4H), 9.21 (d, *J* = 4.4 Hz, 4H); LD-MS obsd 882.6; FAB-MS obsd 883.4362, calcd

883.4300 [$(M + H)^+$, M = $C_{52}H_{58}N_8O_2Si_2$]; λ_{abs} 410, 442, 504 nm.

5,15-Bis(imidazol-4-yl)-10,20-di-*p*-tolylporphyrin (77). A solution of **76** (95 mg, 0.11 mmol) in THF (21 mL) was treated with TBAF (1 M solution in THF, 1.1 mL, 1.1 mmol) at 70 °C under argon for 3 h. The reaction mixture was concentrated. Chromatography [silica, CH_2Cl_2/MeOH (24:1 → 4:1)] afforded a purple solid (22 mg, 33%): LD-MS obsd 622.4; FAB-MS 623.2654, calcd 623.2672 [$(M + H)^+$, M = $C_{40}H_{30}N_8$]; λ_{abs} (ethyl acetate) 420, 517 nm.

5,15-Bis(1-{3-nitro-4-[methyl (2,3,4-tri-*O*-acetyl-β-D-glucopyranoside)uronate]benzyloxycarbonyl}imidazol-4-yl}-10,20-di-*p*-tolylporphyrin (78). SEM-protected porphyrin **76** (14 mg, 16 μmol) was treated with TBAF (1.0 M, 0.16 mL, 0.16 mmol) at 68 °C under argon for 3 h. The reaction mixture was diluted in ethyl acetate (20 mL) and washed with aqueous acetate buffer (pH 7) twice. The organic layer was dried (Na_2SO_4) and concentrated. The crude deprotected product was dissolved in DMF (405 μL) and treated with **31** (53 mg, 81 μmol) and TEA (113 μL, 812 μmol) at room temperature under argon for 43 h. The reaction mixture was diluted in ethyl acetate (20 mL) and washed twice with water. Chromatography [silica, CH_2Cl_2/ethyl acetate (1:3)] afforded a purple solid. LD-MS analysis showed the expected mass peak of the title compound [LD-MS obsd 1644.4, calcd 1644.4518 ($C_{82}H_{72}N_{10}O_{28}$)], whereas HPLC (size exclusion column) analysis indicated the presence of two different compounds present. Further purification was performed by using an SEC column. Two purple bands were observed in the column and were collected separately. However, both fractions showed multiple porphyrin spots on TLC. LD-MS analysis did not show the expected mass peak for the title compound in either fraction.

REFERENCES

(5.1) (a) Tamiaki, H.; Kimura, S.; Kimura, T. *Tetrahedron* **2003**, *59*, 7423–7435. (b) Tamiaki, H.; Miyatake, T.; Tanikaga, R.; Holzwarth, A. R.; Schaffner, K. *Angew. Chem. Int. Ed Engl.* **1996**, *35*, 772–774.

(5.2) (a) Balaban T. S.; Bhise, A. D.; Fischer, M.; Linke-Schaetzel, M.; Roussel, C.; Vanthuyne, N. *Angew. Chem. Int. Ed.* **2003**, *42*, 2140–2144. (b) Sasaki, S.-I.; Omada, M.; Tamiaki, H. *J. Photochem. Photobiol. A: Chem.* **2004**, *162*, 307–315. (c) Balaban, T. S. *Acc. Chem. Res.* **2005**, *38*, 612–623. (d) Tamiaki, H.; Holzwarth, A. R.; Schaffner, K. *Photosynth. Res.* **1994**, *41*, 245–251.

(5.3) Wang, Z.; Medforth, C. J.; Shelnutt, J. A. *J. Am. Chem. Soc.* **2004**, *126*, 15954–15955.

(5.4) Bhyrappa, P.; Wilson, S. R.; Suslick, K. S. *J. Am. Chem. Soc.* **1997**, *119*, 8492–8052.

(5.5) Nagata, N.; Kugimiya, S.-I.; Kobuke, Y. *Chem. Commun.* **2000**, 1389–1390.

(5.6) (a) Tamaru, S.-I., Nakamura, M.; Takeuchi, M.; Shinkai, S. *Org. Lett.* **2001**, *3*, 3631–3634. (b) Csík, G.; Balog, E.; Voszka, I.; Tölgyesi, F.; Oulmi, D.; Maillard, Ph., Momenteau, M. *J. Photochem. Photobiol. B* **1998**, *44*, 216–224.

(5.7) Michelsen, U.; Hunter, C. A. *Angew. Chem. Int. Ed.* **2000**, *39*, 764–767.

(5.8) Balaban, T. S.; Goddard, R.; Linke-Schaetzel, M.; Lehn, J.-M. *J. Am. Chem. Soc.* **2003**, *125*, 4233–4239.

(5.9) Tanaka, T.; Endo, K.; Aoyama, Y. *Bull. Chem. Soc. Jpn.* **2001**, *74*, 907–916.

(5.10) Robertson A.; Waters, R. B. *J. Chem. Soc.* **1930**, 2729–2733.

(5.11) Littler, B. J.; Miller, M. A.; Hung, C.-H.; Wagner, R. W.; O'Shea, D. F.; Boyle, P. D.; Lindsey, J. S. *J. Org. Chem.* **1999**, *64*, 1391–1396.

(5.12) Mikata, Y.; Onchi, Y.; Tabata, K.; Ogura, S.-I.; Okura, I.; Ono, H.; Yano, S.

Tetrahedron Lett. **1998**, *39*, 4505–4508.

(5.13) Geier, G. R., III; Ciringh, Y.; Li, F.; Haynes, D. M.; Lindsey, J. S. *Org. Lett.* **2000**, *2*, 1745–1748.

(5.14) Mareček, V.; Jänchenová, H.; Stibor, I.; Budka, J. *J. Electroanal. Chem.* **2005**, *575*, 293–299.

(5.15) Gao, Y.; Lane-Bell, P.; Vederas, J. C. *J. Org. Chem.* **1998**, *63*, 2133–2143.

(5.16) Srivastava, O. P.; Hindsgaul, O. *Carbohydr. Res.* **1985**, *143*, 77–84. (b) Sabesan, S.; Neira, S. *Carbohydr. Res.* **1992**, *223*, 169–185.

(5.17) Mann, J.; Haase-Held, M. *Tetrahedron* **1990**, *46*, 5377–5382.

(5.18) Florent, J.-C.; Dong, X.; Gaudel, G.; Mitaku, S.; Monneret, C.; Gesson, J.-P.; Jacquesy, J.-C.; Mondon, M.; Renoux, B.; Andrianomenjanahary, S.; Michel, S.; Koch, M.; Tillequin, F.; Gerken, M.; Czech, J.; Straub, R.; Bosslet, K. *J. Med. Chem.* **1998**, *41*, 3572–3581.

(5.19) Zhang, T.-G.; Zhao, Y.; Asselberghs, I.; Persoons, A.; Clays, K.; Therien, M. J. *J. Am. Chem. Soc.* **2005**, *127*, 9710–9720.

(5.20) Kitamura, C.; Yamashita, Y. *J. Chem. Soc., Perkin Trans. 1* **1997**, 1443–1447.

(5.21) Bassetti, M.; Floris, B.; Illuminati, G. *Organometallics* **1985**, *4*, 617–623.

(5.22) Carcel, C. M.; Laha, J. K.; Loewe, R. S.; Thamyongkit, P.; Schweikart, K.-H.; Misra, V.; Bocian, D. F.; Lindsey, J. S. *J. Org. Chem.* **2004**, *69*, 6739–6750.

(5.23) Tamaru, S.-I.; Yu, L.; Youngblood, W. J.; Muthukumaran, K.; Taniguchi, M.; Lindsey, J. S. *J. Org. Chem.* **2004**, *69*, 765–777.

(5.24) Corey, E. J.; Venkateswarlu, A. *J. Am. Chem. Soc.* **1972**, *94*, 6190–6191.

(5.25) Lee, M. J. C; Elberling, J. A.; Nagasawa, H. T. *J. Med. Chem.* **1992**, *35*, 3641–3647.

(5.26) Yan, S. I.; Seth, J.; Balasubramanian, T.; Kim, D.; Lindsey, J. S.; Holten, D.; Bocian, D. F. *J. Am. Chem. Soc.* **1999**, *121*, 4008–4018.

(5.27) Kamogawa, H.; Nakata, T.; Komatsu, S. *Bull. Chem. Soc. Jpn.* **1991**, *64*, 2300–2302.

(5.28) Brückner, C.; Dolphin, D. *Tetrahedron Lett.* **1995**, *36*, 3295–3298.

(5.29) (a) Silva, A. M. G.; Faustino, M. A. F.; Silva, T. M. P. C.; Neves, P. M. S.; Tomé, A. C.; Silva, A. M. S.; Cavaleiro, J. A. S. *J. Chem. Soc. Perkin Trans. 1* **2002**, 1774–1777. (b) Richeter, S.; Jeandon, C.; Gisselbrecht, J.-P.; Ruppert, R.; Callot, H. J. *J. Am. Chem. Soc.* **2002**, *124*, 6168–6179. (c) Xu, Y.; Jaquinod, L.; Wickramasinghe, A.; Smith, K. M. *Tetrahedron Lett.* **2003**, *44*, 7753–7756.

(5.30) (a) Shea, K. M.; Jaquinod, L.; Smith, K. M. *J. Org. Chem.* **1998**, *63*, 7013–7021. (b) Hombrecher, J. K.; Gherdan, V. M.; Ohm, S. *Tetrahedron* **1993**, *49*, 8569–8578. (c) Ostrowski, S.; Szerszeń, D.; Ryszczuk, M. *Synthesis* **2005**, 819–823.

(5.31) (a) Jin, L.-M.; Zeng, Z.; Guo, C.-C.; Chen, Q.-Y. *J. Org. Chem.* **2003**, *68*, 3912–3917. (b) Zeng, Z.; Liu, C.; Jin, L.-M.; Guo, C.-C.; Chen, Q.-Y. *Eur. J. Org. Chem.* **2005**, 306–316.

(5.32) (a) Takanami, T.; Hayashi, M.; Chijimatsu, H.; Inoue, W.; Suda, K. *Org. Lett.* **2005**, *7*, 3937–3940. (b) Zhou, X.; Tse, M. K.; Wan, T. S. M.; Chan, K. S. *J. Org. Chem.* **1996**, *61*, 3590–3593. (c) Zhou, X.; Chan, K. S. *J. Org. Chem.* **1998**, *63*, 99–104.

(5.33) Chen, L.; Jin, L.-M.; Guo, C.-C.; Chen, Q.-Y. *Synlett* **2005**, 963–970.

(5.34) Balasubramanian, T.; Lindsey, J. S. *Tetrahedron* **1999**, *55*, 6771–6784.

(5.35) Balasubramanian, T.; Strachan, J.-P.; Boyle, P. D.; Lindsey, J. S. *J. Org. Chem.* **2000**, *65*, 7919–7929.

(5.36) Lee, C.-H.; Li, F.; Iwamoto, K.; Dadok, J.; Bothner-By, A. A.; Lindsey, J. S.

Tetrahedron **1995**, *51*, 11645–11672.

(5.37) (a) Åhman, J. *Synth. Commun*. **1994**, *24*, 1117–1120. (b) Seitz, D. E., Carroll, J. J.; Cartaya, C. P.; Lee, S.-H.; Zapata, A. *Synth. Commun.* **1983**, *13*, 129–134.

(5.38) (a) DiMagno, S. G.; Lin, V. S.-Y.; Therien, M. J. *J. Org. Chem.* **1993**, *58*, 5983–5993. (b) Aihara, H.; Jaquinod, L.; Nurco, D. J.; Smith, K. M. *Angew. Chem. Int. Ed.* **2001**, *40*, 3439–3441.

(5.39) Barbier, M.; Barton, D. H. R.; Devys, A.; Topgi, R. S. *Tetrahedron* **1987**, *43*, 5031–5038.

(5.40) Abel, E. W.; Rowley, R. J. *J. Organomet. Chem.* **1975**, *97*, 159–165.

(5.41) (a) Smith, K. M.; Bisset, M. F. *J. Org. Chem.* **1979**, *44*, 2077–2081. (b) Hayashi, N.; Naoe, A.; Miyabayashi, K.; Yamada, M.; Miyake, M.; Higuchi, H. *Tetrahedron Lett.* **2004**, *45*, 8215–8219. (c) Arnold, D.; Johnson, A. W.; Winter, M. *J. Chem. Soc. Perkin Trans. 1* **1977**, 1643–1647.

(5.42) Odobel, F.; Blart, E.; Lagrée, M.; Villieras, M.; Boujtita, H.; Murr, N. E.; Caramori, S.; Bignozzi, C. A. *J. Mater. Chem.* **2003**, *13*, 502−510.

(5.43) (a) Johnson, A. W.; Oldfield, D. *J. Chem. Soc. C* **1996**, 794−798. (b) Morozova, Y. V.; Nesterov, V. V.; Yashunsky, D. V.; Antipin, M. Y.; Ponomarev, G. V. *Khim. Geterotsikl. Soedin.* **2005**, 697−704.

(5.44) Muthukumaran, K.; Ptaszek, M.; Noll, B.; Scheidt, W. R.; Lindsey, J. S. *J. Org. Chem.* **2004**, *69*, 5354–5364.

(5.45) Zaidi, S. H. H.; Muthukumaran, K.; Tamaru, S.-I.; Lindsey, J. S. *J. Org. Chem.* **2004**, *69*, 8356–8365.

(5.46) Taniguchi, M.; Balakumar, A.; Fan, D.; McDowell, B. E.; Lindsey, J. S. *J. Porphyrins*

Phthalocyanines **2005**, *9*, 554−574.

(5.47) Borbas, K. E.; Mroz, P.; Hamblin, M. R.; Lindsey, J. S. *Bioconjugate Chem.* **2006**, *17*, 638−653.

(5.48) Quan, C.; Kurth, M. *J. Org. Chem.* **2004**, *69*, 1470−1474.

(5.49) (a) Hunter, C. A.; Sarson, L. D. *Angew. Chem., Int. Ed. Engl.* **1994**, *33*, 2313–2316; (b) Balaban, T. S.; Goddard, R.; Linke-Schaetzel, M.; Lehn, J.-M. *J. Am. Chem. Soc.* **2003**, *125*, 4233–4239.

(5.50) Bhaumik, J.; Yao, Z.; Borbas, K. E.; Taniguchi, M.; Lindsey, J. S. *J. Org. Chem.* **2006**, *71*, 8807–8817.

(5.51) Gryko, D.; Lindsey, J. S. *J. Org. Chem.* **2000**, *65*, 2249–2252.

(5.52) (a) Holmes, S. C.; Gait, M. J. *Eur. J. Org. Chem.* **2005**, 5171–5183. (b) Carrico, D.; Blaskovich, M. A.; Bucher, C. J.; Sebti, S. M.; Hamilton, A. D. *Bioorg. Med. Chem.* **2005**, *13*, 677–688.

(5.53) Strachan, J.-P.; O'Shea, D. F.; Balasubramanian, T.; Lindsey, J. S. *J. Org. Chem.* **2000**, *65*, 3160–3172.

Chapter 6

Enzymatic Formation of a Porphyrin Precipitate From a Water-soluble Porphyrin

6.1. Abstract

In a new therapy that aims to concentrate therapeutic radionuclides within solid tumors, a soluble precipitable reagent (SPR) is administered as the radioisotope carrier and is converted to precipitate by an enzyme located in tumor tissues. To meet the objective of such an SPR, we have prepared and examined a porphyrin diphosphate that is soluble in aqueous solution and that is rendered insoluble upon removal of the two phosphate groups. Dephosphorylation reactions have been carried out using the enzyme shrimp alkaline phosphatase (SAP). The reaction has been examined by absorption spectroscopy, electrospray ionization mass spectrometry (ESI-MS), and nephelometry using non-radiolabeled substrates.

6.2. Introduction

The strategy outlined in the Rose/Oncologic method of cancer therapy relies on a series of steps whereby an insoluble radiolabeled material is accumulated in the diseased (i.e., solid tumor) tissue.[2.10] The first three steps of the process are designed to accumulate solid material to which enzyme molecules are covalently attached. The Step-4 Agent is a soluble precipitable reagent (SPR) that (1) bears a radiolabel, and (2) undergoes conversion from soluble to insoluble form upon action of the bound enzyme. Given that the enzyme functions

catalytically, a large amount of radiolabeled material can in principle be deposited in the diseased tissue.

The design of a Step-4 SPR presents a number of challenges. In addition to the requirement for clean conversion from soluble to insoluble forms, the Step-4 SPR ideally should be compatible with incorporation of one or more radioisotopes. For practical reasons, the Step-4 SPR should be amenable to incorporation of the radioisotopes at the last step of the chemical synthesis. In this chapter, we describe our studies of the soluble-to-insoluble conversion of a *trans*-AB-porphyrin upon enzymatic action in aqueous solution. The porphyrin is not radiolabeled in the studies described herein. However, the *trans*-AB-porphyrin is a free base porphyrin and contains two free meso positions. Radiolabels can be incorporated by use of an appropriate metal (yielding the metalloporphyrin), by halogenation of one or both meso positions, or by both metalation and halogenation. Such labeling procedures can be performed at the last steps of the chemical synthesis.

6.3. Results and Discussion

Low solubility is a common problem with porphyrins because such planar aromatic compounds tend to aggregate upon π-π interactions among the aromatic rings. Substituted phenyl groups such as 3,5-di-*tert*-butyl-phenyl and mesityl groups impart higher organic solubility to the porphyrin than phenyl group.[4.12] A likely explanation is that the alkyl moieties on the meso-phenyl groups "shield" the space above and below the macrocycle, and thus suppress cofacial the π-π interactions. Another type of meso-substituent that solubilizes porphyrins by the same "shielding" strategy is a symmetrically branched alkyl group (swallowtail).[4.12,6.1] One example of a swallowtail substituent is the tridecyl group

symmetrically branched about carbon 7 (Figure 6.1).[4.12] Porphyrins and multiporphyrin rods, bearing the tridec-7-yl swallowtail group, display a high level of solubility in organic solvents.[4.12, 6.2]

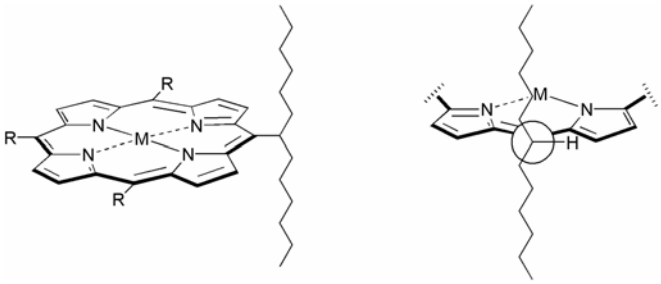

(a) (b)

Figure 6.1. A porphyrin swallowtail bearing a meso-swallowtail substituent. (a) Side view and (b) Newman projection. Adapted from ref. 5.50.

The successes with swallowtail porphyrins inspired the Lindsey group to use a similar structure to improve solubility of porphyrins in aqueous media. The swallowtail group can be derivatized at the terminus of both alkyl groups with polar moieties such as phosphate groups. The rational synthesis of a diphosphate-derivatized swallowtail porphyrin [**Fb-$(PO_4)_2$**] (Equation 6.1) was developed.[5.50] The free base porphyrin **Fb-$(PO_4)_2$** (5-(4-bromophenyl)-15-[1,5-bis(dihydroxyphosphoryloxy)pent-3-yl]porphyrin), which bears one swallowtail substituent, one potentially bioconjugatable group (4-bromophenyl), and no substituents at the flanking meso positions, displays excellent solubility in water.

I performed a series of experiments with **Fb-$(PO_4)_2$** to determine whether the swallowtail diphosphate porphyrin can be converted to a precipitate upon enzymatic treatment as required for a porphyrin-based SPR. **Fb-$(PO_4)_2$** used in the enzymatic assay described in this chapter was provided by Dr. K. Eszter Borbas in the Lindsey group.

Porphyrin **Fb-$(PO_4)_2$** was treated in aqueous solution with shrimp alkaline phosphatase (SAP), an enzyme known to give rapid removal of phosphate groups. The

product of the reaction is a dihydroxyporphyrin [**Fb-(OH)$_2$**, Equation 6.1], which is expected to precipitate. The insolubility of **Fb-(OH)$_2$** was confirmed by testing with an authentic sample. The reaction course was monitored by several methods including absorption spectroscopy, ESI-MS, and nephelometry.

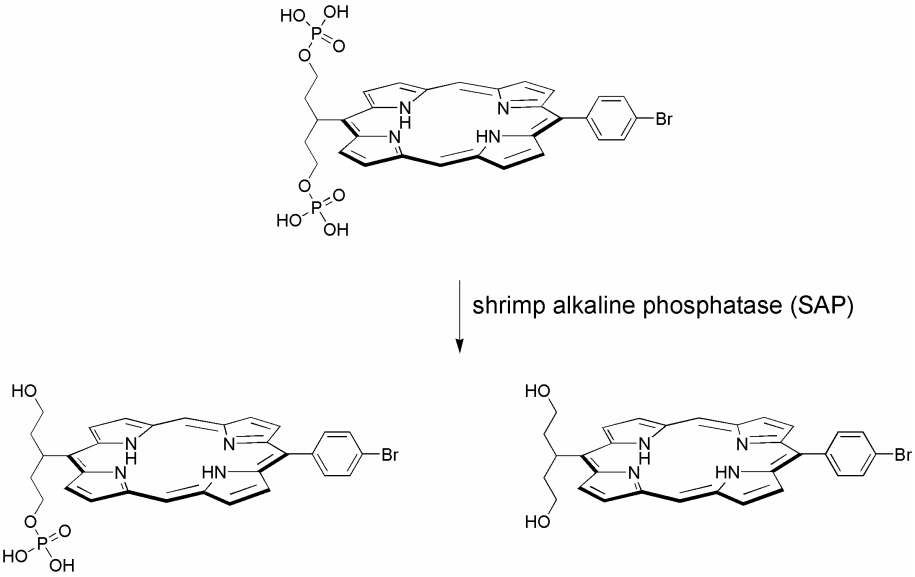

Equation 6.1. A water-soluble porphyrin [**Fb-(PO$_4$)**] and the dephosphorylated products. The porphyrin **Fb-(OH)$_2$** is water-insoluble.

6.3.1. Conditions for Dephosphorylation Reactions

The free base porphyrin **Fb-(PO$_4$)$_2$** shows good solubility in water; however, the porphyrin needs to be soluble in a buffer suitable for the dephosphorylation reaction catalyzed by SAP. Upon mixing the aqueous solution of the porphyrin and a buffer solution provided by the enzyme manufacturer (Promega), a red precipitate was formed immediately. Centrifugation of the sample gave the red precipitate and a slightly yellow supernatant. Aqueous solutions of **Fb-(PO$_4$)$_2$** of a range of concentrations (up to 0.61 mM) were prepared and mixed with the SAP buffer. At high concentrations of porphyrin, a precipitate was

observed by visual inspection to form very rapidly. At low concentrations, a precipitate was observed only upon centrifugation of the sample. In each case, the porphyrin concentration in the supernatant (calculated from absorption spectra) was 1~2 μM.

To avoid such precipitation, a Tris-HCl buffer (50 mM, pH 9.0) was used (lacking SAP and metal salt) to prepare the porphyrin solution. Neither precipitation nor change of color in the solution was observed. Although the lack of Mg^{2+}, which is a cofactor of SAP, may lower the enzyme activity, we prefer a higher starting substrate concentration to better distinguish the reaction composition before and after dephosphorylation. On the other hand, the lower enzyme activity can be compensated by increasing the enzyme/substrate ratio.

To monitor the course of the reaction, we deliberately altered the conditions so as to ensure dephosphorylation would proceed to completion over the course of 30-60 min. The chief means of controlling the conditions was to change the molar ratio of the substrate (phosphoester) to the enzyme. After several preliminary experiments, we found that a suitable molar ratio of phosphoester [each **Fb-$(PO_4)_2$** molecule contains two phosphoesters] to SAP is ~5000.

6.3.2. Analysis of the Dephosphorylation/Precipitation Process

Three experiments were carried out to investigate the enzyme-mediated dephosphorylation process and ensuing precipitation.

Experiment 1: Enzymatic-Mediated Formation of a Porphyrin Precipitate. A dephosphorylation reaction and three negative control reactions were carried out. An aqueous solution of **Fb-$(PO_4)_2$** at 68 μM in a Tris-HCl buffer (50 mM, pH 9.0) was prepared. One enzymatic reaction and three negative control reactions were set up in four 1.5-mL

Eppendorf tubes. Active SAP, heat-inactivated SAP (75 °C for 20 min) and a buffer solution (containing the same ingredients in the SAP storage solution except the SAP enzyme) were added to tubes labeled with "E" (for "enzyme"), "dE" (for "deactivated enzyme") and "MZ" (for "Mg^{2+}/Zn^{2+}"), respectively. The fourth tube was labeled with "NE" (for "no enzyme"). All four tubes were incubated at 37 °C for 2 h followed by centrifugation. Absorption spectra and ESI-MS were obtained for solutions (if there was no visible precipitate) or supernatants (if there was visible precipitate) taken out of the tubes. Any supernatant was isolated, washed with water, dissolved in DMF and analyzed by ESI-MS. Photographs were taken at different stages during the reaction course as described in the following paragraphs.

The aqueous solution of **Fb-$(PO_4)_2$** in a Tris-HCl buffer was light purple (Figure 6.2). After the addition of active SAP, a distinguishable color change was observed within one minute (Figure 6.3, tube E). By contrast, the tubes without SAP or with deactivated SAP did not show any change of color (Figure 6.3, tube NE, MZ and dE).

Figure 6.2. Aqueous solutions of **Fb-$(PO_4)_2$** prior to enzyme treatment in tubes containing no enzyme (NE), a buffer solution (MZ), heat-inactivated SAP (dE) or active SAP (E).

Figure 6.3. Aqueous solutions of **Fb-$(PO_4)_2$** 1 min after the addition of no enzyme (NE), a buffer solution (MZ), heat-inactivated SAP (dE) or active SAP (E).

After the incubation, the reaction mixture containing active SAP was yellow-brown whereas the reaction mixture with deactivated SAP was slightly yellowish (Figure 6.4). The solution in tube MZ did not display any color difference compared to the solution in tube NE. Despite the change of color in tube E, no precipitate was observed by visual inspection. The tubes were then centrifuged. Figure 6.5 clearly shows a brown precipitate in tube E, which contained the reaction mixture with active SAP. Meanwhile, tubes MZ, dE and NE did not display any visible precipitate.

Figure 6.4. Reaction mixtures following treatment of **Fb-$(PO_4)_2$** with no enzyme (NE), a buffer solution (MZ), heat-inactivated SAP (dE) or active SAP (E). No visible precipitate was observed in any tube.

Figure 6.5. Reaction mixture following (1) treatment of **Fb-$(PO_4)_2$** with no enzyme (NE), a buffer solution (MZ), heat-inactivated SAP (dE) or active SAP (E); and (2) centrifugation. A brown precipitate is clearly visible in tube E but not in other tubes.

Prior to the addition of the enzyme SAP, the **Fb-$(PO_4)_2$** exhibited a strong absorption in aqueous solution at 401 nm (Soret band). After incubation, the control reactions without active enzyme (tube NE, MZ, dE) did not show a significant change in the absorption pattern (Figure 6.6a). On the other hand, for the reaction with active SAP, the absorption intensity at 401 nm was significantly diminished, and a new band appeared at 450 nm (attributed to aggregated porphyrin species) (Figure 6.6b). The absorption intensity at 401 nm in water was used as a measure of the amount of **Fb-$(PO_4)_2$** in the reaction mixture.

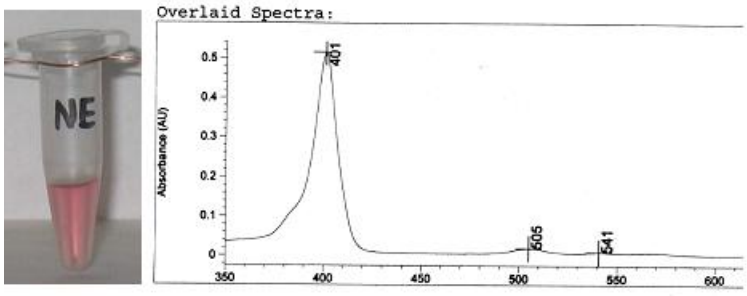

(a)

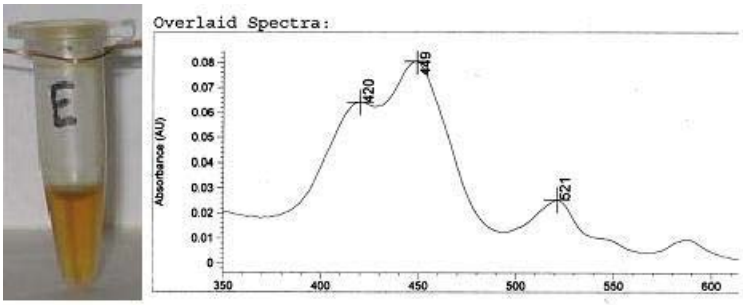

(b)

Figure 6.6. Correlation between the color of the sample and the corresponding absorption spectra. (a) After incubation, the three control reactions (tube NE, MZ, dE) did not display significant change in absorption; (b) the reaction mixture with active enzyme (tube E, after incubation, before centrifugation) displayed a broadened, red-shifted absorption signal that indicates porphyrin aggregates.

The absorption spectra (in aqueous solutions) of the reaction mixtures without active SAP (solutions in tube MZ, dE and NE) showed the same strong absorption at 401 nm as the absorption spectrum obtained before the reactions started. The solution in tube NE showed little change in the absorption intensity at 401 nm (from 0.668 to 0.632) whereas the reaction mixtures in tube MZ and dE showed decreases in the absorption intensity at 401 nm. The decrease (22−25%) may be attributed to the presence of salts (Mg^{2+}, Zn^{2+}, etc). On the other hand, the absorption spectrum of the reaction mixture with SAP (tube E) showed a 450-nm peak but no 401-nm peak. The absence of absorption at 402 nm indicates that porphyrin **Fb-$(PO_4)_2$** was completely dephosphorylated by SAP.

ESI-MS analysis showed the sole presence of starting **Fb-$(PO_4)_2$** in the solutions in

tube NE and MZ (Figure 6.7a and b), whereas the mass spectrum of the reaction mixture treated with deactivated SAP (tube dE) displayed peaks attributed to **Fb-$(PO_4)_2$**, **Fb-$(OH)_2$** and **Fb-OH/PO_4** (Figure 6.7c). It appears that the deactivating condition that we employed (75 °C for 20 min) did not completely deactivate the enzyme. However, the heat treatment seemed to lower the activity of SAP given that **Fb-$(PO_4)_2$** was present after incubation for 2 h.

Figure 6.7. ESI-MS analysis of samples from the three control reactions: (a) without enzyme (NE), (b) without the buffer (MZ), and (c) with deactivated SAP (dE).

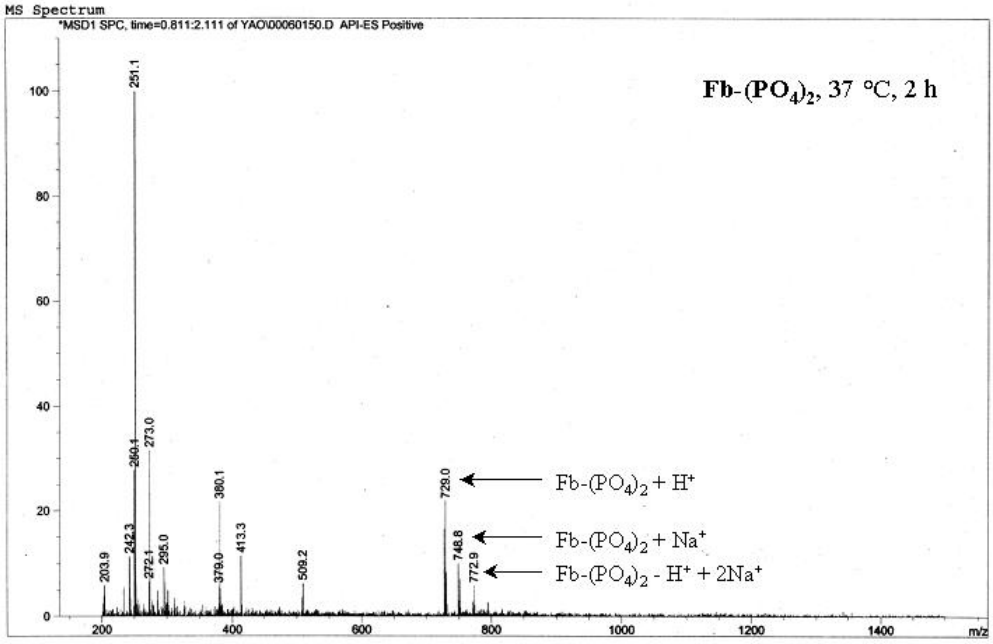
MS Spectrum
*MSD1 SPC, time=0.811:2.111 of YAO\00060150.D API-ES Positive
Fb-(PO4)2, 37 °C, 2 h
Fb-(PO4)2 + H+
Fb-(PO4)2 + Na+
Fb-(PO4)2 - H+ + 2Na+
m/z

(a)

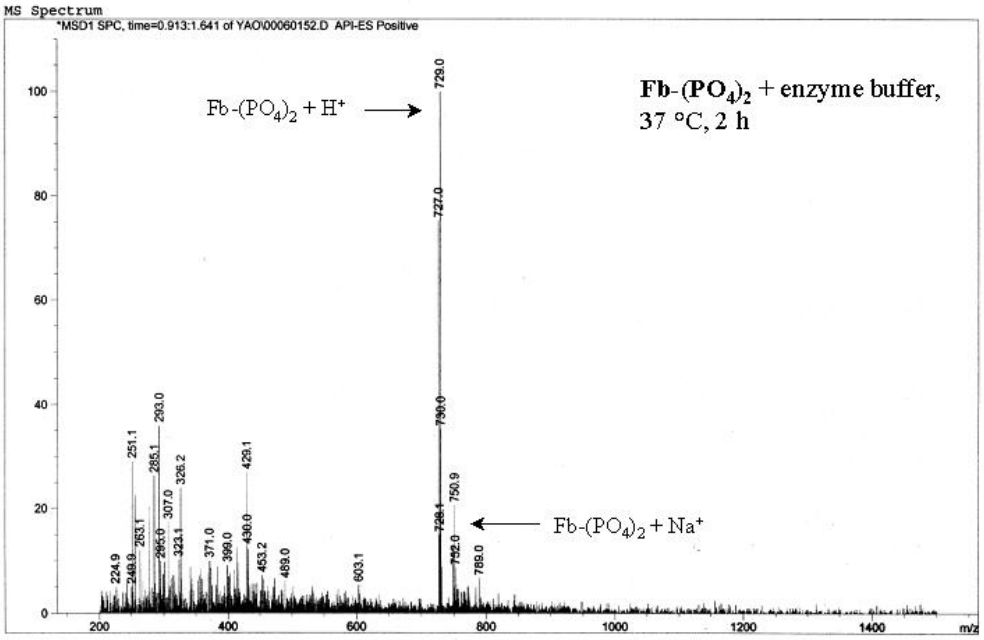
MS Spectrum
*MSD1 SPC, time=0.913:1.641 of YAO\00060152.D API-ES Positive
Fb-(PO4)2 + H+
Fb-(PO4)2 + enzyme buffer,
37 °C, 2 h
Fb-(PO4)2 + Na+
m/z

(b)

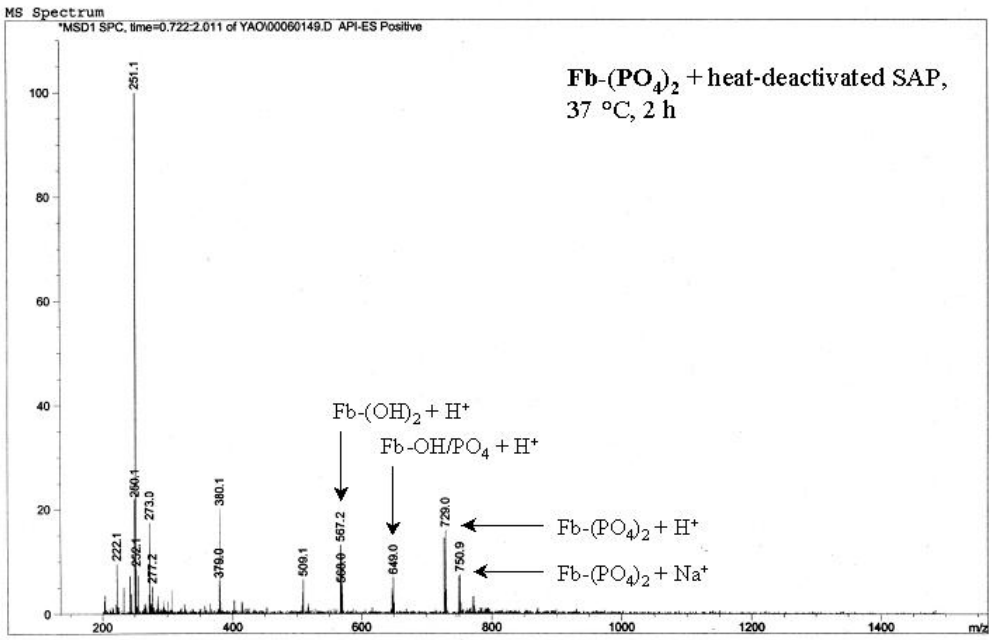

(c)

The mass spectrum of the supernatant in tube E showed the presence of the dephosphorylated porphyrin **Fb-(OH)$_2$** and a small amount of **Fb-OH/PO$_4$** (Figure 6.8a). It was surprising to observe a peak attributed to **Fb-(OH)$_2$**, given that an authentic sample of **Fb-(OH)$_2$** does not dissolve appreciably in water, and attempts to obtain an ESI-MS spectrum from an aqueous sample did not give the corresponding peak. Nevertheless, the formation of **Fb-(OH)$_2$** was confirmed. The precipitate in tube E was isolated, washed with water and dissolved in DMF. ESI-MS analysis showed that **Fb-(OH)$_2$** was the major component in the precipitate (Figure 6.8b).

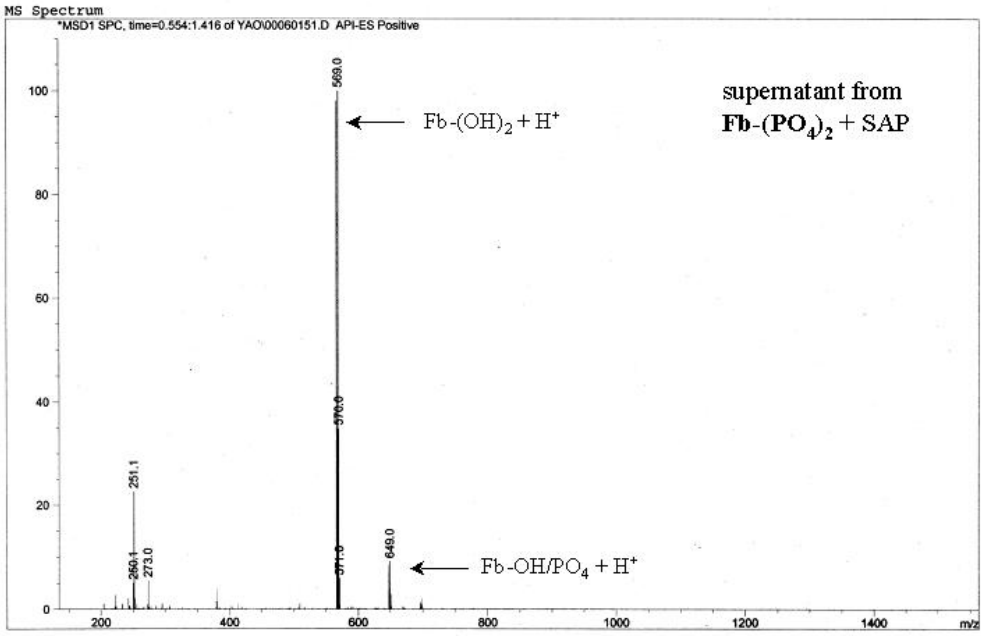

(a)

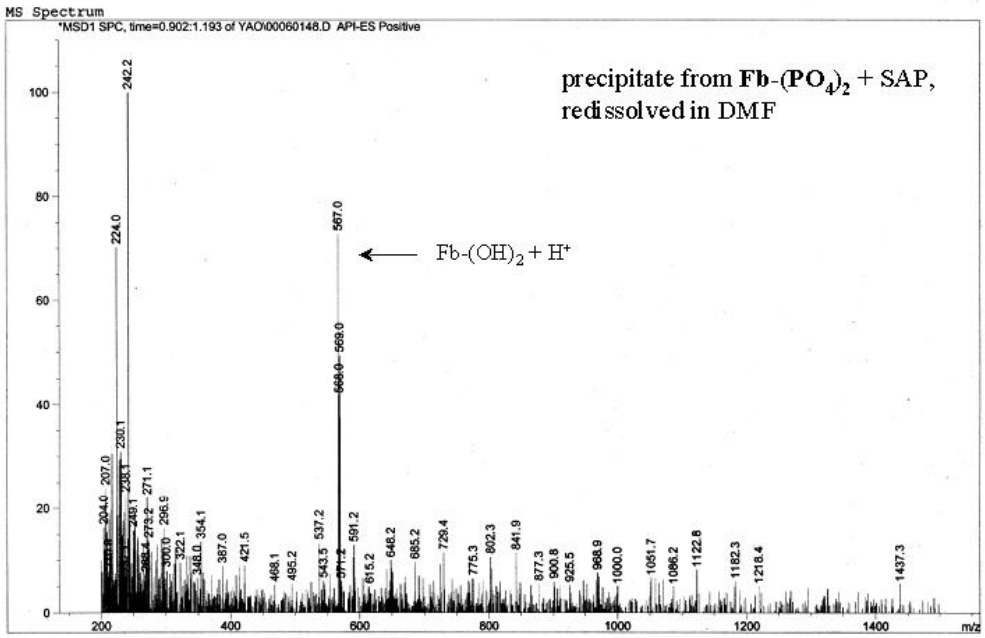

(b)

Figure 6.8. ESI-MS analysis of samples from the enzymatic reaction (E): (a) the supernatant upon centrifugation and (b) the solution obtained by dissolving the precipitate in DMF.

Experiment 2: Kinetic Study of Dephosphorylation Measured by Absorption

Spectroscopy. The dephosphorylation reaction was carried out with the porphyrin **Fb-$(PO_4)_2$** at 60 μM in water containing a Tris-HCl buffer (50 mM, pH 9.0) and SAP at 37 °C in a 1.5-mL Eppendorf tube. To monitor the progress of the reaction, aliquots were periodically removed from the reaction tube and heated to deactivate the enzyme (70 °C at 10 min). The absorption spectra were obtained in both DMF and water for each aliquot. The intensity as a function of time at 402 and 450 nm (aqueous solution) and 406 nm (DMF) was plotted as shown in Figure 6.9.

Since all of the porphyrin species (substrate porphyrin **Fb-$(PO_4)_2$** and the hydrolyzed product porphyrins) dissolve in DMF, the absorption of the reaction mixture in DMF was used to determine the total amount of porphyrin in a given reaction mixture. In DMF, the porphyrin Soret absorption appears at 406 nm. The rationale for monitoring the total amount of porphyrin was to assess the integrity (absence of decomposition) of the porphyrin.

The absorption intensity at 406 nm in DMF changed little during the reaction course. This result indicates that the total amount of porphyrins [**Fb-$(PO_4)_2$**, **Fb-$(OH)_2$** and **Fb-OH/PO_4**] was constant and, thus, negligible porphyrin decomposition occurred. In addition, we set up another enzymatic reaction and dissolved the entire reaction mixture into DMF after incubation for 5 h. By sacrificing the entire reaction mixture, we eliminated any sampling error caused by taking aliquots from heterogeneous media. The absorption intensity at 406 nm changed little after the incubation (0.61 to 0.65; not shown in Figure 6.9). That further proves that decomposition can be excluded as a mechanism for precipitation.

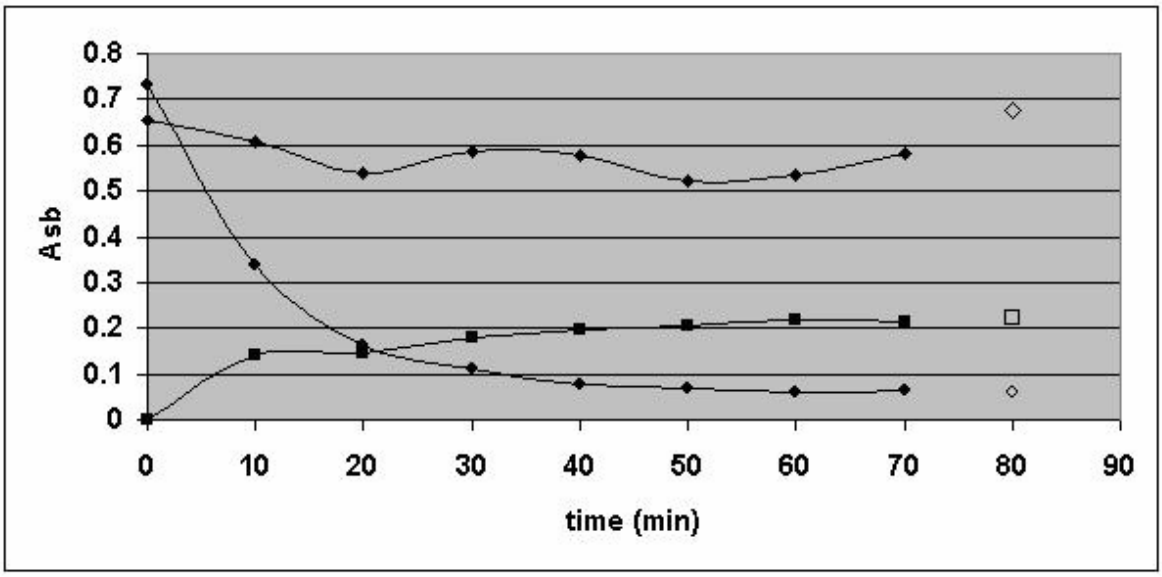

Figure 6.9. Absorption spectral monitoring of the reaction course upon treatment of **Fb-$(PO_4)_2$** with SAP. Legend: 402 nm in water (●); 402 nm overnight (○); 450 nm in water (■); 450 nm overnight (□); 406 nm in DMF (♦); 406 nm overnight (◊).

The absorption intensity at 402 nm in water dropped by more than half (from 0.73 to 0.34) in the first 10 min after the addition of SAP and continued decreasing for another 30 min. The reading after 70 min was around 0.062 and only changed slightly after overnight incubation (0.06). The decrease of intensity at 402 nm was accompanied by the intensification of absorption at 450 nm. An interesting observation is that the addition of several drops of a 5% aqueous NaOH solution to the absorption spectral cuvette caused a decrease of the 450 nm peak and an intensification of the 402 nm peak. The peak at 450 nm likely represents aggregated complexes of **Fb-$(OH)_2$** and **Fb-OH/PO_4** [and possible entrainment of some **Fb-$(PO_4)_2$**]. Since we have ruled out porphyrin decomposition and ionic effects as described previously, the intensity decrease of the 402 nm peak must stem from aggregation and precipitation of **Fb-$(OH)_2$** and/or **Fb-OH/PO_4** formed via enzymatic dephosphorylation.

No visible precipitate was observed immediately upon initiating the reaction.

However, a red-brown precipitate was observed at the bottom of the Eppendorf tubes after standing for several days.

Experiment 3: Kinetic Study of Precipitation Measured by Nephelometry. We assessed the extent of precipitation during the course of the reaction by nephelometry, a technique that measures scattered light. A nephelometer is readily available by use of a fluorimeter, where the light deflected by precipitate in the sample in a cuvette is detected at a right angle from the incident beam.[6.3] For use with porphyrins, the wavelength of the incident beam was chosen as 800 nm to avoid any absorption by the porphyrin. In a photon-counting fluorimeter, the data are obtained as counts/sec (cps). The scattered light was measured continuously as a function of time (cps vs time). The dephosphorylation process was carried out with a gently stirred sample of **Fb-$(PO_4)_2$** at 35 μM in a 3 mL fluorescence cuvette.

The porphyrin solution treated with deactivated SAP gave no increase in the intensity of scattered light over the period examined (3 h). On the other hand, the porphyrin solution treated with active SAP gave a clear increase in scattered light, steadily increasing over the background cps value of ~100,000 over the course of ~6 h (Figure 6.10). A slight increase occurred thereafter as determined upon measurement over the period of 18 to 20 h (Figure 6.11).

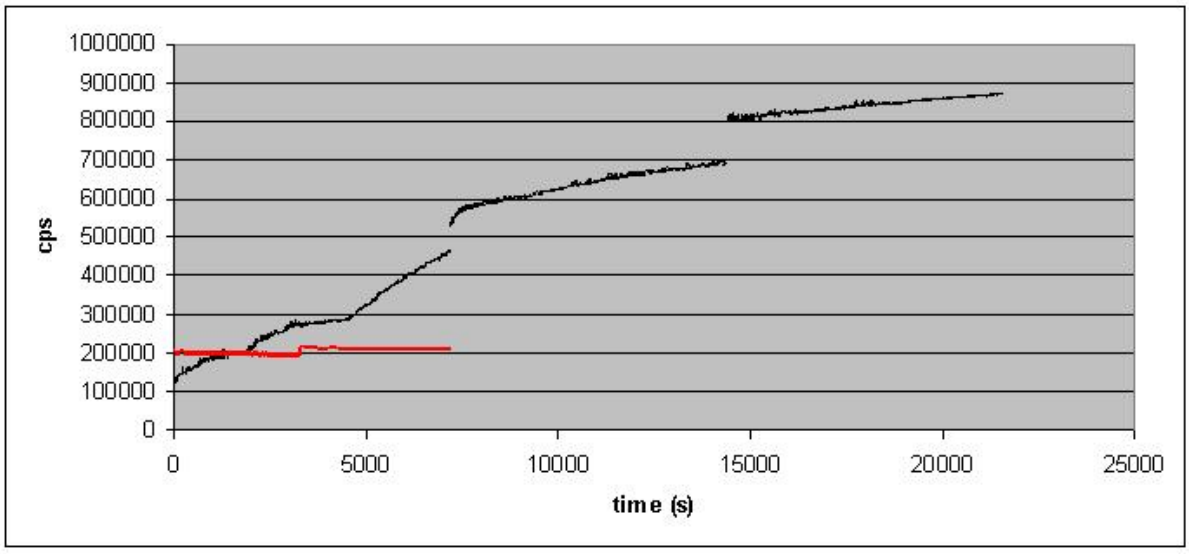

Figure 6.10. Light scattering over time upon treatment of **Fb-$(PO_4)_2$** with SAP in 6 h. Legend: continuous measurement (———); the control reaction with deactivated SAP (— – — –).

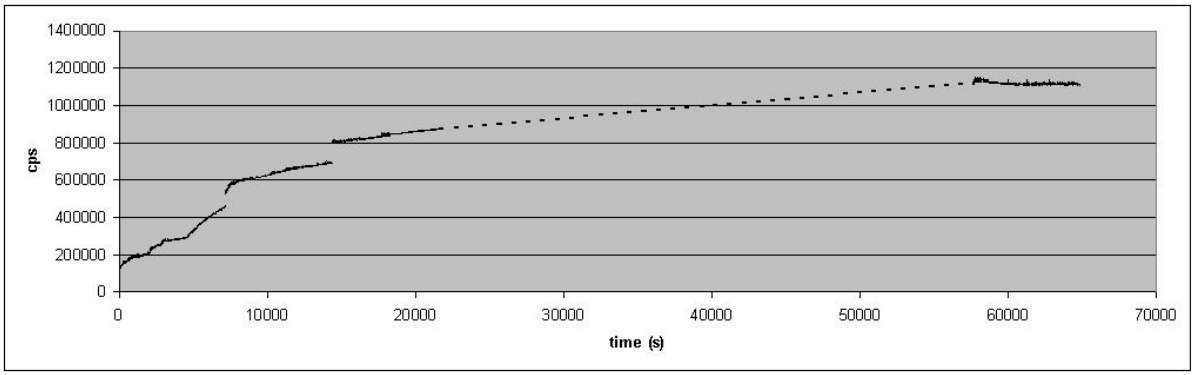

Figure 6.11. Light scattering over time upon treatment of **Fb-$(PO_4)_2$** with SAP in 20 h. The data from 0 – 21,600 seconds are replotted from Figure 3 to show the early time data and late time data (———). The interpolated line (– – –) is provided to guide the eye.

Mass analysis showed the presence of **Fb-OH/PO_4** even when the intensity of the scattered light leveled off. A second batch of SAP was added, but after 6 h the mass peak attributed to **Fb-OH/PO_4** still remained. The **Fb-OH/PO_4** mass peak finally disappeared after several days. The slow dephosphorylation of **Fb-OH/PO_4** may stem from the low temperature (25 °C instead 37 °C) inside the nephelometer.

6.4. Conclusions

The conversion of a soluble porphyrin to an insoluble porphyrin upon enzymatic treatment in aqueous solution has been verified by a series of analytical measurements. Absorption spectroscopy showed the decrease in soluble porphyrin and the formation of an aggregate. Nephelometry showed the formation of a precipitate. Electrospray mass spectrometry confirmed the presence of dephosphorylated porphyrin. The precipitate can be observed after several days by visual inspection, or at earlier times upon centrifugation of the sample. (The sample lacking enzyme remains in solution for days and gives no precipitate.)

As described in Chapter 2.2, two structural features required for a Step-4 SPR are (1) water-solubilizing, cleavable groups and (2) radioisotopes. We demonstrated the soluble-to-insoluble conversion of a diphosphate porphyrin **Fb-$(PO_4)_2$**. Although **Fb-$(PO_4)_2$** is not radiolabeled, such *trans*-AB-porphyrins bear two unsubstituted meso-positions that can conveniently be derivatized with radioactive iodine. Another approach for the design of radiolabeled SPRs entails use of metalloporphyrins. One example of a suitable metal is ^{67}Cu, which forms a stable chelate with porphyrins. A Step-1 SPR may also be constructed based on **Fb-$(PO_4)_2$**. The bioconjugatable group opposite to the swallowtail group may be utilized for attaching other components (e.g., the CTA, Loracarbef, etc.). Alternatively, the two unsubstituted meso-positions can be halogenated and derivatized by subsequent Pd-mediated reactions.

Future research concerning porphyrin-based SPRs includes the design and synthesis of a Step-1 SPR based on a swallowtail diphosphate porphyrin, with subsequent biological assays to assess the tumor targeting ability and platform formation. It must be noted that alkaline phosphatase is present in many biological tissues. The presence of endogeneous

enzyme activity may lead to premature deposition of platform (from the Step-1 SPR) or radioactive precipitate (from the Step-4 SPR). However, the fundamental strategy for solubilizing porphyrins by employing a swallowtail group with polar termini should be compatible with other cleavable water-solubilizing moieties such as galactose or glucuronic acid. Therefore, on the basis of feedback from the biological assays, modifications can be made to improve the effectiveness of porphyrin-based SPRs in this targeted molecular brachytherapy

6.5. Experimental Section.

General. HPLC grade water (Aldrich) was used to prepare all aqueous solutions and in absorption spectral measurements. The concentration of SAP in the storage solution was 2.55 μM, calculated from the unit concentration (unit/μL), specific activity (unit/mg) and molecular weight (g/mol; all data provided by Promega). Porphyrin concentrations were calculated from absorption spectra assuming ε_{Soret} = 500,000 $M^{-1}cm^{-1}$. The enzymatic reaction mixture was analyzed by direct infusion of water/methanol (40:60) solutions by ESI-MS in positive mode.

Experiment 1. A solution of **Fb-$(PO_4)_2$** in 1600 μL of a Tris-HCl buffer (50 mM, pH 9.0) was prepared. A 60-μL aliquot of this solution was diluted in 3 mL of water, and an absorption spectrum was obtained. The concentration calculated from the intensity at 401 nm was 68 μM. The remaining porphyrin solution was distributed evenly into four 1.5-mL Eppendorf tubes, labeled E, dE, MZ, and NE. A 3.8-μL aliquot of SAP storage solution [containing 1 mM of $MgCl_2$, 0.1 mM $ZnCl_2$, 25 mM Tris-HCl (pH 7.6) and 50% (v/v) glycerol] was added to tube E. Another 3.8 μL of SAP storage solution was heated at 75 °C

for 20 min and then added to tube dE. A buffer solution was prepared, which contained 1 mM $MgCl_2$, 0.1 mM $ZnCl_2$, 20 mM Tris-HCl (pH 7.2) and 40% (v/v) glycerol. A 3.8-μL aliquot of the buffer solution was added to tube MZ. All four tubes were incubated at 37 °C for 2 h and then centrifuged at 7,000 rpm for 8 min. From each tube, 60 μL of the solution (tube dE, NE and MZ) or supernatant (tube E) was transferred into 3 mL of water for absorption analysis. The remaining solutions and supernatant were used for mass analysis. The precipitate in tube E was washed with water, dissolved in DMF, and analyzed by ESI-MS.

Experiment 2. A solution of **Fb-$(PO_4)_2$** in 500 μL of a Tris-HCl buffer (50 mM, pH 9.0) was prepared in an Eppendorf tube at a concentration of 60 μM. 5.3 μL of the SAP storage solution was added, and the tube was incubated at 37 °C with shaking. A 50-μL aliquot of the reaction mixture was taken out of tube 1 every 10 min from 0 min (before the addition of SAP) to 70 min. The remaining solution was incubated at 37 °C for 16 h, and then heated to 70 °C for 10 min. Each aliquot was heated to 70 °C in a water bath for 10 min to deactivate the enzyme. Absorption spectra in both water and DMF were recorded for each aliquot and the remaining solution.

A solution of **Fb-$(PO_4)_2$** in 300 μL of a Tris-HCl buffer (50 mM, pH 9.0) was prepared in an Eppendorf tube at a concentration of 38 μM. 100 μL of the solution was transferred to a cuvette filled with 3 mL of DMF, and an absorption spectrum was recorded. 1.7 μL of the SAP storage solution was added to the Eppendorf tube, and the reaction was incubated at 37 °C with shaking for 5 h. The entire reaction mixture was transferred to a cuvette filled with 3 mL of DMF, and a second absorption spectrum was recorded. The absorption intensity at 406 nm in the second spectrum was divided by 2 and compared to the

absorption intensity at 406 nm in the first spectrum.

Experiment 3. A simple nephelometer was constructed using a fluorimeter (Photon Technology International). The photomultiplier voltage was set at 800 V. The enzymatic reaction was performed in a 1-cm pathlength fluorescence cuvette (3 mL) at room temperature. The cuvette was equipped with a stirring bar, and the reaction mixture was stirred at a modest rate (no vortex formation). Excitation and emission monochromators were both set at 800 nm to minimize direct absorption by the porphyrin.

A fluorescence cuvette was filled with 3 mL of an aqueous solution of **Fb-$(PO_4)_2$** in a Tris-HCl buffer (50 mM, pH 9.0). The concentration of the porphyrin solution was 35 μM. An aliquot (16.8 μL) of the SAP storage solution was added to the cuvette, and the light scattering measurement was started immediately. A 500-μL aliquot of the reaction mixture was taken out of the cuvette for mass analysis at 2 h, 4 h, 6 h and 18 h. Once the mass spectrum was obtained, the aliquot was transferred back to the cuvette to keep the total volume constant. A second batch of SAP (16.8 μL) was added at 20 h, and the cuvette was stirred at room temperature. ESI-MS spectra were obtained every 2 h by the same procedure described above.

REFERENCES

(6.1) (a) Tabushi, I.; Sakai, K.-I.; Yamamura, K. *Tetrahedron Lett.* **1978**, *21*, 1821–1824. (b) Rothemund, P. *J. Am. Chem. Soc.* **1939**, *61*, 2912–2915. (c) Runge, S.; Senge, M. O. *Z. Naturforsch.* **1998**, *53b*, 1021–1030. (d) Ema, T.; Senge, M. O. Nelson, N. Y.; Ogoshi, H.; Smith, K. M. *Angew. Chem., Int. Ed. Engl.* **1994**, *33*, 1879–1881.

(6.2) Thamyongkit, P; Lindsey, J. S. *J. Org. Chem.* **2004**, *69*, 5796–5799.

(6.3) Li, F.; Yang, K.; Tyhonas, J. S.; MacCrum, K. A.; Lindsey, J. S. *Tetrahedron* **1997**, *53*, 12339–12360.